Study of radiation induced polymerization of quaternary ammonium based monomers for biomedical and environmental applications

By

Narender Kumar Goel
Enrolment No. CHEM01200804005
BHABHA ATOMIC RESEARCH CENTRE
MUMBAI, INDIA

A thesis submitted to the

Board of Studies in Chemical Sciences

In partial fulfillment of requirements

For the Degree of

DOCTOR OF PHILOSOPHY
of
HOMI BHABHA NATIONAL INSTITUTE

January, 2014

Homi Bhabha National Institute

Recommendations of the Viva Voce Board

As members of the Viva Voce Board, we certify that we have read the dissertation prepared by **Narender Kumar Goel** entitled "**Study of radiation induced polymerization of quaternary ammonium based monomers for biomedical and environmental applications"** and recommend that it may be accepted as fulfilling the dissertation requirement for the Degree of Doctor of Philosophy.

Chairman:	**(Dr. B. N. Jagtap)**		Date: 23/01/14
Guide :	**(Dr. S. Sabharwal)**		Date: 23/01/14
External Referee	**(Prof. P. A. Mahanwar)**		Date: 23/01/14
Member 1:	**(Dr. D. B. Naik)**		Date: 23/01/14
Member 2:	**(Dr. Manmohan Kumar)**		Date: 23/01/14

Final approval and acceptance of this dissertation is contingent upon the candidate's submission of the final copies of the dissertation to HBNI.

CERTIFICATE

I hereby certify that I have read this dissertation prepared under my direction. All the suggestions made by the referees in his evaluation report have been incorporated and the referee has approved these changes. Therefore, I recommend that this dissertation may be accepted as fulfilling the requirement for the Degree of Doctor of Philosophy.

Date: 23/01/2014 **Dr. S. Sabhrawal**

Place: Mumbai **(Guide)**

STATEMENT BY AUTHOR

This dissertation has been submitted in partial fulfillment of requirements for an advanced degree at Homi Bhabha National Institute (HBNI) and is deposited in the Library to be made available to borrowers under rules of the HBNI.

Brief quotations from this dissertation are allowable without special permission, provided that accurate acknowledgement of source is made. Requests for permission for extended quotation from or reproduction of this manuscript in whole or in part may be granted by the Competent Authority of HBNI when in his or her judgment the proposed use of the material is in the interests of scholarship. In all other instances, however, permission must be obtained from the author.

Date: 23/01/2014 **Narender Kumar Goel**

Place: Mumbai

DECLARATION

I, hereby declare that the investigation presented in the thesis has been carried out by me. The work is original and has not been submitted earlier as a whole or in part for a degree/diploma at this or any other Institution / University.

Date: 23/01/2014 **Narender Kumar Goel**

Place: Mumbai

Dedicated to my Grandparents

ACKNOWLEDGEMENTS

From the depth of my heart I express my deep sincere gratitude to the Almighty for the Blessings They had bestowed upon me to do this work.

My heart-felt gratitude I owe to my mentor and my guide Dr. S. Sabharwal, Professor, HBNI & Ex. Head, Radiation Technology Development Division, who has always stood with me and for me throughout my work-cheerfully encouraging, supporting, helping. His insatiable hunger for quality work has ever kept me on my toes and inspires me to produce something up to his expectations for me. I would also express my deepest sense of gratitude to the former Chairman Dr. T. Mukherji, Chairman Dr. B. N. Jagtap, members Dr. D. B. Naik and Dr. Manmohan Kumar of my doctoral committee for their insightful comments and encouragement during the long sessions of my reviews meeting.

It is with immense gratitude that I acknowledge help of my Division Head, Dr. L. Varshney for helping in writing the thesis work with the continuous suggestions and encouragement. It will be not be possible to wind up the thesis without expressing my deepest sense of gratitude to Dr. Y. K. Bhardwaj and Dr. Virendra Kumar for helping me to start my career in scientific world and without whose help, guidance and patience, the thesis wouldn't have been successful.

I also record my appreciation to the all senior researchers and fellow researchers of my division particularly Dr. K. A. Dubey, Mr Sanju Francis, Mr. C. V. Chaudhari, Mr. B. R. Dhanawade, Mr. Nilanjal who were always ready for scientific and personal help through the period. I do thank all non-scientific staff Mr. S. Shejwal, Mrs, Sneha, Mr. M. N. Kadu, and Mr. Y.G. Hilati from my lab to help me during the research. I also pay my deepest gratitude to Mrs Shobita, Mr Sachin, Dr. Ajay Singh for helping me in evaluating and characterizing the samples.

Finally, I take this opportunity to dedicate the work to my grandparents who always taught me the value of education. There is no need for formal word of thanks for my entire family for their love and continuous support – both spiritually and materially and who have stood beside me through every thick and thin, indeed. I shall be failing in my duty if I did not recall the perennial sources of my inspiration and support from my beloved wife Soniya. I have no words for my lovely son Nutan Kumar for his contribution in refreshing me with lot of funny and childish questions at home. I would like to thank almighty for blessing me with twin daughters Jahnavi and Tanvi and with their captivated arrival, I am going to complete my thesis.

Finally, I thank all those who have helped me directly or indirectly in the successful completion of my thesis. Anyone missed in this acknowledgement are also thanked.

I. SYNOPSIS

A polymer is a large molecule (macromolecule) composed of repeating structure units that are typically connected by covalent chemical bonds. It encompasses a large class comprising both natural and synthetic materials with a wide variety of properties. The extraordinary ranges of properties of polymeric materials have made them an essential and ubiquitous material in everyday life [1, 2]. Synthetic and semi-synthetic polymers today provide both necessities and amenities of our life. Among naturally occurring polymers are proteins, starches, cellulose, and latex. Synthetic polymers, Low Density Polyethylene (LDPE), High Density Polyethylene (HDPE), Polypropylene(PP), Polyvinyl Chloride(PVC), Polystyrene(PS), Nylon, nylon 6, nylon 6,6, Teflon(Polytetrafluoroethylene) thermoplastic polyurethanes(TPU) etc, are produced commercially on a very large scale and have a wide range of properties and uses. One trend in modern civilization is to design and produce new materials to meet the growing needs of new technologies such as cleaner energy resources, better health care and green separation process [3]. It is essential to modify the properties of a polymer according to tailor-made specifications designed for target applications. There are several means to modify polymers properties, viz. blending, grafting, and curing. A variety of techniques are available for synthesis and modification of polymeric materials [4]. Over the past several decades, ionizing radiations have emerged as reliable tools for synthesis, processing and modification of polymers for a number of industrial applications. The radiation sources in form of rugged industrial electron beam (EB) machines and high intensity gamma sources have made it possible that the fruits of radiation chemical research are converted into useful industrial products such as polymers designed for

electric and electronic industries, crosslinked wires and cables, heat shrinkable materials, polyethylene foams and surface coatings. The industrial uses of radiation-processed polymers have lead to the development of a new discipline of radiation polymer chemistry [5, 6]

Recent progress in polymer science is unveiling the mystery of marvelous functions of polymer molecules and a new exciting area of '*gel*' technology has now emerged [7]. A lot of interest has been evinced specially in a new class of materials that are termed as *"Hydrogels"*. Hydrogels form a specific class of polymeric biomaterials. hydrogels are defined as two- or multicomponent systems consisting of a three-dimensional network of polymer chains and water that fills the space between macromolecules. Hydrogels are three-dimensional network structures of polymer chains, which swell in aqueous environments without dissolving or losing their structural integrity [8]. The network is often formed by covalently cross-linked polymers, but ionic bonds, crystalline regions, entanglements and Van-der Waals forces can also lead to water swellable network materials. The water-imbibing properties of hydrogels enable them to be employed for several pharmaceutical applications, sensors, separation membranes and adsorbents. Depending on the properties of the polymer (polymers) used, as well as on the nature and density of the network joints, such structures in an equilibrium can contain various amounts of water; typically in the swollen state the mass fraction of water in a hydrogel is much higher than the mass fraction of polymer. Although hydrogels have a number of non-biomedical applications (e.g. in agriculture), it seems that their use in the field of medicine and pharmacy is the most successful and promising [9-11]. The research in this field has resulted in the common

use of hydrogels as soft contact lenses, wound dressings, drug-delivery systems and superabsorbent with a number of products being commercially available.

Cotton fabrics have wide acceptability as clothing material because of their natural abundance and inherent properties like good folding endurance, breathability, moisture absorbency, comfort, durability, easy care, and bio-degradability [12]. However, one of the main drawbacks with the cotton is that it is amenable to bacterial and fungal growth under moist conditions, which leads to mildew, causes bad smell and decreases the life of cloth. Therefore, there exists a keen interest in developing antibacterial fibers and fabrics for various applications such as clothing for hospital workers, hospital beddings, sports clothing, underwear, ladies tights, shoe linings, armbands, sleeping bags and toys for children [13]. Polycationic antimicrobial agents, especially quaternary ammonium and phoshphonium salts containing polymers have been reported to be excellent antimicrobial agents [14].

Synthetic dyes represent a relatively large group of organic chemicals, encountered practically in all spheres of daily life. Various kinds of synthetic dyestuffs appear in the effluents of industries, such as textile, leather, paper printing and plastic industry [15]. Release of these dyes in water stream is not only aesthetically undesirable but also has a serious environmental impact. The intense color reduces the sunlight transmission into water hence affecting photosynthesis phenomenon causing adverse effect on the growth of bacteria and fungi, aquatic plants and other form of aquatic life, which ultimately disturb aquatic ecosystem and food chain. Increased public concern, ecological awareness, as well as strict regulation enforcement by concerned authorities regarding effluent quality have forced industry to pre-treat effluents before discharging and to look

for other economically viable ways to treat the effluents. It is now established that only few dyes can be microbiologically degraded under anaerobic condition, which in most cases leads to the generation of carcinogenic compounds [16] and mutagens [17]. The adsorption process has been found to be comparatively simple, effective and efficient techniques for dye removal from wastewater. Many adsorbents such as activated carbon, peat, chitin, coir pith, banana and orange peel, silica, etc. have been tried for the purpose [18].

Quaternary ammonium compounds (QACs) are frequently used as antibacterial agents that disrupt cell membranes through binding of ammonium cation to anionic sites in the outer layer tissues of bacteria. These compounds are non-toxic at low concentrations and arestable for long periods without losing their antimicrobial activity. In recent years, the derivatives in which QACs are attached to the functional groups that can be readily polymerized have become commercially available. It is therefore of importance to stdy the polymerization characteristics as well as their binding or grafting behavior onto other substrates and to evaluate the resulting end products for their antibacterial behavoiur. Radiation induced grafting is one of the promising synthesis strategies in the development of new materials for a cvariety of applications. The present study is aimed at investigating the polymerization and grafting behavior of derivatices of QACs, characterization of the resulting end products and evaluating them for the desired characteristics. The results of the work done are reported in the following six chapters.

Brief chapter wise work in thesis is explained below:

Chapter: 1 Fundamental aspects of radiation chemistry, polymers and radiation induced grafting

The chapter introduces fundamental aspects related to polymers and radiation technology. These include an understanding of the basic principles of interaction of radiation with matter as well as macro effects of radiation on the monomer and the polymeric substrates. Different processes for energy loss by electromagnetic radiation and charged particles when they pass through different media. The radiation chemistry of aqueous solution is discussed in details starting from typical time scales of different events, which finally leads to formation of primary (1^o) as well as secondary (2^o) radicals. Basic properties of both 1^o and 2^o radicals have been summarized. The chapter also briefly introduces the subject of grafting, different methods of radiation induced grafting and advantages of radiation graft co-polymerization method over conventional methods. The chapter also introduces various types of gels along with historical development of the subject. In the last little description is given about the Quaternary ammonium based germicides with its probable mode of action on germs.

Chapter: 2 Experimental Methodology and techniques for characterization of Polymers

During the course of this study, a variety of methods has been used to modify and synthesis of polymeric materials and characterize the end products with various characterization techniques. These include steady-state irradiation facilities like ^{60}Co gamma radiation chamber for irradiation and characterization techniques like Scanning Electron Microscopy (SEM), Fourier Transform Infrared spectroscopy (FTIR), Elemental

Analysis (EA), Thermogravimetric analysis (TGA), UV-visible spectroscopy for the characterization of radiation induced synthesized and modified polymer materials. The chapter details the principle and methodologies used in these studies. Some of the principles regarding the swelling of hydrogel have also been explained to provide a view of the experimental and theoretical aspects of the process. At the end of the chapter qualitative and quantitative methods of determining the antibacterial efficacy of poly-QACs and poly-QACs grafted cotton have been elaborated.

Chapter: 3 Radiation induced Synthesis 2-Hydroxy- ethylmethacrylate-co-[2-(Methacryloyloxy)ethyl]Trimethylamm -onium Chloride Hydrogels & swelling response under various-*In Vitro* Conditions

---

High-energy ^{60}Co gamma radiation has been used to synthesize 2-hydroxyethylmethacrylate-co-[2- (methacryloyloxy)ethyl]trimethylammonium chloride (HEMA-co-MAETC) polyelectrolyte hydrogels. HEMA-co-MAETC co-polymer gels formed were characterized and investigated for swelling behaviour in different swelling conditions. Fourier transformed infrared spectroscopy (FT-IR) and scanning electron microscopy (SEM) techniques were used to characterize the co-polymer gels. Swelling extent of the gels was found to be a linear function of MAETC content in the gels. The effect of ionic strength, temperature, pH, some solutes of biological importance like glucose, urea, and surfactants such as Triton-X and deoxycholic acid on swelling behavior have been investigated. The swelling of gels at higher temperature enhanced the swelling rates but not the swelling extent. HEMA-co-MAETC hydrogel exhibited an excellent responsive characteristic to the ionic strength of the swelling medium. The results showed that the swelling of the co-polymer gel at 60◦C reduced the swelling–

deswelling cycle time by approx. 30% without altering the swelling extent. The gels were also investigated for their swelling in aqueous solutions of anionic dyes, Acid Blue 25 (AB25), Acid Blue (AB74) and Acid Yellow 99 (AY99), and were found to be suitable for dye uptake applications. The details of these studies have been presented in this chapter.

Chapter 4: Synthesis of antibacterial cotton fabric by radiation-induced grafting of [2-(Methacryloyloxy)ethyl] trimethyl amm- onium chloride (MAETC) onto cotton

As discussed earlier, there is a keen interest in modifying the properties of cotton fabrics specially to impart antifungal and antibacterial properties into them for specific applications. The antibacterial property can be introduced into the fiber, either at the manufacturing step itself by incorporating antibacterial chemicals or by coating the finished product with antibacterial compounds [19]. However, such products have the limitation of leaching of physically trapped antibacterial compounds leading to induced toxicity and decreased antibacterial efficacy of the substrate. Immobilization of antimicrobial agents through covalent bonding can be a solution of this problem. In the present work, radiation grafting of MAETC, a quaternary ammonium monomer with amphiphilc character, onto finished cotton has been carried out in order to impart antibacterial property. Radiation grafting has been carried out in aqueous medium by mutual grafting method and effect of various experimental variables like total dose, dose rate, monomer concentration, ambiance, effect solvents and homopolymer inhibitor on the grafting extent has been investigated. Mutual radiation grafting has the disadvantage of homopolymer formation during grafting reaction, which leads to unproductive use of

monomer and necessitates removal of physically adsorbed homo-polymers on the grafted copolymer. Addition of certain inorganic salts has been reported to suppress the production of undesirable homopolymer during radiation induced grafting. Various metal salts viz. Fe^{2+}, Cu^{2+}, Ce^{4+} were used to study their efficacy in inhibition of homo-polymerization. The grafted product has been characterized with various techniques like FTIR, elemental analysis, SEM, water uptake etc. Grafted samples were also investigated for their antibacterial efficacy. The qualitative test for antibacterial activity of radiation synthesized PMAETC in nutrient broth indicated it to be bactericidal as there was no significant increase in turbidity and number of colonies formed on solid media reduced with time. The minimum bactericidal concentration (MBC) of the polymer ranged from 0.025% to 0.075% depending on the organism used. The lowest MBC was found to be for *S. aureus*, followed by *E. coli*, *B. cereus* and *P. fluorescens*. Maximum activity was found against *S. aureus*, as there was approximately 5-log cycle kill in 24 h. In case of *B. cereus* and E. coli, up to 4-log cycle was observed with 19% grafting followed by P. fluorescens where only 3-log cycle kill was observed. The details of these investigations are presented and discussed in this chapter.

Chapter 5: Radiation induced synthesis of antibacterial cotton fabric by grafting of [2- (Acryloyloxyethyl)]trimethyl- ammonium chloride and co-grafting of 2-Hydroxyethyl methacrylate onto cotton fibrils

This chapters deals with the study of covalently binding of quaternary ammonium based agent [2-(Acryloyloxyethyl)]trimethylammonium chloride (AETC) through gamma irradiation on the surface of cotton to impart antibacterial activities. AETC has side chain (hydrophobic part) which is different from MAETC and as positive charge and hydrophobic nature of the antibacterial reagent are important factors of cationic

disinfectants [20]. Quaternary ammonium compounds have a broad spectrum of antimicrobial activity against both gram-positive and gram-negative bacteria [21]. As compared with small molecule antimicrobial agents, polymeric antimicrobials have advantages in terms of being nonvolatile, chemically stable, long-term antimicrobial activity, and hard to permeate through the skin [22-24]. Mutual radiation induced grafting method was used as it is well established that grafting is an ideal and efficient technique for attaching polymer chains containing desired chemical groups via covalent bonding to existing polymeric backbones. The results showed that due high reactivity of AETC monomer in aqueous solution; homo-polymerization was predominant over graft copolymerization. Hence 2-Hydroxyethyl methacrylate (2-HEMA) monomer was used as AETC grafting facilitator. Grafting of only AETC was also studied in various solvents like water, DMF, alcohols and their mixture to enhance the graft co-polymerization. The effect of various other experimental variables like dose, dose rate, monomer concentration as function of AETC and HEMA, ambiance, solvents, additives like salts as an homopolymer inhibitor and acid on grafting extent was studied. Grafting extent increased with dose and monomer concentration whereas high dose rate, presence of O_2 and salts suppressed grafting. The grafting was also observed to be a function of the ratio of the monomers in the feed solution. The grafted samples have been characterized for water-uptake, surface morphology and thermal stability. AETC-grafted and AETC-HEMA co-grafted cotton samples were tested for their antibacterial efficacy against various bacteria and were found to possess significant antibacterial activity particularly against gram positive bacteria like S. aureus and B. cereus. The presence of HEMA in the grafting mixture though increased the grafting extent but decreased the antibacterial

activity of the grafted matrix. The details of these studies have been presented in this chapter.

Chapter: 6 Functionalization of textile adsorbent from textile cotton cellulose waste via radiation grafting process for acid dye removal: Equilibrium and kinetic adsorption studies

---

A large amount of cellulose based waste by-products are generated from agriculture and the cotton based industries has no salability and creates environmental pollution. India alone consumes cotton fibers approximately 26 million tons per year, of which approximately 0.21 million tons of cotton waste is generated during yarn manufacture [25]. The utilization of textile cotton waste for the production of functional adsorbent for treatment of textile dye effluent offers an attractive waste processing method. The objective of the present work is to develop an efficient functionalized adsorbent from a textile cotton waste and to examine the possibility of its use for the treatment of another textile industrial waste, i.e., dye effluent. In present work, experimental conditions have been optimized to produce the cotton cellulose based cationic adsorbent by radiation induced grafting of polyvinylbenzyltrimethylammoinum chloride (PVBT). The adsorbent was further studied for the adsorption of three acid dyes, AB25, AY99 and AB74. PVBT-g-Cellulose exhibited equilibrium adsorption capacities of ~540 mg/g, ~474 mg/g and ~122 mg/g for AB25, AY99 and AB74, respectively. Based on coefficient of determination (r^2) values, the degree of agreement between adsorption isotherm models and experimental equilibrium adsorption data followed the order: Langmuir-Freundlich>Redlich-Peterson>Langmuir>Freundlich. Higher value of r^2 (>0.99) and better agreement between the $q_{e,cal}$ and $q_{e,exp}$ values suggested that the

pseudo-second order model better represents the kinetic adsorption data. The adsorption rate of AB74 was found to be an order faster than that of AB25 and AY99. The multi-linearities in the intra-particle kinetic plots suggested the involvement of different processes in the adsorption kinetics of acid dyes. The elution extent of ~95%, ~70% and~20% could be achieved for AB25, AY99 and AB74, respectively, using optimized eluent composition. This chapter will discuss the optimization studies carried out to produce the functional adsorbent and its subsequent performance for removing textile dyes from aqueous solution.

Summary

This thesis contains results from the research work towards radiation polymerization and/ or radiation induced grafting behavior of derivatives of QACs and their evaluation for health care and environmental applications. In this work, efforts have been made to acquire new insights in obtaining the well characterized grafted and / or copolymerized QACs through radiation technology. The results have been interpreted in terms of their antibacterial and dye uptake studies for healthcare and environmental applications.

References

[1] P. C. Painter, M. M. Coleman, Fundamentals of polymer science: an introductory text. Lancaster, Pa.: Technomic Pub. Co.p.1. ISBN 1-56676-559-5 (1997)

[2] N. G. McCrum, C. P. Buckley, C. B. Bucknall, Principles of polymer engineering. Oxford; New York: Oxford University Press. p.1. ISBN 0-19-856526-7 (1997)

[3] C. A. M. Afonso, J. G. Crespo Green Separation Processes: Fundamentals and Applications. John Wiley & Sons, New York. (2006)

[4] A. Bhattacharyaa, B. N. Misra, Prog. Polym. Sci. 29, 767 (2004)

[5] K. Makuuchi, S. Cheng, Radiation Processing of Polymer Materials and Its Industrial Applications. John Wiley and Sons, New York. (2011)

[6] G. C. Andrzej, H. S. Mohammad, A. Shamshad. Nucl. Instrum. Meth. B. 236 (1–4), 44 (2005)

[7] T. Tanaka, Gles. Sci. Am. 244, 110 (1981)

[8] M. Tokita, M. J. Tanaka. J. Chem. Phys. 95, 4613 (1991)

[9] H. Singh, P. Vasudevan, A. R. Ray, J. Scient. Ind. Res., 39, 162 (1980)

[10] I. Kaetsu, Radiat. Phys. Chem., 18, 343 (1981)

[11] N. A. Peppas, Hydrogels in Medicine and Pharmacy; CRC Press, Boca Raton (1986)

[12] V. R. Gowariker, N.V. Viswanathan, J. Sreedhar, Individual polymers. In: Polymer Science. Wiley Eastern Limited, New Delhi, 215–262 (1993)

[13] G. Reyerouck, W. B. Hugo, A. D. Russel, Evaluation of antibacterial and antifungal efficiency: Principles and practice of disinfection, preservation and sterilization Blackwell Scientific Publications, Oxford, 124-148 (1992)

[14] C. Kuo-Yu, L. Yu-Sheng, , Y. Chun-Hsu, L. Ming-Hsien, L. Jui-Che, J. Biomater. Sci., Polym. Ed. 21(4), 429 (2010)

[15] H. Zollinger, Color Chemistry-Synthesis, Properties and Application of Organic Dyes and Pigments, VCH Publishers, New York (1987)

[16] C. A. Fewson, Trends Biotechnol. 6, 148 (1988)

[17] K. T. Chung, C.E. Cerniglia, Mutat. Res. 277, 201 (1992)

[18] V. Kumar, N. K. Goel, Y. K. Bhardwaj, S. Sabharwal, Sep. Sci. Technol. 47, 1937 (2012)

[19] B. Gottenbos, H. C. Van der Mei, F. Klatter, P. Nieqwenhuis, H. J. Busscher, Biomaterials. 23, 1417 (2002)

[20] T. Tashiro, Macromol. Mat. Eng., 286, 63 (2001)

[21] N. Kawabata, M. Nishiguchi, Appl. Environ. Microbiol. 54, 253 2(1988)

[22] E.-R. Kenawy, J. Appl. Polym. Sci. 82, 1364–1374(2001)

[23] I. Cakmak, Z. Ulukanli, M. K Tuzcu, S. K. Genctav, Eur. Polym. J. 40, 2373 (2004)

[24] J.-H. Jeong, Y.-S. Byoun,, Y.-S. Lee, React. Funct. Polym. 50, 257 (2002)

[25] C. Sundar Raj, S. Arul, S. Sendilvelan, C. G Saravanan, The Open Waste Manage J. 2, 1 (2009)

S. No.	Table Caption	P. No.
Table 1.1	Spur Reactions in Water	15
Table 1.2	Properties of e_{aq}^-	17
Table 1.3	Properties of $H^\bullet$ atom	17
Table 1.4	Properties of $^\bullet OH$ radical	18
Table 2.1	IR Absorptions for Representative Functional Groups used in the study	45
Table 3.1	Composition and EDS of HEMA-co-MAETC gels synthesized at a dose rate of 5.0 $kGyh^{-1}$ for total dose of 3.75 kGy in water and NaCl solution	63
Table 3.2	Dynamic swelling parameters of different HEMA-co-MAETC gels in distilled water at different temperatures	69
Table 3.3	Diffusion coefficients of water into different HEMA-co-MAETC gels at different temperatures and activation energy of diffusion	70
Table 3.4	Dynamic swelling parameters of HEMA-co-MAETC gels in NaCl solution at 28^oC	74
Table 3.5	Dynamic swelling parameters of different HEMA-co-MAETC gels in solution of various solutes at 28^oC	77
Table 4.1	Elemental analysis of grafted samples	93

International Journals

1. **N. K. Goel**, V. Kumar, Y. K. Bhardwaj, J. Biswal, C. V. Chaudhari, K. A. Dubey, S. Sabharwal (2009). Swelling response of radiation synthesized 2-Hydroxyethylmethacrylate-co-[2-(Methacryloyloxy)ethyl] trimethylammonium chloride hydrogels under various in-vitro conditions. J. Biomat. Science: Polymer Edition. 20(5-6), 785-805
2. **N. K. Goel** , M. S. Rao, V. Kumar, Y. K. Bhardwaj , C. V. Chaudhari, K. A. Dubey, S. Sabharwal (2009). Synthesis of antibacterial cotton fabric by radiation-induced grafting of [2-(Methacryloyloxy)ethyl]trimethylammonium chloride (MAETC) onto cotton. Radiat. Phys. Chem. 78 (6), 399-406
3. **N. K. Goel**, V. Kumar, M. S. Rao, Y. K. Bhardwaj, S. Sabharwal (2011). Functionalization of cotton fabrics by radiation induced grafting of quaternary salt to impart antibacterial property, Radiat. Phys. Chem. 80(11), 1233–1241
4. V. Kumar, **N. K. Goel**, Y. K. Bhardwaj, S. Sabharwal (2012). Development of functional adsorbent from textile cotton waste by radiation induced grafting process: Equilibrium and kinetic studies of acid dye adsorption. Sep. Sci. Technol. 47, 1937-1947

Conference papers/ BARC news letter (Poster)

1. **N. K. Goel,** V. Kumar, Y. K. Bhardwaj, S. Sabharwal. Radiation synthesized stimuli-responsive HEMA-co-MAETC hydrogel, BARC NEWS letter Founder's day: Special issue October 2011, Paper No. 68 pp.310-312

2. **N. K. Goel,** V. Kumar, Y. K. Bhardwaj, S. Sabharwal, Radiation synthesized stimuli-responsive HEMA-co-MAETC hydrogels, RC-05, APSRC-TSRP-2010, Sept 14-17, 2010, Lonavala, India.
3. **N. K. Goel,** V. Kumar Y. K. Bhardwaj, S. Sabharwal, Radiation grafted PMAETC-g-cellulose adsorbent for waste water treatment: Equilibrium and kinetic dye adsorption, NIC-2010, Dec. 13-15, PM-18, 358-362, 2010, Mumbai, India
4. **N. K. Goel,** S. R. Kannat, Y. K. Bhardwaj, V. Kumar, S. Sabharwal, Radiation induced grafting of QAS monomer AETC in presence of HEMA on to cotton fibrils and its effect on antibacterial activity. **"**2nd DAE-BRNS international symposium on materials chemistry. 2-6 December, 2008, , BARC, Mumbai, India
5. **N. K. Goel,** V. Kumar, Y. K. Bhardwaj, K. A. Dubey, C. V. Chaudhari, S. Sabharwal. Antibacterial cotton fabric prepared by radiation grafting technique. "An international conference on Frontiers of Radiation and Photochemistry" 8-11 February 2007, Mahatma Gandhi University, Kottayam, Kerala, India
6. **N. K. Goel,** V. Kumar, Y. K. Bhardwaj, S. Sabharwal, Radiation induced co-grafting of Acryloyloxyethyltrimethylammmonium chloride (AETC) and 2-Hydroxyethylmethacrylate (HEMA) onto cotton threads: optimization and characterization. "Trombay symposium on Radiation and Photochemistry" (TSRP-2008), 7-11 January 2008, YASHADA, Pune, India
7. V. Kumar, **N. K. Goel**, S. Pahan, Y. K. Bhardwaj, S. Sabharwal, Synthesis of Adsorbents from Polymer Waste Using Radiation Induced Grafting Process: Equilibrium and Kinetic Adsorption of Dyes, NIC-2010, Dec. 13-15, PM-18, 385-389, 2010, Mumbai, India

8. V. Kumar**, N. K. Goel**, Y.K. Bhardwaj, S. Sabharwal, Cationized cellulose synthesized by radiation grafting for removal of acid dyes fom aqueous solutions-Equilibrium and kinetic studies, RC-62, APSRC-TSRP-2010, Sept 14-17, 2010, Lonavala, India.

Presentation

9. **N. K. Goel,** V. Kumar, V. S. Thakur, Y. K. Bhardwaj, H. D. Sharma, S. Sabharwal, Radiation induced polymerization to make cationized cotton fibrils for its antibacterial and faster wound healing applications, RPP-2(15), PSE-2010, 26-27 Nov.2010, Chandigarh, India.
10. **N. K. Goel,** V. Kumar, V. S. Thakur, Y. K. Bhardwaj, H. D. Sharma, S. Sabharwal, Radiation induced polymerization to make cationized cotton fibrils for its antibacterial and animal testing for faster wound healing applications " NIC-2010, Dec. 13-15, 2010, Mumbai, India
11. **N. K. Goel**, M. S. R. Rao, Y. K. Bhardwaj, S. Sabharwal, Radiation induced synthesis of Polyquats for their application in biomedical science**,** Polymer congress APA-2009 on Polymer Science and Technology: Vision & Scenario. Dec. 17-20, 2009 New Delhi, India

Best Poster Award

1. **N. K. Goel,** V. Kumar, Y. K. Bhardwaj, S. Sabharwal, Radiation synthesized stimuli-responsive HEMA-co-MAETC hydrogels, RC-05, APSRC-TSRP-2010, Sept 14-17, 2010, Lonavala, India.
2. **N. K. Goel,** V. Kumar, Y. K. Bhardwaj, and S. Sabharwal. Radiation induced co-grafting of Acryloyloxyethyltrimethylammmonium chloride (AETC) and 2-

Hydroxyethylmethacrylate (HEMA) onto cotton threads: optimization and characterization. "Trombay symposium on Radiation and Photochemistry" (TSRP-2008), 7-11 January 2008, YASHADA, Pune, India

3. **N. K. Goel,** V. Kumar, Y. K. Bhardwaj, K. A. Dubey, C. V. Chaudhari, S. Sabharwal, Antibacterial cotton fabric prepared by radiation grafting technique. "An international conference on Frontiers of Radiation and Photochemistry" 8-11 February 2007, Mahatma Gandhi University, Kottayam, Kerala, India

Chapter 1

Fundamental aspects of radiation chemistry, polymers and radiation induced grafting

Keywords: Polymer, Grafting, Hydrogel, Polyelectrolytes, Quaternary ammonium monomer

1.1 Introduction

Polymer surfaces can be modified to achieve a variety of goals, including increasing adhesion, improving wettability and biocompatibilty, reducing friction, reducing susceptibility to harsh chemicals or environmental agents, bio-functional surfaces in tissue engineering and antibacterial surfaces. Polymer surfaces may also be modified by functionalization with various chelating groups for their application in the treatment of waste water like toxic metals and dyes from textile effluents to address the serious environmental pollution problem [1, 2]. Surface-modified polymers are of substantial importance in many diverse aspects of modern technology, and whilst there are a number of existing physical and chemical methods like UV, plasma, conventional chemical methods, enzymatic [3] and most recently laser surface modification for surface modification of polymers, the frequent requirement for significant infrastructure, harsh reaction conditions and limitation to specific polymer types led to explore high energy radiation (gamma-ray, electrons beams etc.) based technology known for convenience, high efficiency, high purity, easy and environmental friendly process for such modifications. It started back in 1950s and continued to be a subject of intensive research for obtaining modified materials for various applications based on the wide range of properties available when different polymer chains are connected to form hybrid branched polymers. These surface modifies surfaces have many applications like

antibacterial properties [4], odor absorbent fabrics, ion exchange separation of metal ions, dyes, pesticides, purification of proteins, immobilization of enzymes, extraction of uranium from sea water, recovery of precious/rare earth metals, desalination of seawater, toxic gases [5] and compatibilization in heterogeneous composites. Some of the pioneer progress in the area of radiation induced surface grafting of polymers are elaborated below.

Extensive investigations of adsorbents capable of recovering uranium from seawater which has about 4.5 billion tons of uranium in seawater and aqueous systems have been carried out during the last two decades especially in Takasaki Radiation Chemistry Research Establishment. By using the radiation grafting method, the group from Japan Atomic Energy Research Institute designed a fabric absorbent based to extract uranium from seawater in 2002 [6]. They prepared a polymeric absorbent in a nonwoven fabric by radiation induced grafting of acrylonitrile and subsequently converted to amidoxime group that was capable of forming a complex with uranyl tricarbonate ions. In their marine experiments, the group already has collected one kg of uranium yellow cake. Efforts are being made to decrease the cost and increase the efficiency of uranium uptake by incorporating two amidoxime per monomer unit to increase the capacity of the adsorbent for uranium uptake [7]. Smart polymers, especially PNIPAAM have been grafted by radiation induced polymerization to explore to have smart surfaces for the various applications in the field of tissue engineering by various groups. Okano and Yamato and co-workers have been pioneer in the area of smart polymers cell cultures. This group grafted PNIPAAM, which behave like hydrophobic above 37^{o}C and hydrophilic below 37^{o}C, by radiation induced grafting method. This dual

behavior of the grafted film was applied for the cell culture to avoid the cell adhesion without damaging it [8].

Radiation grafting has also been used to combine the proton-conducting properties of a graft component, hydrophilic polystyrenesulfonate, with the thermal and chemical stability of the partial and fully fluorinated polymer base films together in membranes suitable for the application in Polymer Electrolyte Membrane Fuel Cells (PEMFC) [9]. Considerable work has been recently devoted to develop new cation exchange membranes by radiation-induced graft copolymerization of styrene onto various fluorinated and partially fluorinated polymer films such as PTFE, FEP, PVDF, and ETFE requirements include high ionic conductivity, defined swelling behavior, high chemical resistance, and mechanical integrity and thermal stability [10].

During the last two decades continuous efforts have been made to develop polymers with antimicrobial properties. Positive charge and hydrophobic nature of the antibacterial reagent are important factors of cationic disinfectants [11]. Quaternary ammonium compounds (QACs) have been widely used in water treatment, textiles and food industries because of their low toxicity and broad antibacterial spectrum [12]. In the present thesis surface modification of cottons by covalently attaching QACs has been investigated with high energy gamma radiation technology to smart surfaces with antibacterial properties. These smart surfaces are aimed for adding the antibacterial properties for number of possible applications in the field of healthcare like antibacterial bandages for faster wound healing and antibacterial clothes for undergarments, shoe lining, hospitals and sportswear etc. To add these QACs, radiation induced grafting method was adopted which is further explained in later section of this chapter. Grafted samples, having quaternary ammonium group a strong anion exchanger, have also been

investigated for the treatment of textile effluents containing toxic acid dyes to address the serious problem of environmental pollution.

1.2 Basic aspects of radiation chemistry

Radiation chemistry deals with the study of chemical changes induced by high-energy electromagnetic radiation (γ-rays, X-rays), charged particles (electrons, protons, deuterons, α-particles) or uncharged particle (neutron), termed as "ionizing radiation", with energy in the range of 10^2 to 10^7eV.

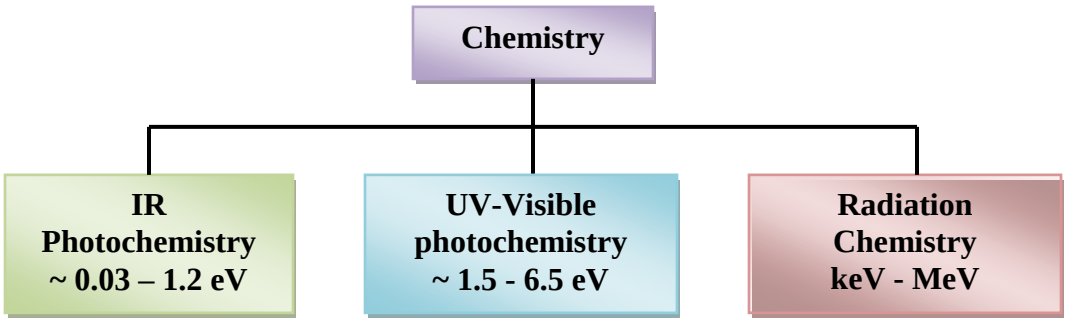

Figure 1.1: Energy ranges for electromagnetic radi*a*tion

Interaction of ionizing radiation with atoms and molecules in their path is non-specific and thus non-selective in nature. It can cause ionization and excitation of varied types of molecules and atoms in many possible ways resulting in the formation of a variety of reactive species. Interaction of high energy ionizing radiation are non-selective process because of much higher energy which is much higher than the chemical bond in organic compounds, unlike in photochemistry where one can selectively excite, ionize or break a particular bond in a given molecule by choosing the energy of a photon (figure 1.1).

A thorough knowledge of the processes by which high-energy radiation interacts with matter is a pre-requisite for understanding the radiation chemical effects, as it is the absorbed energy, which results in the observed chemical changes in the substrate. The

extent and process of energy absorption depends upon the nature of radiation and properties of the material. The important parameters on which the interaction will depend are energy, mass and charge of the radiation, and atomic number or electron density of the material [13]. Mechanisms of interaction of (i) electromagnetic radiation (ii) electrons (iii) heavy charged particles and (iv) neutrons, which are of relevance in radiation chemistry, are explained in brief in the following sections.

1.2.1 Interaction of electromagnetic radiation

Electromagnetic radiations of wavelength less than 100 A° belong to the class of ionizing radiation. They are usually called X-rays (extra nuclear origin) or γ rays (produced from the atomic nuclei). The gamma rays emitted by radioactive isotopes are mono-energetic, possessing one or more discrete energies, for example ^{60}Co emits γ-photons of energy 1.332MeV and 1.173MeV. For a narrow beam, the intensity of gamma radiation transmitted through an absorber is given by

$$I = I_o\, e^{-\mu x} \qquad (1.1)$$

Where, I_o is the incident radiation intensity, x is the thickness of material through which radiation has traversed and μ is the linear attenuation coefficient, which is the sum of a number of partial coefficients representing different processes occurring inside the absorber. These are (i) Photoelectric effect, (ii) Compton scattering, (iii) Pair production (iv)coherent scattering and (v) photonuclear reactions. The relative importance of each process depends on the photon energy and the atomic number of the absorbing material. Coherent scattering is of importance for low energy photons (<0.1MeV), photonuclear reactions are possible with photons of energies in the range of 2 to 8MeV for low Z

materials and in the region of 7-20MeV for high Z materials. Thus, for gamma radiation emitted by ^{60}Co source, only the first three interaction processes are of importance and are discussed below briefly.

(i) Photoelectric effect: This process is the principal interaction process at low photon energies. In photoelectric process photon interacts with a bound electron in an atom and transfers all its energy to eject it from the atom (figure. 1.2).

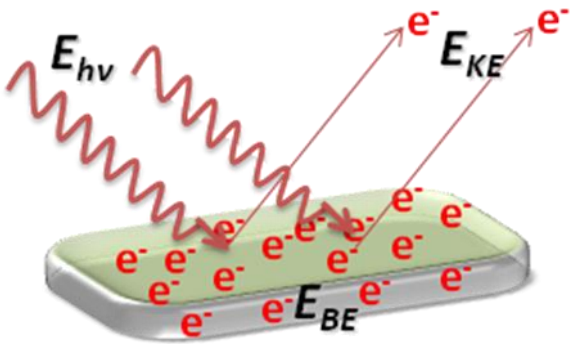

Figure 1.2: Photoelectric Effect

The kinetic energy of the ejected electron (E_{KE}) is equal to the difference between the energy of the incident photon (E_{hv}) and the binding energy of the electron (E_{BE}) as given by equation 1.2.

$$E_{KE} = E_{hv} - E_{BE} \quad (1.2)$$

(ii) Compton scattering: Compton scattering is an inelastic scattering, which occurs when a photon with energy E_o interacts with a loosely bound or free electron (as shown in figure 1.3). The resulting photon is deflected with reduced energy E' at an angle θ to the direction of the incident photon and the electron gets accelerated at an angle ϕ with recoil energy E_e. The relation between the various parameters is given by equation (1.3). The energy of recoil electron is given by the equation (1.4).

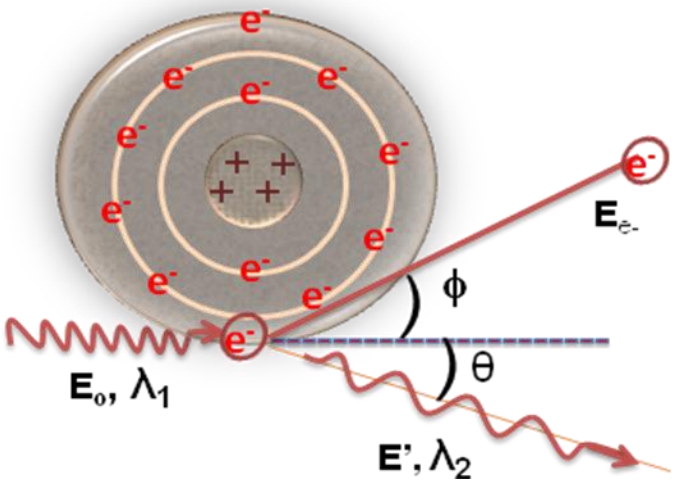

Figure 1.3: Compton Scattering

$$E' = \frac{E_0}{1+\left(E_0/m_e c^2\right)(1-\cos\theta)} \tag{1.3}$$

$$E' = E_0 - E_{e^-} \tag{1.4}$$

Compton scattering predominates for photon energies between 30keV to 20MeV for low Z materials like water and polymeric materials.

(iii) Pair production: In the pair production process, as diagramed in the figure 1.4 below labeled "Pair Production - Energy Conversion to Mass," the photon is literally split into an electron and its anti-particle, called a positron. Both have a rest mass energy equivalent of 0.511MeV ($2m_ec^2$). (Since mass and energy are equivalent, the mass energy equivalent is just the amount of energy that it would take to form the mass of the particle. Pair production is a phenomenon of nature where energy is converted to mass (equation 1.5). It involves the complete absorption of a photon in the vicinity of an atomic nucleus.

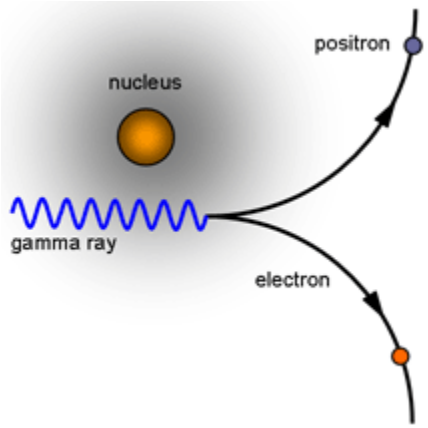

Figure 1.4: Pair Production

$$E_0 = E_{e^-} + E_{e^+} + 2m_e C^2 \quad (1.5)$$

The electron and positron can move in opposite directions (at an angle of 180^o) meaning they have a total momentum of zero or they can move at an angle of less than 180^o resulting in a net combined momentum. However, if the photon had only just enough energy to create the mass of the electron-positron pair then the electron and positron will be at rest. This could violate the conservation of momentum since the photon has momentum and the two resulting particles have none if they are stationary (since momentum = mass × velocity). This means that the pair production must take place near another photon or the nucleus of an atom since they will be able to absorb the momentum of the original photon. In other words, since the momentum of the initial photon must be absorbed by something, pair production by a single photon cannot occur in empty space; the nucleus (or another particle) is needed to conserve both momentum and energy [14]. Thus depending on the incident photon energy, the photon gets attenuated and the total linear attenuation coefficient (μ) is given by equation (1.6).

$$\mu = \tau + \sigma + \kappa \quad (1.6)$$

Where, τ, σ, κ are the linear attenuation coefficient of photoelectric, Compton and pair production process respectively.

1.2.2 Interactions of charged particles

(a) Electrons

Electron interacts with matter via four processes namely, emission of Bremsstrahlung radiation, inelastic collision, elastic collision and Cerenkov emission. The relative importance of these processes depends mostly on the energy of the electrons and to a lesser extent on the nature of the absorbing material.

(i) Bremsstrahlung: High energy electrons passing close to the nucleus of an atom are decelerated due to their interaction with the electric field of the nucleus and radiate electromagnetic radiation called bremsstrahlung radiation. Bremsstrahlung emission is negligible below 100KeV but increases rapidly with increasing energy, and is the dominant process at electron energy between 10-100MeV.

(ii) Inelastic collision: This is the major process for electrons having energy more than that at which bremsstrahlung emission occurs. The average amount of kinetic energy lost per unit length by electron through coulomb interaction with atomic electrons in a medium is defined as the specific energy loss or stopping power (S) of the medium and is defined by the Bethe's equation (1.7).

$$S = -\frac{dE}{dx} = \frac{2\pi e^4 N_o Z}{m_o v^2}\left[\ln\frac{m_o v^2 E}{2I^2(1-\beta^2)} - (2\sqrt{1-\beta^2} - 1 + \beta^2)\ln 2 + 1 - \beta^2 + \frac{1}{8}(1-\sqrt{1-\beta^2})^2\right] \qquad (1.7)$$

Where, e and m_o represents the charge rest mass of electron, v is the velocity of electron, N_o is the number of atoms cm^{-3} in the medium, Z is the atomic number and *I* is the mean

excitation potential of the electrons in the stopping material, β is the ratio of v to the speed of light c and is numerically represented in equation (1.8)

$$\beta = \sqrt{\{1 - (m_0 c^2/(E - m_0 c^2)\}^2} \quad (1.8)$$

(iii) Elastic collision: This is a quite frequent phenomenon because of the small mass of electrons and happens when electrons get deflected by the electrostatic field of an atomic nucleus. This essentially leads to a change in the direction of motion of electrons and is more probable for electrons with low energy and target with high atomic number.

(iv) Cerenkov emission: Electrons with velocity higher than that of light in a particular medium interacts and emits electromagnetic radiation, called Cerenkov radiation. This phenomenon is responsible for the blue glow observed around high intensity γ-sources stored under water.

(b) Heavy charged particles

The interaction of heavy charged particles with matter is the same as that of electrons, i.e., Bremsstrahlung emission, inelastic collision and elastic scattering. The most important among these processes by which charged particle interact with matter is inelastic collision. As heavy charged particles have higher mass than electrons, for a given energy, they have a much higher linear energy transfer (LET), which give rise to high local concentration of primary species and leads to recombination in spurs to yield molecular products.

(c) Neutrons

Neutrons do not produce ionization directly in matter but interact almost exclusively with the atomic nuclei of the material. The main processes by which neutron interacts with matter are: elastic scattering, inelastic scattering, nuclear reaction and

capture. The products of neutron interactions often cause ionization and thus produce typical radiation chemical changes. The main products of neutron interactions being protons and heavy positive ions, the chemical effects of neutron interactions are similar to those of charged particles.

1.2.3 Distribution of active species in the system – track structure

The electrons from Compton scattering of ^{60}Co ϒ-rays have an average energy of 440keV. These electrons, also termed as δ-rays, bring about further ionization and excitation. Such events along the main track or the δ-ray branch track are called isolated spurs. In water, the isolated spurs contain on an average ~ 6 active species and ~ 100eV energy is involved. When δ-ray electron energy is < 5keV, its penetration becomes very less and the spurs so formed in close vicinity overlap and take cylindrical shape, known as short tracks. As the electron energy becomes less than 500eV, even denser regions of ionization, which look like large spurs, called as blobs, are produced (figure 1.5).

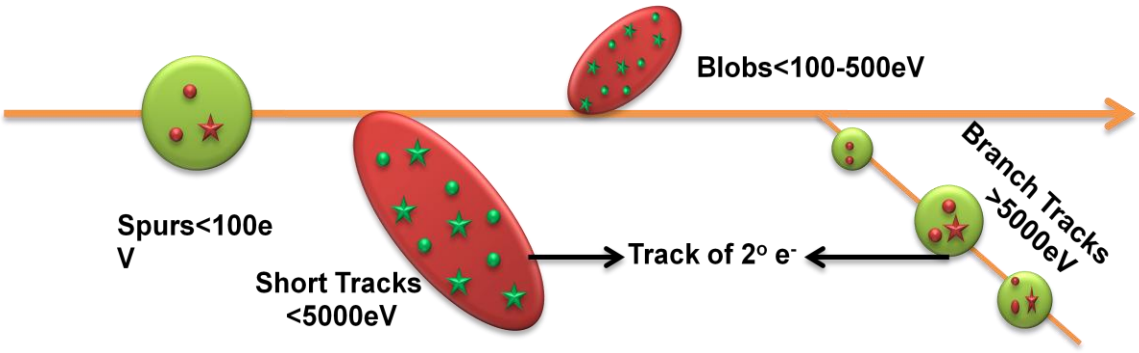

Figure 1.5: Distribution of ions and exited species along the track of fast electron; (•) represents the ions and (★) represents the excited species

The typical energy distribution ratio for a 440keV electron in water is spur (64%), short tracks (25%) and blobs (11%). In contrast to this, for heavy charged particles (high LET), more energy will be deposited in blobs and short tracks than in isolated spurs.

1.3 Radiation dosimetry

Management of the physical, chemical or biological changes produced by ionizing radiation necessitates knowledge of the amount of energy absorbed per unit mass of the absorber, and distribution of the absorbed energy in the absorbing material. Radiation dosimetry constitutes determination of these quantities.

(i) Absorbed dose: The absorbed dose is the amount of energy absorbed per unit mass of the irradiated material. The SI unit for the absorbed dose is Joules per kilogram (Jkg^{-1}), which is known as gray (Gy). The old unit is rad (1 rad = 0.01Gy).

(ii) Absorbed dose rate: The absorbed dose rate is the absorbed dose per unit time.

1.3.1 Radiation-chemical yield

Traditionally, radiation chemical yields have been reported in terms of G values, which represents the number of molecules of the product formed or changed per 100eV of energy absorbed [14]. The SI unit of radiation chemical yield is defined as change in the number of moles of material formed or decomposed by energy absorption of 1Joule. G-values reported in terms of number of species formed per 100eV can be converted to SI units using the following relationship (1.9).

$$\mathrm{G(mol\ J^{-1})} = \mathrm{G(as\ 100ev)\ X\ 1.036\ X\ 10^{-7}} \qquad (1.9)$$

1.3.2 Gamma Radiation Dosimetry (Fricke Dosimeter)

The radiation-induced oxidation of the ferrous ions to the ferric ions in aqueous solutions forms the basis of Fricke dosimeter [15].The standard Fricke dosimeter consists

of an aerated solution of 1.0 x 10^{-3} mol dm^{-3} ferrous ammonium sulphate, 1.0 x 10^{-3} mol dm^{-3} NaCl and 0.4 mol dm^{-3} sulphuric acid. The yield of Fe^{3+} ions produced is determined by absorption spectrophotometry employing Beer's law ($\Delta A = \Delta \varepsilon.c.l$) at 30 nm with $\varepsilon(Fe^{3+})$ = 220.5 ± 0.3 m^2mol^{-1} and $\varepsilon(Fe^{2+})$ =0.1m^2mol^{-1} at 25^oC. The $G(Fe^{3+})$.ε value accepted for electron and photon radiation in the range 1 to 30MeV is 3.52 x $10^4m^2J^{-1}$at 25^oC [16]. The Fricke dosimeter can be used to accurately determine dose only up to 400Gy because of depletion of oxygen present in the system. Fricke dosimeter is independent of dose rate between 0.2 to 2.0 x 10^6Gys^{-1}. A modified version of Fricke dosimeter, also called as super Fricke dosimeter, containing 10^{-2} mol dm^{-3} ferrous ions, oxygenated but without any sodium chloride, is dose rate independent up to absorbed dose rates of the order of 10^8Gys^{-1}. The upper limit of absorbed dose that can be measured using a super Fricke dosimeter is 2.0kGy.

1.4 Radiation chemistry of water

Understanding of radiation chemistry of water is of importance as water is present in most biological and chemical systems. For water, the sequence of events like formation and solvation of the primary species, and the time scale of events initiated either by fast electrons from an accelerator or by ^{60}Co gamma-rays is illustrated in figure 1.6. High energy radiation is deposited in energy in 10^{-16} seconds in the substrate forming positively charged ions, electrons and excited species. Energetically unstable positively charged ions (H_2O^+) undergo ion-molecule reaction in 10^{-14} seconds producing $^{\bullet}OH$ radicals [17]. The excited water molecules decompose in 10^{-14} seconds yielding $H^{\bullet}$ and $^{\bullet}OH$ radicals. The electron released during ionization can also bring about further ionization provided it has sufficient kinetic energy. Eventually, its energy will fall below

the ionization threshold of water and then it dissipates rest of its energy by exciting vibrational and rotational modes of the solvent molecules. Finally, it would be localized in a potential energy well long enough to become solvated as a result of molecular dipoles rotating under the influence of the negative charge, and thus get stabilized [18]. The electrons get thermalised in about 10^{-13} seconds and subsequently get hydrated or solvated in less than 10^{-12} seconds and called hydrated electron (e_{aq}^-) [19].

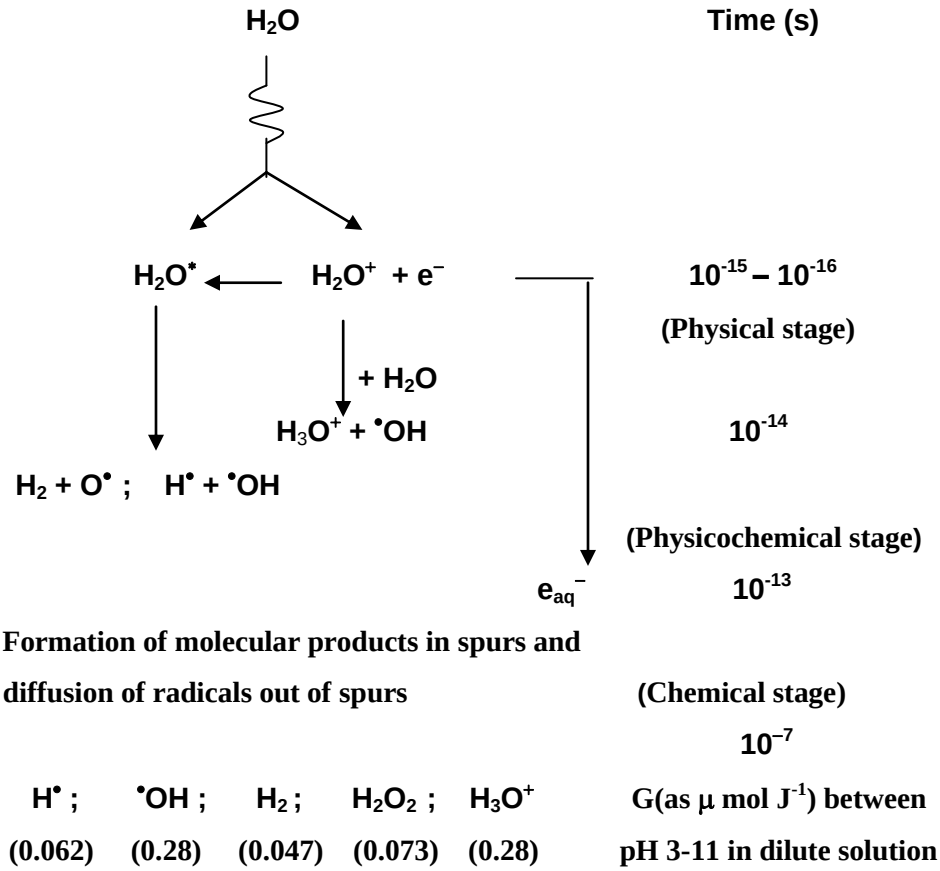

Figure 1.6: Sequence of events in water Radiolysis and formation of primary species from 10^{-16} to 10^{-7}second.

These species viz. hydrated electrons, hydrogen atoms and hydroxyl radicals, formed in the spurs, can react with one another to reform water or molecular products, H_2 and H_2O_2, while the remaining escape into the bulk solution. This spur expansion is complete in about 10^{-7}s. The reactions occurring during spur expansion are listed in

Table1.1. After about 10^{-7} second, the species are distributed homogeneously in the bulk are known as primary species. Main species produced are hydrated electrons (e_{aq}^-), $OH^\bullet$, $H^\bullet$ and molecular products H_2 and H_2O_2. These species can subsequently react with solutes present in the system. In water, 10^{-7} seconds is the lifetime of the radicals reacting at a diffusion-controlled rate with a solute whose concentration is 10^{-3}mol dm^{-3}. Under these conditions the G-values of e_{aq}^-, $H^\bullet$ and $^\bullet OH$ radicals at 10^{-7} second are shown in the figure 1.7.

Table 1.1 Spur Reactions in Water

Reactions	**k x 10^{-10} ($dm^3mol^{-1}s^{-1}$)**
$e_{aq}^- + e_{aq}^- \longrightarrow H_2 + 2^\bullet OH$	0.55
$e_{aq}^- + {}^\bullet OH \longrightarrow OH^-$	3.0
$e_{aq}^- + H_3O^+ \longrightarrow H^\bullet + H_2O$	2.3
$e_{aq}^- + H^\bullet \longrightarrow H_2 + OH^-$	2.5
$H^\bullet + H^\bullet \longrightarrow H_2$	1.3
$^\bullet OH + {}^\bullet OH \longrightarrow H_2O_2$	0.53
$^\bullet OH + H^\bullet \longrightarrow H_2O$	3.2
$H_3O^+ + OH^- \longrightarrow 2H_2O$	14.3

1.4.1 Primary yields

Primary yields are the yields of the species remaining when all spur reactions are complete, that is, ~10^{-7} seconds after the ionization event. At this time the radiolytic change in water is represented by:

$$H_2O \xrightarrow{\text{Gamma or EB}} e_{aq}^-, H^\bullet, {}^\bullet OH, HO^\bullet{}_2, H_2O_2, H_2, H_3O^+$$

and the material balance equations are:

$$G(-H_2O) = 2\,G(H_2) + G(H^\bullet) + G(e_{aq}^-) - G(HO^\bullet{}_2)$$

$$= 2\,G(H_2O_2) + G(^{\bullet}OH) + 2G(HO^{\bullet}_2) \quad (1.10)$$

or if $HO^{\cdot}_2$ is neglected, which is justified for low LET radiation

$$G(-H_2O) = 2\,G(H_2) + G(H^{\bullet}) + G(e^{-}_{aq})$$

$$= 2\,G(H_2O_2) + G(^{\bullet}OH) \quad (1.11)$$

Primary yields were measured particularly for low LET radiations using scavengers in dilute solutions. In very dilute solutions the radical and molecular yields are constant, but in the presence of a reactive solute at concentrations more than 10^{-2}mol dm^{-3}, the yields of H_2 and H_2O_2 decrease and radical yields increase due to spur scavenging by the solute molecules [20].

1.4.2 Important reducing radicals in aqueous solutions

The hydrated electron, e^{-}_{aq}, and the hydrogen atom ($H^{\bullet}$) are the primary radicals falling in this category. The redox-potential value $\xi° = -2.9$ V vs NHE for e^{-}_{aq} suggests that it is a powerful reducing agent (Table 1.2). Its reactions with solutes are best understood in terms of availability of a suitable vacant orbital in the solute molecule (S) for the electron to get localized. A typical reaction is represented as in equation (1.12) where the n represents the positive charge on the solute.

$$e^{-}_{aq} + S^{n} \longrightarrow S^{n-1} \quad (1.12)$$

The rate constant values for typical hydrated electron reactions support the above requirement. For water, the rate constant, k is only $16 dm^3 mol^{-1} s^{-1}$ as a low-lying vacant orbital is absent in water. It also explains the sufficiently long half-life of e^{-}_{aq} in water. With solutes having low lying π^* orbital, the k value approaches the diffusion controlled limit. In neutral and acidic pH, the $H^{\bullet}$ is an important reducing species with its redox

potential value, ξ° = -2.3 V vs NHE (Table 1.3). It can be thought of as a weak acid with pK_a of 9.6. While it readily reduces substrates with more positive redox potential, the corresponding rates are slower than for e_{aq}^- reactions. With substrate having center of unsaturation, it is known to add readily to form H-adduct.

Table 1.2 Properties of e_{aq}^-

Radius of charge distribution	0.25-0.30 nm
Diffusion coefficient	4.9×10^{-5} cm^2 s^{-1}
Spectral characteristics	e_{aq}^-, λ_{max} = 715 nm,
	$\varepsilon = 1.85 \times 10^4$ dm^3 mol^{-1} cm^{-1}
Redox potential (Vs NHE)	ξ° ($e_{aq}^- + H^+ \rightarrow$ ½ $H_2 + H_2O$) - 2.9 V
Half life: pH ≥ 7.0	6.6×10^{-4} seconds.

From a solute devoid of π electrons, it abstracts hydrogen atom giving rise to a solute transient radical. Optical absorption of $H^\bullet$ lies around 200 nm with very low extinction coefficient, which is normally not accessible with the available experimental facilities. Thus, measurements of $H^\bullet$ reaction parameters are made by competition kinetics method or from the transient formation kinetics.

Table 1.3 Properties of $H^\bullet$ atom

Diffusion constant	8.0×10^{-5} cm^2 s^{-1}
Spectral characteristics	$H^\bullet$, λ_{max} = 200 nm
Reduction potentials (vs. NHE)	ξ° ($e_{aq}^- + H_3O^+ \rightarrow H + H_2O$) - 2.3 V
	pK_a: 9.6

1.4.3 Important oxidizing radicals in aqueous solutions

Hydroxyl radical ($^{\bullet}OH$) is a strong oxidizing radical ($\xi° = 2.8$ V vs NHE) and like $H^{\bullet}$, it absorbs in the far UV, therefore, its kinetic parameters are olso estimated by competition kinetics or transient formation kinetics. In strongly basic solution (pH > 11.9), it is deprotonated to give $O^{\bullet-}$. The properties of $^{\bullet}OH$ radical are listed in Table 1.4.

Table 1.4 Properties of $^{\bullet}OH$ radical

Diffusion constant	2.2×10^{-5} cm^2 s^{-1}	
Spectral characteristics	$^{\bullet}OH$, $\lambda_{max} = 235$ nm, $\varepsilon = 530$ dm^3 mol^{-1} cm^{-1}	
Reduction potentials (vs. NHE)	$\xi°$ ($e^- + {}^{\bullet}OH + H^+ \rightarrow H_2O$)	+ 2.8V, acid
	($e^- + {}^{\bullet}OH \rightarrow OH^-$)	+ 1.8 V, alkali
	pK_a: ($^{\bullet}OH \Leftrightarrow O^{\bullet-} + H^+$)	11.9

1.5. Radiation effects on Polymers

It has been approximately 50 years since researchers first began exposing polymeric materials to ionizing radiation, and reporting the occurrence of cross linking [21], surface modification (grafting and curing) [22, 23] and other useful effects. Today, a substantial commercial industry is in place based on processing of polymers with radiation like radiation cross-linked wire and cables, smart surfaces for tissue engineering, separation of toxic metal ions, treatment of textile effluents, fuel cells etc.

Irradiation of polymers causes modification of properties which is currently the basis of major industries in heat shrinkable film and tubing, crosslinked polymers and graft copolymers [24]. Irradiation of polymers with high energy radiation leads to the formation of very reactive intermediates in the forms of excited states, ions and free

radicals. These intermediates are almost instantaneously guided in several reaction pathways which result in the arrangement or formation of new bonds structures. The ultimate effects of these reactions are the formation of oxidized products, grafts copolymer, crosslinking and scissioning of main or side chains which is also called degradation. Schematic of various processes has been shown in the figure 1.7. Generally, scission and crosslinking coexist, although the prevalence of each relies on many factors, such as the initial molecular structure, polymer morphology and the experimental irradiation conditions of treatment before, during and after irradiation and close control of these factors make the modification of polymers possible by radiation processing [25] The degree or dominance of these transformations depends on the nature of the polymer and the conditions [26].

1.5.1 Crosslinking and degrading polymers

Polymers are generally divided into two groups: crosslinking type (which predominantly crosslink) and degrading type (which predominantly undergo chain scission). In general, polymer chain with at least one hydrogen atom (as in the structure I) with each carbon atom undergo crosslinks and if a tetra-substituted carbon atom is present in the repeat unit (as in the structure II), the polymer degrades predominantly.

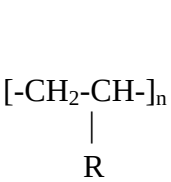

Structure I (crosslinking)

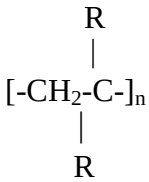

Structure II (degrading)

Thus, polyethylene, polystyrene, are crosslinking type of polymers, and polymethyl methacrylate, polytetrafluoroethylene are degrading type of polymers. In general, crosslinking reactions in polymers are favored by the presence of unsaturated

groups particularly vinyl groups, absence of oxygen, high chain mobility and molecular entanglements. Chain scission on the other hand is favored by restrictions to chain rotation i.e. glassy state, high levels of crystallinity and presence of oxygen. Usually radiation stability of the polymer increases in the presence of aromatic ring in its structure. Crosslinking reaction transforms a linear polymer into a single three-dimensional molecule with significantly different properties. The crosslinked structure has ultra high molecular mass, is practically insoluble in any solvent and has improved mechanical properties. Degradation on the other hand results in a reduction of molecular mass as chains are fractured and results in a general degradation of the physical properties of the polymer.

Crosslinking reactions have been intensively studied for a long time, and continue to this date for the improvement of the thermal resistance, mechanical, physicochemical properties of polymers. The desired change of physical and mechanical features is induced and can be tuned by the choice of individual irradiation parameters. There are number of applications of cross-linking, mainly with radiation technology, like wire and cable insulation, heat shrinkable products, polymeric positive temperature coefficient products, gaskets and seals, hydrogels, vulcanization etc. Other cross linking applications like hydrogel will be further elaborated in respective chapter. The opposite of crosslinking chain, scission is the basis of other radiation treatment aimed at enhancing processing characteristics of polymers. For example, radiation degradation of Polytetrafluoroethylene (PTFE) found large applications for thickener of various oils, lubricants, material for coatings and inks [27].

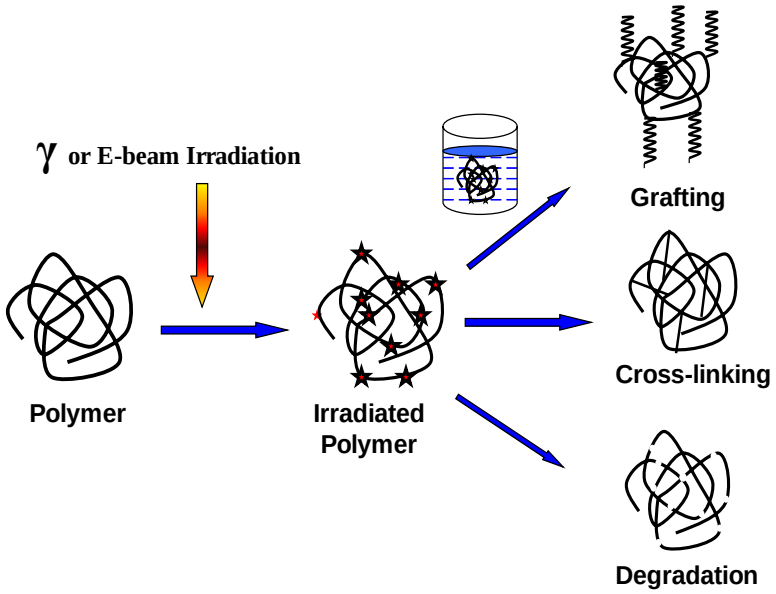

Figure 1.7: Schematic diagram for radiation effect on polymers

There were number of problems with the high MW PTFE in grease and other lubricants. Grease containing degraded PTFE was claimed by US patent in 1966. It was claimed that PTFE retained its low coefficient of frictions even with loss of tensile strength and was easier to disperse in a lubricant than high MW PTFE. It was also observed that degraded PTFE gives smoother grease and reduce the amount of PTFE required [28].

1.5.2 Surface modification

(a) Basics of Radiation Induced grafting

Graft copolymers are branched copolymers in which the branches are of a different type from the base polymer to add the desired functionality for various directed applications. In graft copolymerization, the role of the trunk polymer is to provide an appropriate practical shape and dimension and to maintain physical and chemical stability, whereas, the grafted polymer branch adds various functionalities.

There are various methods for the graft polymerization like conventional method, radiation induced method, plasma induced method, enzymatic method [3] etc. But using high energy radiation is hot topic now days in which radiation chemist produces radicals by breaking C-H bonds on a trunk polymer by irradiating it with ionization radiation (gamma rays or electron beams). Then a polymer branch with desired functional capabilities is grafted onto the trunk polymer as shown in figure 1.8.

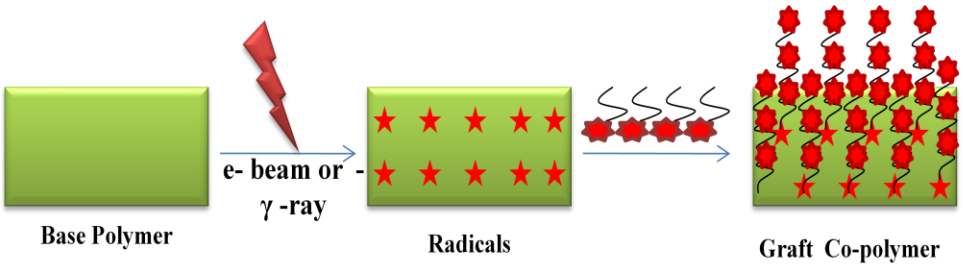

Figure 1.8: Radiation induced Graft Copolymerization

Therefore, one can easily and effectively incorporate the desired properties onto a polymer backbone using graft polymerization by selecting suitable monomer without destroying or affecting the basic properties of the of the trunk polymer, e.g. crystanillity, melting point or mechanical properties [29-31].

(b) Classification of graft polymerization

Radiation grafting technique can be classified into two categories in terms of irradiation opportunity [5].

(i) Simultaneous or mutual irradiation grafting: Simultaneous irradiation is the simplest irradiation technique for preparation of graft copolymers. In this method a polymer backbone is irradiated in the presence of a monomer available in different forms: vapor, liquid or in bulk solution. Irradiation can be carried out in air, inert atmosphere (e.g. N_2) or preferably under vacuum leading to the formation of active free radicals on

both polymer backbone and monomer units (figure. 1.9a). In this method, the trunk polymer in contact of a monomer is irradiated simultaneously. The best condition for the method is preferred for base polymer having higher G-value as compared to the monomer to be grafted.

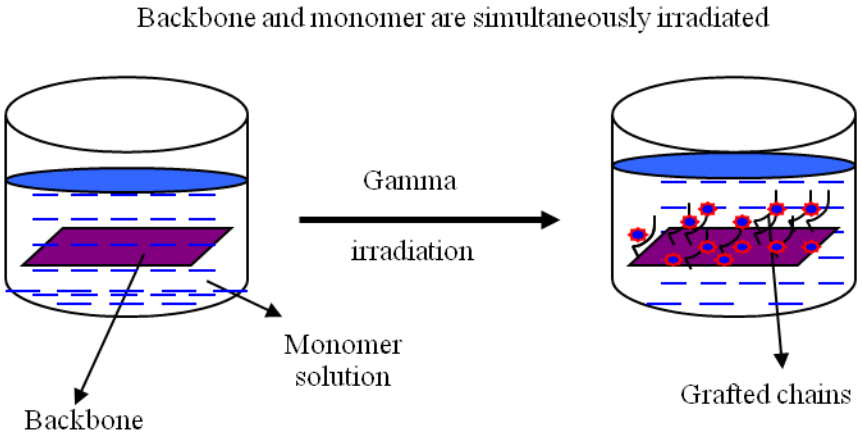

Figure 1.9a: Schematic diagram for Mutual Irradiation Grafting

(ii) Pre-irradiation grafting: In this method, the trunk polymer is first irradiated to generate reactive radical sites and then brought into contact with the monomer (figure 1.9b). The best condition for the method is preferred for base polymer having lower G-value as compared to the monomer to be grafted.

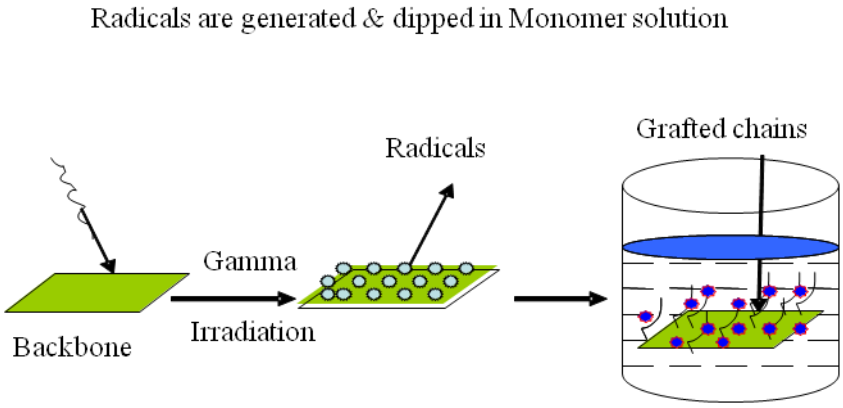

Fig 1.9b: Schematic diagram for Post Irradiation Grafting

(c) Parameters affecting Graft Polymerization

There are number of parameters, which strongly affect radiation-induced graft copolymerization process and subsequently the grafting yield in the copolymer membranes. Variation of parameters as mentioned in figure 1.10 causes considerable changes in the amount of degree of grafting in the resulting membranes and therefore, control of the compositions and the properties of the membranes can be achieved. A combination of parameters has to be adapted to achieve successful grafting reactions and obtain desired membrane structure economically. This includes parameters directly related to irradiation source and others related to the grafting mixture and its components.

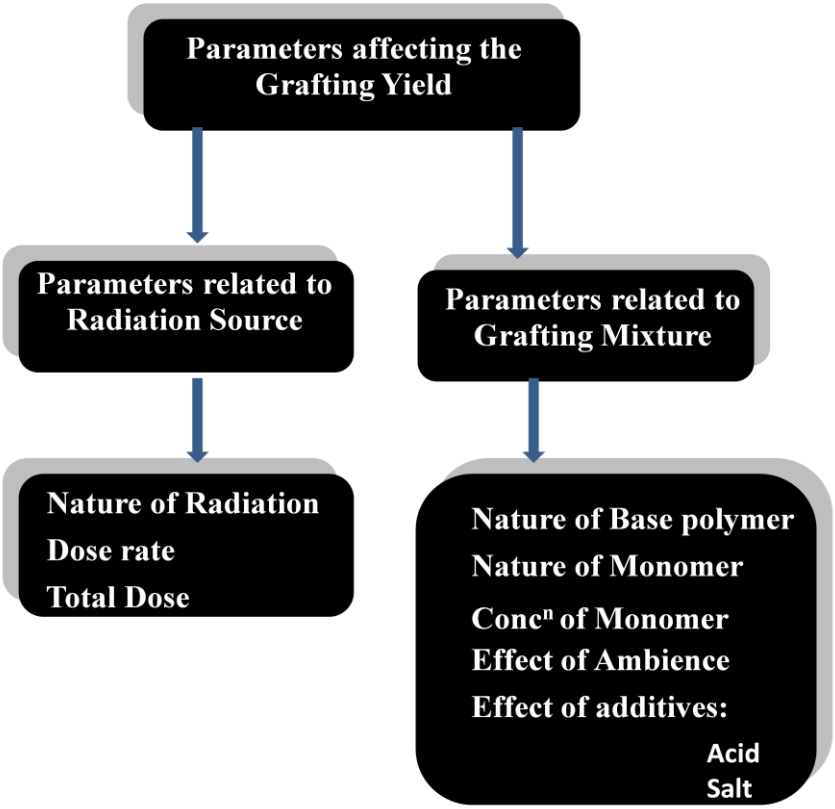

Figure 1.10: Schematic representation of parameters affecting the degree of grafting prepared by radiation-induced graft copolymerization.

Figure 1.10 shows a schematic representation of parameters affecting the degree of grafting in membranes prepared by radiation-induced graft copolymerization [32]. The effect of each one of these parameters on the degree of grafting of the membrane is discussed in the corresponding chapters.

(d) Advantages of radiation grafting*:* Radiation grafting is superior to other conventional grafting techniques because of the following reasons:

(i) Selective absorption, low penetration and requirement of additive like photo initiators or photo sensitizers make the photo initiation process a handicap one. However, radiation induced grafting methods are limitless, owing to the unselective absorption of radiation energy in matter, and can in principle, be used to prepare any desired combination of polymers. Unlike conventional grafting methods, radiation grafting reaction can either be conducted homogeneously throughout thick layers of polymers or limited to the surface zone of desired thickness only, depending upon the type of radiation, the total energy absorbed, the depth of penetration and radiation sensitivity of trunk polymer and monomer.

(ii) Some polymers such as solid fiber are difficult to be grafted by chemical initiators, because they can hardly induce reactive centers homogeneously in the solid fiber. As far as radiation grafting is concerned, it is easier, especially for gamma radiation and high-energy electrons, which have high penetration power, to induce radicals homogeneously onto any arbitrary shapes of polymers, such as a hollow fiber, woven/non-woven fabric and films.

(iii) Radiation grafting does not require any additives such as initiators or sensitizers, unlike photo grafting or thermal grafting methods. Therefore, in radiation grafting

method, high purity copolymer is obtained, which have vast applications as biocompatible and bio-functional materials where impurity of any type is not acceptable.

1.6 Hydrogel

At present there is no precise and limiting definition of the term hydrogel but it is commonly defined as three dimensional networks of cross-linked hydrophilic polymer chains that imbibe substantial amounts of water (>20%) without losing its physical integrity. Hydrogels are highly absorbent (>99.9% water) based on natural or synthetic polymers. It is a solid material in dried state, but when water is added; the hydrogel swells until it reaches the swelling equilibrium as shown in figure 1.11. Hydrogels also possess a degree of flexibility very similar to natural living tissue, due to their high water content, more than any other type of synthetic biomaterial. Due to this resemblance to living tissues, hydrogel have a number of biomedical applications, such as wound care products, dental and ophthalmic materials, drug delivery systems, elements of implants, constituents of hybrid-type organs, as well as stimuli-sensitive systems superabsorbents etc. with a number of products being commercially available [33]. Among the above mentioned applications of hydrogel, most notably, research has been advanced in the commercialization of burns and wound dressing hydrogels. In India, wound dressing material has been commercialized with the brand name ‘HI-ZEL’by Varshney and group [34]. These hydrogel maintain a moist environment, barrier to bacterial contamination, excess to oxygen, transparent in nature, which allows monitoring the healing progress of wound without removing the dressing. Most importantly faster wound healing was reported than dry gauze dressing [35].

Figure 1.11: Schematic representation of gel structure before and after swelling

Another fascinating class of hydrogel which is subject of extensive investigation is responsive to small transition in solvent composition, pH, temperature, and intensity of light as well as magnetic and electric fields called Stimuli Responsive Hydrogel. For example, the change in pH causes volume transition in polyacrylic acid hydrogel as shown in figure 1.12. Depending on the pH of the medium as the polyacrylic acid goes from non-ionized state (relaxed configuration) to ionized state (stretched configuration), the polyacrylic matrix may swell or de-swell. The applications of such hydrogels in devices as actuators, artificial muscles, controlled drug delivery; controlled molecular separators have been suggested [36]. Carenza and group have reported control release of insulin in response to glucose blood levels in their vivo studies on diabetic rats.

The properties, which decide the applications of a hydrogels, are: equilibrium degree of swelling, swelling kinetics, permeability, biocompatibility, mechanical and optical properties and change in extent of swelling with external environment like pH, ionic strength, temperature.

The introduction of ionic monomers results in gels which normally swell more than the non-ionic gels [37-39]. Incorporation of monomers like acrylic acid and methacrylic acid produces anionic polyelectrolyte gels, whose ionization is a function of pH, thermo

responsive gels poly-N-isopropylacrylamide (PNIPAM) are the functions of temperature which undergo phase transition in pure water, from a swollen state at low temperature to a collapsed state at high temperature [40] by breaking hydrogen bonding at higher temperature whereas incorporation of the sulfonate, tertiary and quaternary amines group produces polyelectrolyte gels relatively insensitive to pH [41]. Poly(2-hydroxyethyl methacrylate) (PHEMA) based gels have been the subject of interest for scientists and technologists because of their versatile properties, such as biocompatibility, good mechanical strength, high gel fraction, and ease of synthesis. However, low swelling of non-ionic polymer matrix like PHEMA at higher crosslinking extent restricts their applications where high swelling is desired. This problem can be overcome by either functionalization of the base matrix or by co-polymerization with ionic monomers. The introduction of ionic monomers results in gels which normally swell more than the non-ionic gels [37-39].

In the present study, poly[2-(methacryloyloxy)ethyl]trimethylammonium chloride (MAETC), a strong cationic polyectrolyte, was incorporated in Poly(2-hydroxyethyl methacrylate) (PHEMA) based gels by radiation induced polymerization to improve the swelling extent and also to add ionic strength responsive properties. Electrostatic interactions between the ionized groups, as well as the presence of small electrolyte ions in the nearby solution, convey to polyelectrolyte system a host of properties distinct from those displayed by neutral polymer systems. Industrial applications and academic interests lead to more studies on the polyelectrolyte behavior in solutions, gels, adsorbed layers, and grafted brushes.

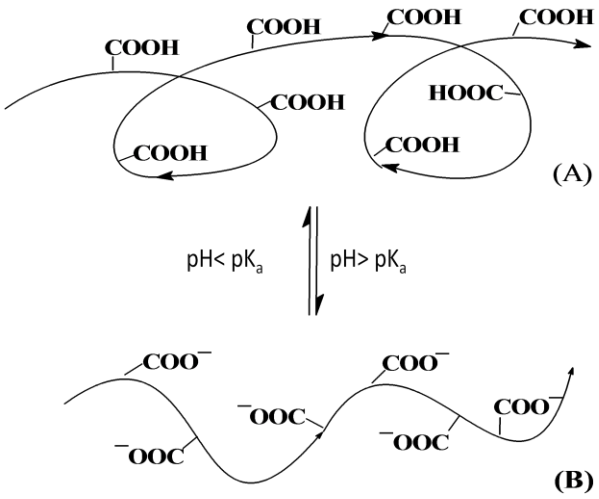

Figure: 1.12: Effect of pH on pH stimuli Hydrogel

1.7 Quaternary cationic polyelectrolytes

Cationic polyelectrolytes are polymers with basic groups, either a weak amine or a quaternary ammonium groups, situated along the main chain of the polymer. Therefore they retain many of the properties of polymer from which they are derived, but these properties are considerably modified by the presence of the basic groups. Examples of weak cationic polyelectrolytes are polyvinylamine, polyethyleneamine, and poly (4-vinyl-pyridine), where examples of strong polyelectrolytes are polyvinyl-bezyltrimethylammonium chloride and polyvinylmethylpyridinium bromide. Quaternary ammonium cations, also known as quats and corresponding polymer containing quaternary ammonium cations as polyquats, are positively charged polyatomic ions of the structure NR_4^+, R being an alkyl group or an aryl group [42]. Unlike the ammonium ion (NH_4^+) and the primary, secondary, or tertiary ammonium cations, the quaternary ammonium cations are permanently charged, independent of the pH of their solution.

1.7.1 Quaternary ammonium compounds as an anti-microbial compounds

Antimicrobial agent or germicides are the chemicals which inhibit or kill microorganisms' e.g bacteria, fungi or viruses. Halogens (iodine, chlorine), alcohols, peroxygen compounds (H_2O_2, peracetic acid), phenolic compounds, aldehydes and ionic surfactants are the well-known examples of antimicrobial agent. Among the various classes of surfactants, the cationic, and more particularly the quaternary ammonium compounds are the most effective germicides. Quaternary ammonium compounds (QACs) are amphoteric surfactants that are widely used for the control of bacterial growth in clinical and industrial environments [43]. Quaternary ammonium compounds have a broad spectrum of antimicrobial activity against both Gram-positive and Gram-negative bacteria. As compared with small molecule antimicrobial agents, polymeric antimicrobials have advantages, such as that they are nonvolatile, chemically stable, have long-term antimicrobial activity, and are hard to permeate through the skin [11]. These compounds kill or inhibit the growth of both gram-positive and gram-negative bacteria, and are effective over wide pH range. On the other hand, the anionic surfactants are frequently effective against gram-positive bacteria but very rarely effective against gram-negative bacteria. Their action tends to be much slower than that of the cationic surfactants and more susceptible to the changes in the pH of the system [44].

1.7.2 Mechanism of the germicidal action

Although large amount of work has been carried out to study the biochemical mechanism by which cationic surfactants exert their germicidal action, no complete theory has yet been developed. It appears probable that the surfactant can attack the cell through many different routes, and the particular mechanism, which is effective in a single case, depends on the organism and the concentration of the surfactant. Simple

adsorption may not be sufficient disturbing to kill unless it seriously upsets the osmotic balance between the organism and the medium. This class of chemical reduces the surface tension at the interfaces, and is attracted to the negatively charged surfaces, including microorganism. Some of the mechanism suggested include: (i) denaturation of the cell proteins. (ii) Combination of the cationic compound with the cell lipids. (iii) Interference with the enzyme balance within the organism and affecting the metabolic reactions of the cell (iv) Interference with the osmotic balance in such a manner as to release vital solute materials outward through the cell wall, finally causing death [45, 46]. Most of these compounds bearing quaternary ammonium groups appear to act by interacting with and disrupting negatively charged bacterial cell membrane followed by release of K+ ions and other cytoplasmic constituents, resulting in immediate death of the bacterial cell. In contrast to the soluble polycations, insoluble quaternary ammonium macromolecules act on the surface of the microbial cell and display their antimicrobial activity only on contact without permeation [47]. An alternative mechanism of action was proposed by Kugler et al. for cationic surfaces which appear to induce an ion exchange between the positive charges and cations within the membrane. Upon approaching a cationic surface, the structurally essential divalent cations of the membrane are relieved of their role in charge neutralization of the membrane components and are thus free to diffuse out of the membrane. The loss of these structural cations results in a loss of membrane integrity [48].

1.8 Scope of the thesis

As discussed in the earlier part of this chapter, water-soluble polyelectrolytes have been suggested as important polymeric materials having immense potential in

different field of life. New method of synthesis of polyelectrolytes, their gels and grafted copolymers using radiation polymerization method have been developed.

High energy gamma radiation has been used to initiate the synthesis HEMA-co-MAETC hydrogels of good swelling extent and mechanical strength which has number of advantages over conventional methods viz. high purity products, easy process control, room temperature synthesis and possibility of sterilization during synthesis. The properties, which decide the applications of a hydrogels, are: equilibrium degree of swelling, swelling kinetics, permeability and hence incorporation of strong polyelectrolyte PMAETC has been studied extensively. Equilibrium swelling study gives the idea about the equilibrium degree of swelling (EDS) of the hydrogel, which is the one important factor that decides the application of the gel matrices. On the other hand, dynamic swelling kinetics provides information regarding solvent sorption rate (diffusion constant), the rate of approach to the EDS and transport mechanism (type of diffusion) controlling the solvent sorption. Therefore, equilibrium swelling and dynamic swelling studies of any gel are of vital importance for developing technological applications. The equilibrium and dynamic swelling study of polyampholytic gels were carried out in different experimental conditions.

PMAETC and PAETC have a strong anion exchanger (quaternary ammonium) group and also exhibit anti-microbial activity. Therefore, PMAETC and PAETC were grafted onto cotton cellulose matrix, which is the most abundant biopolymer in the nature but very prone to attack by the microorganisms like bacteria, fungi, by mutual radiation grafting method in order to incorporate bactericidal. The grafted samples were then tested for antibacterial property group of gram positive and gram negative bacteria. In the last, one of the monomer VBT containing quaternary ammonium groups, a strong anion

exchanger which is grafted onto cotton, has been investigated for the treatment of textile effluents containing acid dyes.

Chapter: 2 Experimental methodology and techniques for characterization of Polymers

Keywords: Gamma radiation, Radiolysis, Characterization techniques, Hydrogel, Antibacterial

2.1 Introduction

In the present work, Cobalt-60 gamma radiation source was used for steady-state radiolysis studies, synthesis of linear polymers, grafted co-polymers and hydrogels. The different characterizations techniques like UV-visible spectrophotometry, Fourier Transform infrared spectroscopy (FTIR), Scanning Electron Microscopy (SEM), Elemental Analysis (EA), Thermogravimetry (TG), equilibrium and dynamic swelling analysis were utilized to characterize the radiation synthesized polymer, grafted polymers and cross-linked polymer gels. The techniques and instruments used are briefly described in this chapter with emphasis on ^{60}Co gamma radiation source.

2.2 Gamma radiation source

Gamma irradiation of the samples was carried at room temperature using Gamma Chamber 5000, supplied by the Board of Radiation & Isotope Technology (BRIT), Mumbai, INDIA. Figure 2.1 shows the schematic of gamma chamber used for studies. Gamma chambers mainly consist of a set of stationary Cobalt-60 (written ^{60}Co) sources placed in a cylindrical cage surrounded by a lead shield provided around the source to keep external radiation field well within the permissible limits. The sample for irradiation is placed in an irradiation chamber located in the vertical drawer inside the lead flask. The drawer can be moved up and down with the help of a system of motorized drive which enables precise positioning of the irradiation chamber at the center of the

radiation field. ^{60}Co radioisotope is produced by irradiating natural cobalt (^{59}Co) in the form of pellets, small slugs or thin disks in nuclear reactor by $^{59}Co(n,\gamma)^{60}Co$ reaction to give a uniformly active material which emits two γ rays of energies 1.33 and 1.17 MeV after β^- emission as shown below in the decay scheme 2.1.

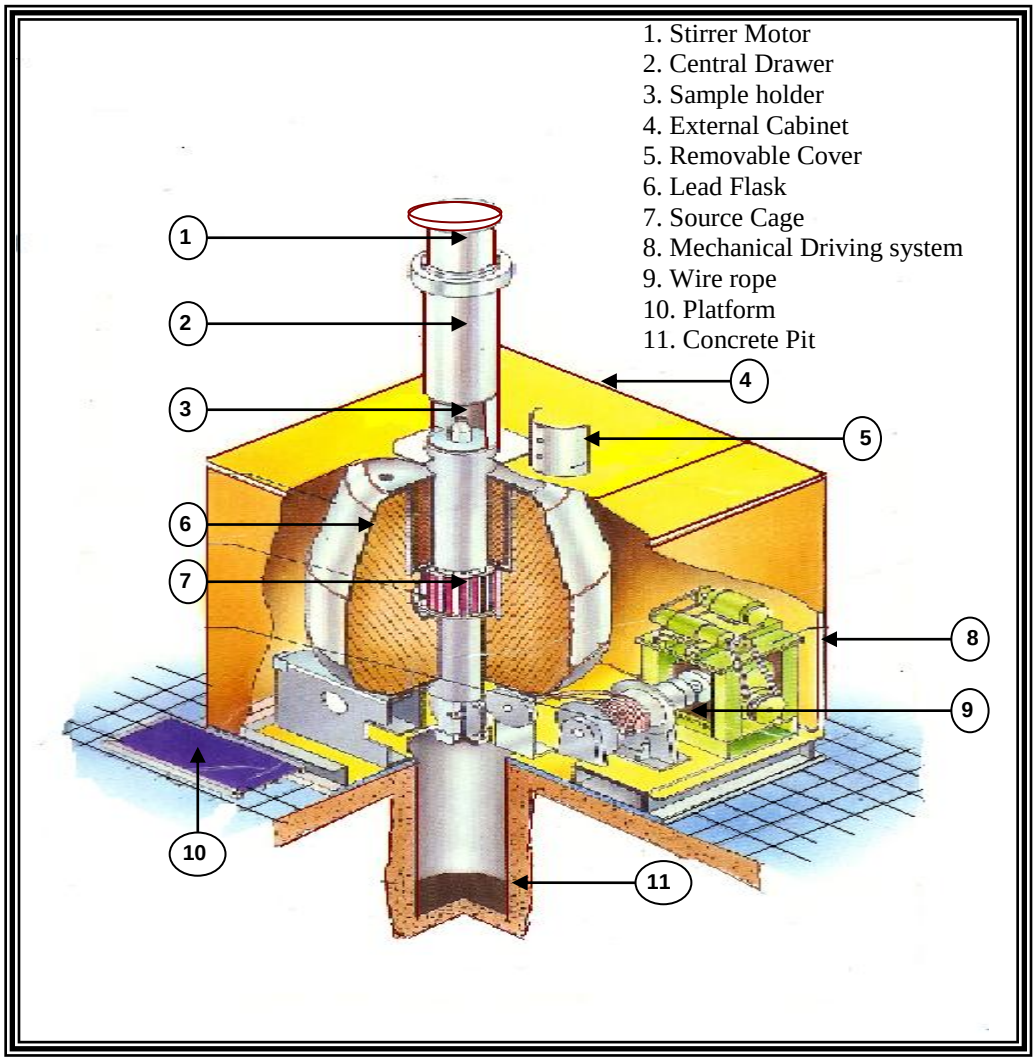

Figure 2.1: Schematic of Gamma chamber 5000

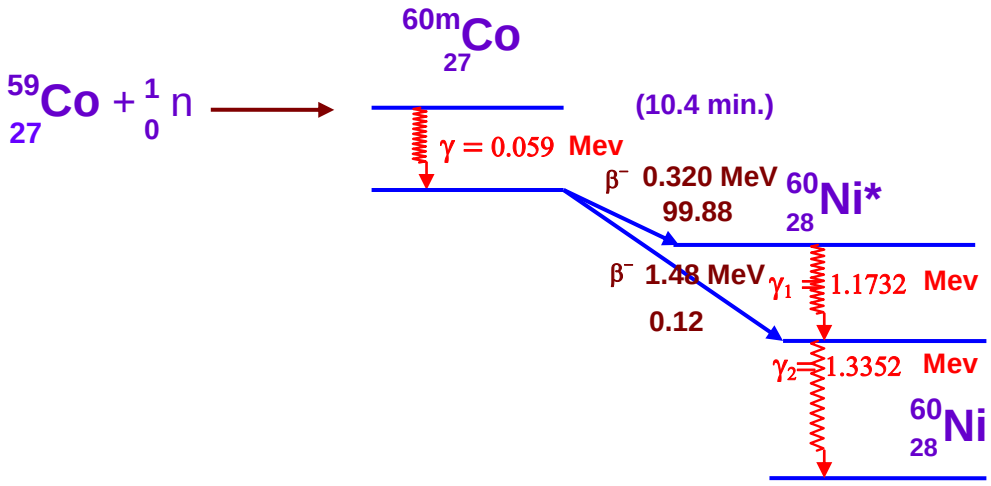

Scheme 2.1: Production and decay scheme for ^{60}Co

2.2.1 Dosimetry of gamma chambers

Before using gamma chambers for irradiation experiments, dosimetry of gamma was carried out to determine the radiation dose inside the gamma chamber by Fricke dosimetry [49]. The reaction involved in the Fricke dosimeter is the radiation-induced oxidation of ferrous ion to ferric ion at low pH and in the presence of oxygen in accordance with the series of reactions (2.1) – (2.7) [50-53].

$$H_2O \rightsquigarrow H^{\bullet}, {}^{\bullet}OH, e_{aq}^{-}, H_2, H_2O_2, HO^{\bullet}_2, H_3O^{+} \quad (2.1)$$

$$e_{aq}^{-} + H^{+} \longrightarrow H^{\bullet} \quad (2.2)$$

$$H^{\bullet} + O_2 \longrightarrow HO_2^{\bullet} \quad (2.3)$$

$$Fe^{2+} + {}^{\bullet}OH \longrightarrow Fe^{3+} + OH^{-} \quad (2.4)$$

$$Fe^{2+} + HO_2^{\bullet} \longrightarrow HO_2^{-} + Fe^{3+} \quad (2.5)$$

$$HO_2^{-} + H^{+} \longrightarrow H_2O_2 \quad (2.6)$$

$$Fe^{2+} + H_2O_2 \longrightarrow Fe^{3+} + OH^{-} + {}^{\bullet}OH \quad (2.7)$$

The chemical yield of ferric ion (chemical yield G value is defined as number of species produced or destroyed per 100 eV energy absorbed) is related to the primary radical and molecular yields by equation (2.8)

$$G(Fe^{3+}) = 2G(H_2O_2) + 3[G(e_{aq}^{-}) + G(^{\bullet}H) + G(HO_2^{\bullet})] + G(^{\bullet}OH) \quad (2.8)$$

Since each molecule of hydrogen peroxide oxidizes two ferrous ions by reactions (2.7) and then (2.4), while the each reducing radicals (e_{aq}^{-} and $H^{\bullet}$) oxidize three ferrous ions as given by sequential reactions involving $HO_2^{\bullet}$, H_2O_2 and $^{\bullet}OH$ in equations 2.4, 2.5 and 2.7 respectively. Substituting the G values of various species in equation 2.8, the G (Fe^{3+}) has been reported to be 1.61 $\mu molJ^{-1}$ [54, 55]. Absorbed doses (D_d) can be determined in Gray using relation

$$D_d = 2.77 \frac{\Delta D}{I} \quad (2.9)$$

Where, ΔD is change in the absorption (at 304 nm) of solution and I is the path length in meters.

For carrying out dosimetry of the gamma chambers nine vials containing about (10 ml) of Fricke solution were fixed to a rectangular thermocol sheet and placed it at the center of irradiation chamber vertically. Three vials equidistant from each other were placed at upper and lower ends and three along the horizontal central axis as shown in figure 2.2. Three sets of dosimeters for different duration of time were irradiated and their absorption was measured immediately after irradiation. Dose variation along the horizontal axis was ~8% and along the vertical axis ~10%. Lead attenuators of suitable thickness were used for reducing the dose rates.

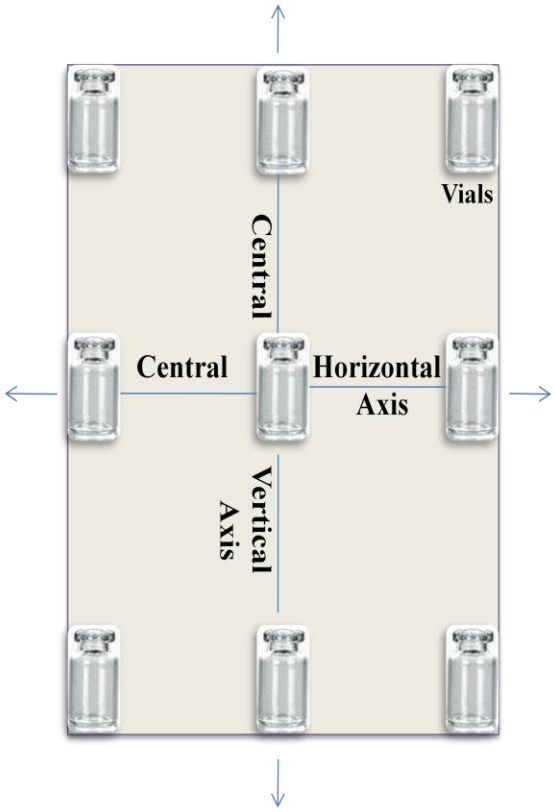

Figure 2.2: Schematic diagram of sample cell of gamma chamber showing position of vials for gamma chamber dosimetry

2.3 Swelling and de-swelling measurements

The amount of water absorbed by a hydrogel i.e. swelling at equilibrium is a function of (i) hydrophilicity of the polymer (ii) the extent of crosslinking of the network structure (iii) the number of ionized groups on the polymer (iv) the swelling medium. The swelling degree is central to any application of the hydrogel, therefore it is important to examine changes in its swelling degree due to composition of gels as well as due to swelling medium. These studies provide an idea about the water imbibing capacity of the gel matrix in various kinds of swelling environments, which decides its applicability for various applications.

For swelling/de-swelling studies, crosslinked cylindrical gel samples were cut into thin disc form. The samples were repeatedly swollen (in distilled water) and dried several times, at room temperature, to leach out the sol-fraction and then used for further studies.

These measurements were made by a simple gravimetric method [56] using a Sartorius single pan weighing balance (accuracy ±0.00001 g). The percentage equilibrium degree of swelling (EDS %) of gels were determined gravimetrically using equation (2.10)

$$\text{EDS}\ (\%) = \frac{W_{eq} - W_i}{W_i}\ X\ 100 \qquad (2.10)$$

Where, Weq and W_i are the weights of gel in swollen at equilibrium and dry states, respectively.

The swelling ratio (SR) of the gels swelled to equilibrium were determined using equation (2.11)

$$SR = \frac{W_s}{W_i} \qquad (2.11)$$

Where, W_i and W_s are weight of dry gel and weight of swollen gel at time t respectively.

2.4 Analysis of data for kinetics of swelling

2.4.1 Types of diffusion

The dynamic swelling properties of a polymer include the solvent sorption rate, the rate of approach to equilibrium and the transport mechanism controlling the solvent sorption. Alfrey et. al. [57] proposed that the diverse responses of polymers to the presence of a penetrant may be categorized into three classes based on the relative rates of diffusion and relaxation of the polymer chains:

1. Fickian Diffusion: When the rate of diffusion is significantly slower than the rate of relaxation of the polymer chains, the transport is characterized as Fickian or Case I diffusion.

2. Case II transport: Case II diffusion arises when the rate of diffusion is greater than the rate of the relaxation of the polymer chains. The main feature of this second limiting

model is the establishment of a sharp boundary between the glassy core and the swollen shell that advances at a constant velocity.

3. Anomalous transport or Non-Fickian: Anomalous diffusion occurs when the rates of diffusion and polymer relaxation are comparable and is connected with the transition region between the two limiting cases of Case I and Case II.

The mechanism of transport of solvents into polymers can be determined by a variety of experimental techniques, the simplest and most common one is the sorption technique. In a sorption experiment, the polymer is exposed to a penetrant and the gain or loss in mass of the polymer, M_t, is monitored as a function of time, t. The quantity M_t is normalized to the mass of the polymer at its equilibrium hydration level M_∞ and analyzed according to power law equation 2.12 [58].

$$\frac{M_t}{M_\infty} = k\, t^n \qquad (2.12)$$

Where, M_t is the mass of solvent absorbed at time "t", M_∞ is the mass of the solvent absorbed at equilibrium; k is a kinetic constant, characteristics of the polymeric system, n is an empirical number called as transport exponent, which is indicative of the mechanism of solvent transport in the polymer gel.

A value of n=0.5 for planar systems indicates Fickian diffusion, while non-fickian or anomalous behaviour is characterized by an n lying between 0.5 and 1.0, with a limit of n=1.0 identifying Case II transport. Peppas [59] reported an extension of the analysis to other geometries. Hopfenberg [60] have reported that a polymer may exhibit all of the three types of diffusion by traversing a wide range of temperature, penetrant activity and penetrant type.

2.4.2 Determination of the diffusion coefficient

The sorption experiment involves exposing a specimen of polymer with aspect ratio (length/thickness) greater than 10 to the penetrant and the gain (absorption) or loss (desorption) in mass of the specimen is monitored as a function of time. The results for a sorption experiment are presented as a plot of M_t/M_∞ versus $t^{1/2}/L$, where M_t is the amount of the penetrant sorbed at time t, M_∞ is the amount of the penetrant sorbed at equilibrium and L is the thickness of sample. The features of the Fickian sorption have been summarized by Fujita [61]. The pertinent features for Fickian type transport are:

(a) Both absorption and desorption curves should be linear, with respect to $t^{1/2}$ in the initial portion, generally up to 60% of equilibrium.

(b) Beyond the linear region, curves are concave towards the time axis.

(c) The curve for films of different thickness superimpose with each other.

The failure of any of these criteria classifies the sorption process as either anomalous or case II.

The rate of approach to equilibrium can be characterized by a diffusion coefficient value "D" which can be calculated from the equation 2.13 [62].

$$\frac{M_t}{M_\infty} = 4\left(\frac{Dt}{\pi l^2}\right)^{1/2} \qquad (2.13)$$

From this "D" value obtained experimentally, a sorption curve can be simulated using equation 2.14 [63], which can be compared with experimentally determined diffusion plot.

$$\frac{M_t}{M_\infty} = 1 - \sum_{n=0}^{\infty}\left\{\frac{8}{(2n+1)^2\pi^2}\right\} e^{\left\{-(2n+1)^2\pi^2\left(\frac{Dt}{L_0^2}\right)\right\}} \quad (2.14)$$

The mathematical calculations and non-linear curve fitting were carried out using Mathcad and Origin 6.1 software program.

In order to investigate the swelling rate of different copolymer gels in water medium, the mean swelling time (MST) was estimated according to following equation (2.15) [64].

$$MST = \left(\frac{n}{1+n}\right) k^{-1/n} \quad (2.15)$$

Where, n and k having same meaning as in power law equation (2.12)

Further, the rate of swelling at different temperatures was evaluated in terms of the penetration velocity (V) of solvent, determined by weight-gain method as described elsewhere [65]. The penetration velocity was calculated from the slope of the initial portion of water uptake curve by following equation (2.16)

$$V = \left(\frac{1}{r*A}\right) * \left(\frac{dW}{dt}\right) \quad (2.16)$$

Where, dW/dt is the slope of the weight gain vs time curve, r is the density of the solvent, A is the area of one face of the disc.

Arrhenius equation was used to estimate the activation energy of diffusion for gels. Arrhenius equation in modified form (equation 2.17) was applied to the experimental data to estimate the activation energy for the diffusion of water through hydrogel matrices as reported earlier [66].

$$D = D_0 \exp\left(-\frac{E_D}{RT}\right) \quad (2.17)$$

Where, E_D is the apparent activation energy for the diffusion process.

2.5 Characterization Techniques

2.5.1 UV-Visible Spectroscopy

UV/Vis spectroscopy is used in the quantitative determination of solutions of transition metal ions and highly conjugated organic compounds. The method is most often used in a quantitative way to determine concentrations of an absorbing species in solution, using the Beer-Lambert law (equation 2.18):

$$A = \log_{10}\left(\frac{I_0}{I}\right) = \varepsilon * c * L \quad (2.18)$$

Where:

I_o = intensity of incident light

I = intensity of transmitted light

ε = molar extinction coefficient

c = concentration of the absorbing species (mol/L)

L = path length of the light-absorbing sample (cm)

A spectrophotometer model Evaluation 300 by Thermo Electron with single xenon lamp source, wavelength range 190nm to 1100nm, wavelength accuracy $\pm$ 0.3nm and silicon photodiode detector was used to carry dye adsorption study.

2.5.2 Fourier-Transform Infra-red spectroscopy (FTIR)

Infrared spectroscopy (IR) is an important analytical technique by which liquids, solutions, pastes, powders, films, fibres, gases and surfaces can all be examined with a proper choice of sampling technique. IR is used both to gather information about the structure of a compound and as an analytical tool to assess the purity of a compound.

The wave numbers (ν cm^{-1}) is the frequency of vibration as given by the equation 2.19 depends upon the nature of the functional groups in a molecules and therefore, synthesized and modified compounds can be characterized by this technique. In our study as we have added number of molecules to the surface of the base polymer by the surface modification grafting process and also studied the copolymerization of different monomers. Therefore, FTIR technique can be useful in characterization of the radiation induced synthesized materials. Some of important functional groups used to characterize the samples are listed in Table 1.1 with their corresponding wave numbers.

$$\nu\ (cm^{-1}) = \frac{1}{2\pi c}\sqrt{\frac{f(m_1+m_2)}{(m_1 m_2)}} \qquad 2.19)$$

Where, ν (cm^{-1}) is the frequency of the vibration which has been derived from Hook's law for diatomic molecule and m_1 and m_2 are the mass of atoms 1 and 2, respectively, in g, c is the velocity of light (cms^{-1}).

Table 2.1 IR Absorptions for Representative Functional Groups used in the study

Functional Groups	Molecular Motion	Wavenumber (cm^{-1})
Alkanes	C-H stretch	2950-2800
	CH_2 bend	~1465
	CH_3 bend	~1375
	CH_2 bend (4 or more)	~720
Aromatic	C-H stretch	3020-3000
	C=C stretch	~1600 & ~1475
	C-H bend (mono)	770-730 & 715-685
	C-H bend (ortho)	770-735
	C-H bend (meta)	~880 & ~780 & ~690
	C-H bend (para)	850-800
Carboxylic	O-H stretch	3400-2400
	C=O stretch	1730-1700
	C-O stretch	1320-1210
	O-H bend	1440-1400
Esters	C=O stretch	1750-1735
	C-C(O)-C stretch (acetates)	1260-1230
	C-C(O)-C stretch (all others)	1210-1160
Amines	N-H stretch (1 per N-H bond)	3500-3300
	N-H bend	1640-1500
	C-N Stretch (alkyl)	1200-1025
	C-N Stretch (aryl)	1360-1250
	N-H bend (oop)	~800

Therefore grafted and hydrogels samples were characterized using Fourier transformed infrared (FTIR) spectroscopy to confirm the grafting of AETC, MAETC, VBT on to cotton fibrils and copolymerization of MAETC-HEMA hydrogel and measurements were performed using FTIR spectrophotometer (JASCO, model FT/IR-610). Samples were ground at liquid nitrogen temperature and mixed with KBr to prepare

discs by compression molding press. FTIR spectra were recorded in the range from 400 to 4000 cm^{-1} with a resolution of $4cm^{-1}$ and averaged over 100 scans.

2.5.3 Elemental Analysis (EA)

Elemental analysis is the technique which gives elemental and sometimes isotopic composition of the compounds by analyzing the corresponding flash combusted compounds like carbon dioxide, water and nitric oxide. It examines the weight percent of each element in the compound to determine the compound's composition. The most common form of elemental analysis is CHN analysis. Compounds which are modified with the MAETC, AETC, and VBT containing the quaternary ammonium group which has nitrogen elements. Percentage of nitrogen elements was analyzed by using model Thermo Finnigan Flash EA112 elemental analyzer. Further the composition of the Nitrogen was correlated with percentage of grafting.

2.5.4 Thermogravimetric Analysis (TGA)

Thermogravimetric analysis (TGA) is one of the members of the family of thermal analysis techniques in which the amount and rate (velocity) of change in the mass of a sample as a function of temperature [67] or time in a controlled atmosphere is measured to characterize a wide variety of materials. TGA is the technique which can insight the thermal stability and also gives the upper use temperature of a material, particularly surface modified samples in the study. Beyond this temperature the material will begin to degrade. Three ways a material can lose mass during heating are through chemical reactions, the release of adsorbed species, and decomposition. All of these indicate that the material is no longer thermally stable. In the present study of radiation induced grafting, it is very important to investigate the thermal stability and upper temperature

limit of use of the end products. Therefore, TGA technique have been used to check the thermal stability of the grafted samples using Mettler 3000 instrument in air atmosphere at a heating rate of $10^{o}C\ min^{-1}$ and temperature range of room temperature to $600^{o}C$. Instrument has temperature range from room temperature to 1100 °C with cooling rate 60 °C in 8.8 min with balance resolution 1µg.

2.5.5 Scanning Electron Microscope (SEM)

Scanning electron microscope (SEM), which is a type of electron microscope, images a sample by scanning it with a high-energy focused beam of electrons in a raster scan pattern (line-by-line scanning is what creates a raster or rectangular area pattern). The electrons interact with the atoms that make up the sample producing signals that contain information about the sample's morphology (texture), chemical composition, crystalline structure and orientation of materials making up the sample. Secondary electrons are generally detected which gives the morphology and topography on samples. The surface morphology of grafted samples and copolymer hydrogels were characterized by using TS5130 model, TESCAN with resolution 3.5nm and max magnification is one Lac times. It had a Tungsten Filament with microscope VEGA MV2300T/40 (TS 5130MM). The Maximum acc. Voltage that can be used is 30KV. The stage is 3-axis (x,y and rotation) motor controlled and two axis(tilt a& z axis) manual.

2.6 Chemicals reagents and Microorganism

[2-(Methacryloyloxy)ethyl]trimethylammonium chloride (MAETC), Molecular weight. 207.7 in form of 75% (w/v) aqueous solution, [2-(Acryloyloxy)ethyl] trimethyl-ammonium chloride (AETC), 80% (w/v) aqueous solution in water from Aldrich chemicals and Vinylbenzyltrimethylammonium chloride (VBT) (Molecular weight

=211.74) from Fluka was used. 2-Hydroxyethyl methacrylate (HEMA), Molecular weight 130.14 from Aldrich chemicals (purity~97%), was further purified by vacuum distillation at 78^{o}C and 5mmHg pressure. Only the middle 70% of the distillate was collected and used. All other chemicals used were of AnalaR (Purity 99%) grade. Dyes Acid Blue 25 (AB25, dye content approx. 45%, Molecular Weight 416.39), Acid Blue 74 (AB74, dye content approx. 85%, Molecular Weight 466.36) and acid yellow 99 (AY99, dye content approx. 40%, Molecular Weight 496.35) from Aldrich were used as received. KSCN (AnalaR grade, purity >99%) and methanol (AnalaR grade, purity >99%) from S.D. Fine Chem Limited, India, were used as received without further purification. Double distilled water (conductivity 1.9μScm^{-1}) was used for preparing all solutions and for swelling studies. The cotton fabric procured from a local supplier in cloth form was washed and dried for 5 cycles finally followed by rinsing with double distilled water. The washed cotton samples were dried in vacuum at 50^{o}C and stored in desiccator for further use. All other chemicals were of AnalaR grade. Double distilled (DD) water and Methanol (Purity >99%) were used for preparation of all solutions. The grafted samples were soxhlet extracted for 8 hours using water as an extractant to remove any homopolymer.

Escherichia coli JM109, *Pseudomonas fluorescens* (lab isolate), *Staphylococcus aureus* ATCC 6538P, *Bacillus cereus* MTCC 470 cultures were maintained at 4^{o}C. Before the start of the experiment, the cultures were grown on nutrient agar for 2 days at 37^{o}C. The isolates were sub-cultured twice before inoculation. The long-term storage of cultures was done in 20% glycerol (v/v) at 20^{o}C. All the bacterial counts were done on plate count agar, (Himedia, Mumbai, India) incubated at 37^{o}C for 24 h during the course of this work.

2.7 Anti-bacterial studies

The two purposes of antimicrobial test method were to determine the susceptibility of the textile materials to mildew and rot and to evaluate the antimicrobial efficacy of fungicides on textile materials. The performance of antimicrobial susceptibility testing is important to confirm susceptibility to chosen empirical antimicrobial agents, or to detect resistance in individual bacterial isolates. In general, there are two methods of testing antibacterial efficacy i.e. qualitative and quantitative methods which are explained in details below were used to perform the antibacterial characteristics of the samples.

2.7.1 Qualitative test (Agar Diffusion assay)

Agar diffusion refers to the movement of molecules to be tested for their susceptibility against test microorganism, through the matrix that is formed by the gelling of agar. When the seaweed extract known as agar is allowed to harden, it results a porous matrix which is permeable. Molecule such as antibiotics, QUATS are able to diffuse through the agar. In this method, molecule to be tested is applied to a well cut into the agar on which the bacterium in question is swabbed uniformly across a culture plate. Thus, the molecule will tend to move from well region of high concentration to the surrounding regions of lower molecule concentration through the porous structure of agar. If the compound is effective against bacteria at a certain concentration, no colonies will grow where the concentration in the agar is greater than or equal to the effective concentration. This is called zone of inhibition (D) as shown in figure 2.3. The diameter of the inhibition zone is a function of the amount of compound in the well and susceptibility of the microorganism. The larger the clear area around the agar well, the more effective the compound.

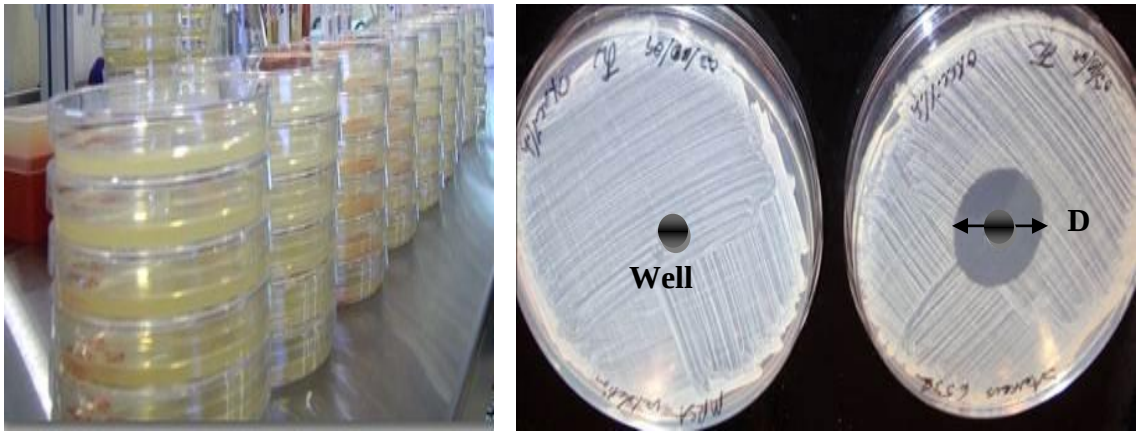

Figure 2.3: Agar well cup method for qualitative determination of efficacy and efficiency of an antibacterial compound

Method must be rigorously standardized since zone size is also dependent on inoculum size, medium composition, temperature of incubation, excess moisture and thickness of the agar.

2.7.2 Quantitative Test (Serial dilution method)

Because of very small size of microorganism like bacteria, counting the number of bacteria in a sample can be difficult. Although direct counts are possible with a microscope but it requires a lot of time and expertise. An easier method is to spread bacteria over a wide area (i.e. nutrient agar plate) and count the number of colonies that grow. If the bacteria are spread out enough, each bacterial cell in the original sample should produce a single colony. Dilution of suspension with higher bacterial counts can be useful for getting more manageable results [68]. Therefore, proper dilution of the suspension to be plated has to be made in such a way that colonies developed after incubation comes in the range of 30-300. Greater than 300 colonies on the agar plate and less than 30 lead to a high degree of error. A high count can be confounded by error in counting too many small colonies, or difficulty in counting overlapping colonies and less

than 30 CFU are not statistically reliable. Serial dilution is a common technique used in many immunologic procedures where serial dilutions are made by making the same dilution step over and over, using the previous dilution as the input to the next dilution in each step as shown in figure 2.4. Serial dilution is adopted technique over single step dilution because of very high volume of diluents and very low volume (in µl) of suspension to be diluted is required for single step dilution which leads to very high consumption of diluents and experimental error in measurement of microlitre of suspension. Once the culture has been diluted it can be spread on agar plates. Agar plates allow for individual bacterial cells to be separated spatially with low probability of having two cells very close to each other. When each of these spatially separated cells multiplies, spatially separated colonies are formed. These are called clonal colonies as each visible colony arises from a single progenitor cell. The number of colonies observed is thus a direct measure of the number of bacteria spread on the surface of the plate. The purpose of serial dilution is to determine the number of bacteria per unit volume in the original culture, determination of the culture density in cells per ml.

Determination of antibacterial activities gives rise to three possible results as:

1) A significant increase of the initial bacteria population

2) An inhibition of the bacteria growth comparing the antimicrobial product with the control sample for which there is a multiplication of test bacteria population inoculated at the beginning of the time contact.

3) A quantitative reduction of the number of test bacteria inoculated at the beginning of the time contact. The second and the third cases indicate an antibacterial activity from the modified cotton fibrils and the terms used to differentiate the two performances are biostatic and biocide.

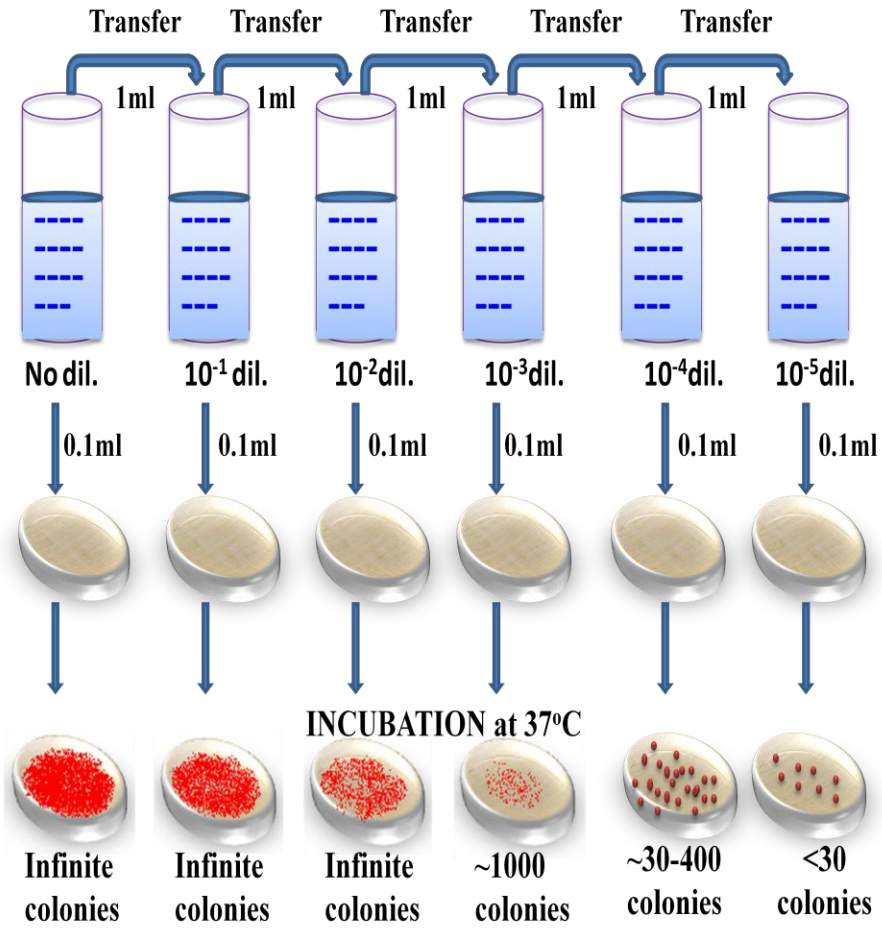

Figure 2.4: Serial dilution plate counting method for quantitative testing of antibacterial compound

Chapter 3

Radiation induced synthesis of 2-Hydroxyethylmethacrylate-co-[2-(Methacryloyloxy)ethyl] trimethylammonium chloride hydrogels: Dynamic and equilibrium swelling kinetics

Keywords: Gamma radiation, Copolymer, 2-Hydroxyethylmethacrylate, [2-(Methacryloyloxy)ethyl]trimethylammonium chloride, Hydrogel, Swelling

3.1 Introduction

Hydrogels are three-dimensional networked structures of polymer chains, which swell, in the aqueous environment without dissolving or losing their structural integrity [69]. The network is often formed by covalently crosslinked polymers, but ionic bonds, crystalline regions, entanglements and Van der Waals forces can also lead to water swellable network materials [70, 71]. Water imbibing properties of hydrogels enable them to be employed for several pharmaceutical applications, sensors, separation membranes and adsorbents [72-76]. The multitude of hydrogels synthesized in recent years has made available a number of choices for polymeric formulations. The most appropriate approach for development of a hydrogel with desired properties is to correlate the macromolecular structure of the polymer with the desired swelling, mechanical and other required characteristics. The applications of a hydrogel are mainly governed by factors like, equilibrium swelling degree, dynamics of swelling and stimuli responsive property.

Stimulus responsive hydrogels have received considerable attention due to their ability to exhibit reversible volumetric changes in response to external stimuli like pH, temperature, electric field. In order to incorporate the specific characteristics stimuli responsiveness or controlling the swelling behavior required for specific applications, a variety of copolymers such as poly(acrylic acid) [77], polymethacrylic acid [78]. Poly

NIPAM poly(N-isopropylacrylamide) [79] and similar copolymers have been synthesized. The judicious choice of the components of binary hydrogels can lead to hydrogels that exhibit a combination of unique physiochemical properties, thus permitting their wide-range of applications and often exceptional possibilities for practical applications. For radiation-synthesized gels, properties of gel may be programmed by the choice of the main polymer that forms the framework, the co-monomer, co-monomers content, and the radiation dose.

Poly(2-hydroxyethyl methacrylate) (PHEMA) based gels have been subject of interest for scientists and technologists because of its versatile properties like biocompatibility, good mechanical strength, high gel fraction, and ease of synthesis [80]. Modification of the swelling behavior of PHEMA by co-polymerizing HEMA with other co-monomers has been studied to achieve optimum levels of swelling for various applications [81-83]. Ratner et al have investigated the copolymerization of polyHEMA and poly methyl methacrylate that make the gel thinner for easy diffusion of oxygen and increase its water of hydration otherwise pure polyHEMA is too thick to diffuse sufficient oxygen [84]. In little contrasting application Jorge et. al. studied the copolymer of HEMA (2-hydroxy-methyl-methacrylate) and MMA (methyl-methacrylate) and explored potential use to relieve injured articular cartilage. In the studies, they incorporated the MMA to increase the mechanical strength and decrease the water contents [85]. HEMA does not produce a high swelling hydrogel unless it is combined with a polar monomer. Introduction of ionic segments in neutral hydrogels is an easy method to regulate the swelling extent [86]. However, the addition of another polar monomer with a different solubility nature can produce undesirable structural heterogeneity in the final product. Therefore, the formulation should contain very little of

the comonomer; moreover, high concentration of a more water soluble monomer can offset the expected mechanical properties of HEMA. Various research groups have tried to incorporate hydrophilic co-monomer to increase the hydrophilicity of polyHEMA. Hossain et al studied the copolymerization of polyHEMA and polyacrylic acid to make the super porous hydrogel with various compositions of 2-PHEMA and acrylic acid [87]. Belma and group have also increased the hydrophilicity of polyHEAM by adding polyethylene glycol in the gel matrix [88]. Goel et al had earlier incorporated the Vinybenzyltrimethyl ammonium chloride (VBT) monomer, with high charge density quaternary ammonium group, in polyHEMA matrix to increase the hydrophilicity and ionic strength responsive characteristics [89]. As VBT containing the benzene moiety, it is proposed that MAETC not bearing the benzene moiety might enhance the more hydrophilicity in poly HEMA with very low concentration than the VBT. Therefore, in this chapter we studied the incorporation of MAETC as comonomer bearing quaternary ammonium group. Swelling kinetics and equilibrium swelling extent depend on the type and proportion of ionic monomer in the co-polymer hydrogel [90, 91]. Therefore in the chapter equilibrium and kinetics parameters have been investigated in details.

The conventional thermo-chemical technique, gamma irradiation or electron beam irradiation has been utilized to synthesize binary or ternary co-polymer hydrogels to combine the desired properties of all the parent components in the form of interpenetrating polymer network (IPN), grafted matrices or random copolymers gels [92-95]. Radiation induced synthesis of hydrogels has several advantages over conventional methods viz. high purity products, easy process control, room temperature synthesis and possibility of sterilization during synthesis [96-98]. Therefore, gamma radiation induced synthesis method has been investigated. Radiation induced copolymer

hydrogel has also been characterized by SEM and FTIR spectroscopy. In the end chapter will include the investigation about the effect of introducing [2-(Methacryloyloxy)ethyl]trimethylammonium chloride (MAETC), a cationic monomer, on swelling extent and swelling kinetics of radiation co-polymerized PHEMA gel. Perturbation on swelling due to temperature change and ionic interaction with various ionic moieties present in swelling medium has also been studied.

3.2. Synthesis and characterization of copolymers of PolyHEMA & PolyMAETC

2-Hydroxyethyl methacrylate (HEMA), molecular weight 130.14, from Aldrich (purity >97%), was further purified by vacuum distillation at 78°C and 700 Pa pressure. Only the middle 70% of the distillate was collected. Cuprous chloride was added to the distillation flask to inhibit polymerization during distillation. Rests of the chemicals used in the study have been listed in chapter 2.

3.2.1 Radiation induced synthesis of hydrogels

HEMA, MAETC solution and water were mixed in various ratios for synthesizing gels of different compositions. The solutions were thoroughly stirred and filled in clean glass tubes (inner diameter=2 cm and length=7-8 cm), deoxygenated at $<10^{-3}$ torr vacuum at liquid nitrogen temperature, freeze-thawed and sealed. Polymerization was carried out by irradiating the sealed samples at room temperature with gamma rays from a ^{60}Co γ-source at a dose rate of 5 $kGyh^{-1}$ as determined by Fricke dosimetry. After irradiation the glass vials were carefully broken to obtain copolymer gels in cylindrical form. The samples were rubbery and transparent at room temperature. These samples were cut into 0.6-1.8 mm thick disks with a sharp edged blade and left in double distilled water to swell to equilibrium and dried. Swelling drying was continued for several cycles and finally the

samples were dried in an oven at 35^{o}C under vacuum to constant weight. The dried samples were stored in a desiccator for further use.

3.2.2 Radiation induced Mechanism of preparation of the copolymer hydrogel

Radiation synthesis of copolymer of MAETC and HEMA can be illustrated by considering the radical reaction mechanism. Copolymer hydrogel has been synthesized by taking corresponding aqueous solution of monomers MAETC and HEMA in a fixed ratio.

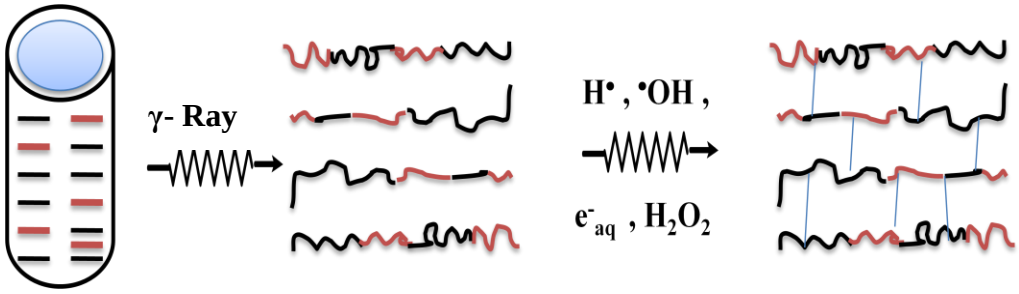

Scheme 3.1: Radiation induced synthesis of Copolymer Hydrogel

In the first step as shown in scheme 3.1, radiolysis of aqueous solution have produced number of radicals species like OH, H, e^-_{aq} which have polymerized the copolymer by radical reaction mechanism. Further, Hydroxyl radicals have been shown to be the main species responsible for reactivity transfer from water to the polymer chains. They abstract hydrogen atoms from macromolecules (copolymer), thus polymer radicals are formed. These macro-radicals are localized on carbon atoms and recombine with nearby macro- radical's gives the 3D network called copolymer hydrogel. Depending upon the concentration of polymer and dose rate may also give the microgel which is out of scope of the present studies.

3.3 Characterization of radiation induced synthesized hydrogel

3.3.1 FTIR Studies

Samples were thoroughly ground at liquid nitrogen temperature and mixed with KBr. The mixture was compressed to prepare disc for FTIR analysis. FTIR spectra were recorded in the range from 400 to 4000 cm^{-1} with a resolution of 4 cm^{-1} and averaged over 100 scans. Figure 3.1 shows the FTIR spectra of PHEMA, HEMA-co-MAETC polymer (HM31) and MAETC. The chemical structures of MAETC and HEMA are same except the terminal groups i.e. OH group in HEMA and $–N(CH_3)_3Cl$ group in MAETC. So the IR spectra of all the three polymers gels are almost similar except the extra peak for CN stretching at 1240 cm^{-1} appeared in MAETC and HEMA-co-MAETC gel. The appearance of sharp peak at 1735 cm^{-1} gives the signature of C=O stretching vibrations of methacrylate group in HEMA-co-MAETC copolymer gel.

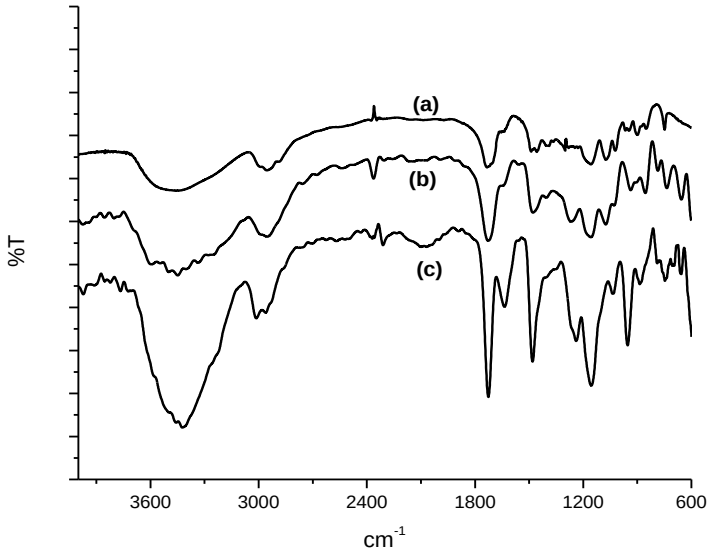

Figure 3.1: FTIR spectra (a) PHEMA (b) HEMA-co-MAETC (HM31) (c) MAETC

3.3.2 Scanning Electron Microscopy (SEM)

HEMA-co-MAETC copolymer gels with different content of MAETC were investigated using SEM to understand the inner morphology of the gels. The hydrogel samples for SEM were prepared by initially lyophilizing the gel samples swelled to equilibrium in liquid nitrogen.

The lyophilized hydrogel samples were then fractured carefully and mounted on the base plate by carbon tape and coated with gold using vapor deposition technique. The gel surfaces were scanned at 1000X magnification to investigate their pore structure. The morphology of gels is shown in figure 3.2. Although, the freeze-drying of hydrogel may lead to some structural artifacts of the specimens, the dramatic differences in the morphology observed between hydrogels are presumably of intrinsic nature since the fixation procedures were identical among all hydrogels. The results showed that the HM35 gel showed poor porous architecture and the pore size of the gel increased gradually with MAETC content. SEM micrograph of gel with highest ionic monomer content (HM31) showed lump structure with highly porous architecture. The increased porosity of the gels was also confirmed by the degree of swelling of the gels (Table 3.1). The pore boundaries of copolymer gels were more distinct with the increase in the MAETC content in the gel.

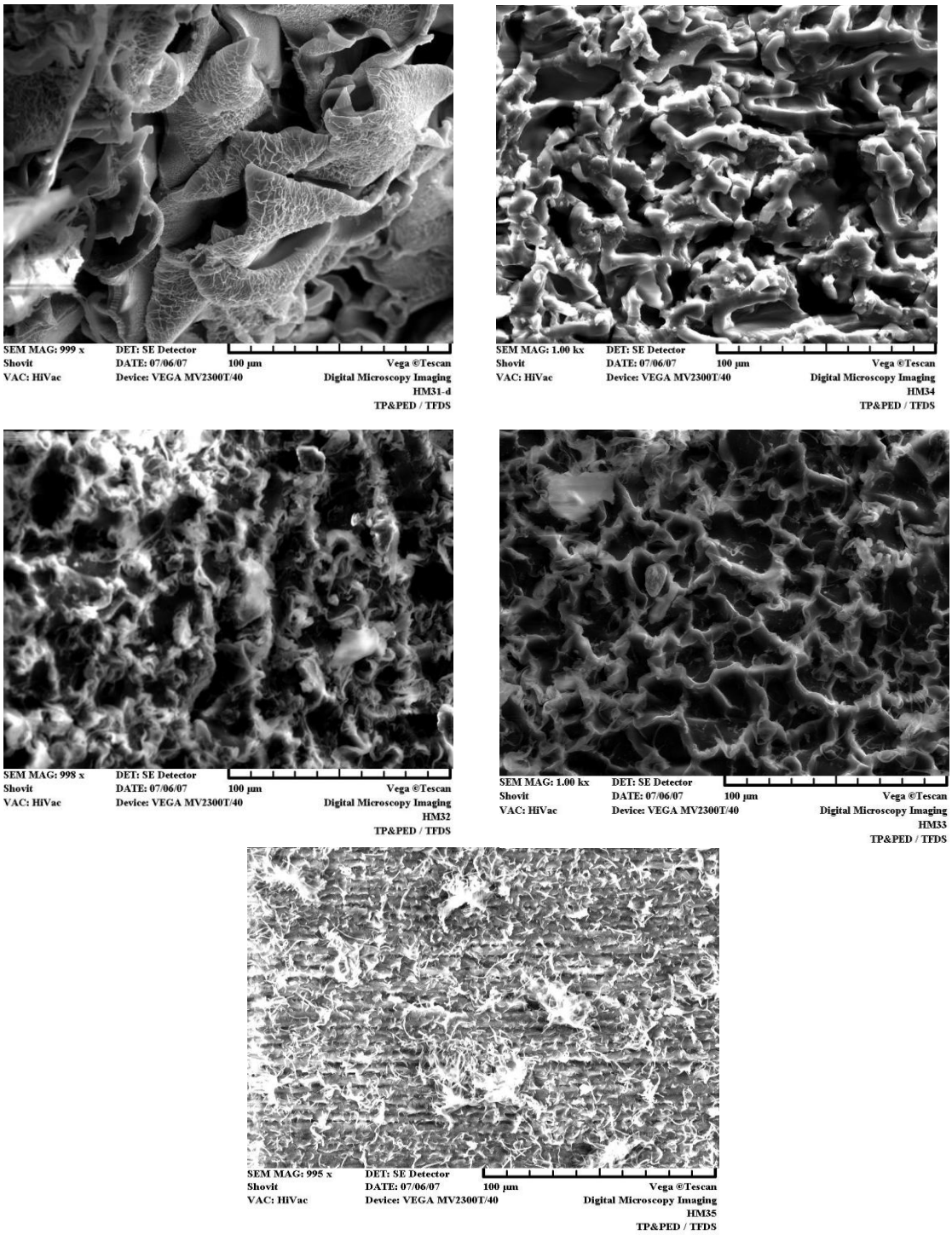

Figure 3.2: SEM micrographs of MAETC-co-HEMA gels

3.4. Swelling of gels and swelling extent measurements

The progress of the swelling process was followed gravimetrically by monitoring the increase in the mass of samples at different time intervals. In a typical swelling experiment, a pre-weighed circular piece of gel was immersed into a definite volume of swelling media, taken out at different time intervals, blotted free the surface water using laboratory tissue paper, weighed and returned to the swelling medium. The percentage equilibrium degree of swelling (EDS %) and swelling ratio (SR) of the gels were determined using equations 2.10 and 2.11 (refer to chapter 2) respectively.

3.4.1 Equilibrium swelling

(a) Effect of gel composition on swelling in water and NaCl solution

Introduction of small amount of ionic monomer into the non-ionic matrices have been found to affect equilibrium swelling and swelling mechanism of parent gel matrix [72, 99, 100]. The effect on the extent of swelling of the PHEMA matrix**,** due to the incorporation of MAETC was investigated by varying the concentration of the ionizable monomer MAETC in the feed solution. Table 3.1 shows the change in swelling extent of the gel with MAETC concentration. It can be seen that EDS increased almost linearly with the amount of MAETC in the matrix.

When dry hydrogel is kept in water, water diffuses into the hydrogel, it swells and eventually reaches equilibrium swelling when no further swelling takes place. The total osmotic swelling pressure for polyelectrolyte gel is expressed by equation (3.1) [101].

$$\pi_{tot} = \pi_{mix} + \pi_{elast} + \pi_{ion} + \pi_{elect} \qquad (3.1)$$

Where, π_{mix} = osmotic swelling pressures due to mixing of polymer chains with solvent,

π_{elas} = osmotic swelling pressures due to elastic response to changes in the configuration of the polymer network,

π_{ions} = osmotic swelling pressures due to mixing of ions from solution and from the polymer network,

π_{elec} = osmotic swelling pressures due to changes in the electrostatic interactions of ionized groups upon swelling.

At equilibrium, there are mainly four pressure components that balance each other and determine the extent of swelling of a hydrogel [101]. However for a non-ionic gel like PHEMA in equilibrium with the solvent, the π_{ions} and π_{elect} components of pressure do not contribute and therefore, the total osmotic swelling pressure is given by equation (3.2).

$$\pi_{tot} = \pi_{mix} + \pi_{elas} \qquad (3.2)$$

The parameters π_{mix} and π_{elas} are related to crosslink density and the Flory-Huggins parameter (χ). Thus, the key parameters that determine the swelling of non-ionic gel in a solvent are the crosslink density and Flory-Huggins parameter (χ) [102]. If the gels contain ionizable groups, the additional ion related terms π_{ions} and π_{elec} have to be included in equation (3.2) [101, 102].

Unlike ionizable polymers, such as poly (acrylic acid), MAETC polymers are strong polyelectrolytic salt. The positively charged, fixed ions generated on the polymer chains due to ionization repel each other, and this repulsion tends to stretch polymer chains to an extended state from a closed coiled state, which causes opening of the polymer chains and overall swelling of the hydrogels.

Table 3.1 Composition and EDS of HEMA-co-MAETC gels synthesized at a dose rate of 5.0 $kGyh^{-1}$ for total dose of 3.75 kGy in water and NaCl solution

Sample	[HEMA] (mole fraction)	[MAETC] (mole fraction)	EDS (%)				
			Water	0.01 N NaCl	0.05N NaCl	0.1 N NaCl	0.5 N NaCl
HM31	0.85	0.15	7394	2729.7	1191.1	766.1	325.7
HM32	0.89	0.11	3997	1665.3	742.3	500.1	207.9
HM33	0.91	0.09	2817	1436.3	581.3	393.4	165.6
HM34	0.93	0.07	2063	1316.7	471.9	326.4	139.8
HM35	0.97	0.03	268	198.9	115.4	98.6	71.9

Thus, the extent of swelling increases with an increase in the number of ionizable groups in the network. Also, the water binding sites, such as tetra-alkylammonium ions, are known to have a net structure causing effect [103]. Their high electric fields not only polarize, immobilize and electrostrict the nearest neighbor molecules, but they also induce additional order beyond the first layer of water molecules. The higher attractive field that can be felt to several layers in the case of $-N^{+}(CH_3)_3$ probably causes many more layers of water associated to the first layer, which is in immediate vicinity of the polymer than in comparison to the OH group in PHEMA and hence, more water uptake is seen in gels containing MAETC. Similar significant increase in equilibrium degree of two different parent matrixes on introduction of similar segments having tetra-alkyl ammonium groups have been reported recently in our studies [104, 105].

(b) Swelling behavior at different pHs

It has been reported that incorporation of a highly ionizable group, such as tetra-alkylammonium chloride or sulphonates results in polyelectrolyte gels relatively

insensitive to pH, whereas, introduction of monomers such as acrylic acid produces anionic polyelectrolyte gels whose ionization is a function of pH [41].

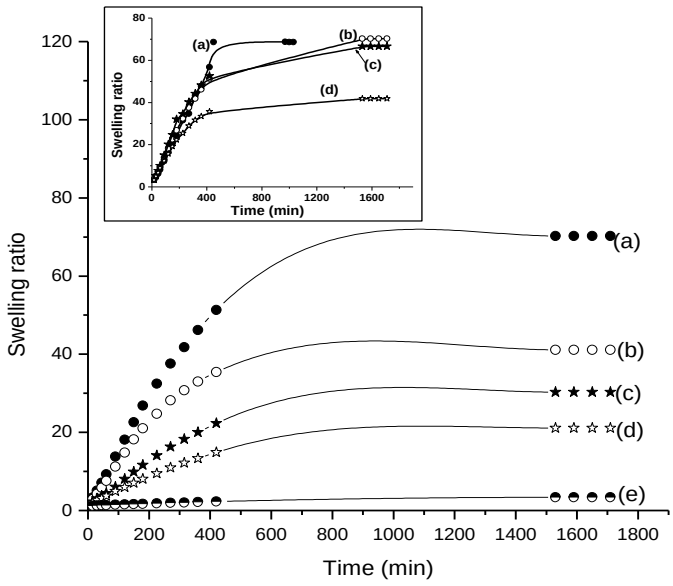

Figure 3.3: Swelling of gels at pH 10 (a) HM31 (b) HM32 (c) HM33 (d) HM 34 (e) HM35. Inset: Swelling of gel HM 31 at different pH (a)water (b) pH 10 (c) pH 8 (d) pH 3

The effect of pH on the swelling of HEMA-co-MAETC hydrogel was investigated in the pH range 3-10. The pH of the swelling medium was adjusted using $HClO_4$ and NaOH as the ions furnished by standard buffers were seen to themselves interfere with the swelling of gels. The results of these studies are shown in figure 3.3. As shown in figure 3.3 and its inset, EDS at low pH was less than that in water however at pH>7 the gels swelled almost to the same extent as in water. This observation is contrary to earlier observation reported [105] for a co-polymer gel containing vinylbenzyltrimethylammmonium chloride (VBT), a monomer similar to MAETC. For HEMA-co-VBT gels it has been reported that the EDS of the matrix did not vary with pH, when pH was maintained using $HClO_4$ and NaOH but EDS was influenced when pH

was maintained using buffers due to the ions furnished by the buffers in the aqueous medium.

(c) Swelling of gels in dye solutions

MAETC gels due to their anion exchange capability, can act as an effective anion exchange vehicles. However, pure MAETC gels, because of their very high water uptake capacity, have poor strength and dimensional stability. The copolymer matrices of MAETC with HEMA results in gel with good swelling, as well as better strength, which are easy to handle and can uptake anionic dyes. The copolymer gels were investigated for swelling in aqueous solution of monovalent anionic dyes, namely AB25, AY99 and a divalent dye AB74. Extent of swelling of gel HM31 in different dye solutions of 250ppm concentration is shown in figure 3.4. After reaching equilibrium swelling, the otherwise transparent gels showed intense color of the dyes absorbed. The dye molecule that diffuses with water into the gel gets bound to oppositely charged MAETC sites through ionic interaction. These dyes were only held through ionic interaction was confirmed by the fact that pure PHEMA matrix didn't show any affinity for any of the dyes. As the dye binds to the gel the degree of ionization of the gel decreases and so does the EDS. This observation was similar to observation reported earlier for HEMA-VBT gel [105] where presence of dye molecule showed significant decreases in EDS. Another noticeable feature was that though the dye AB74 had two binding sites instead of one in AB25 and AY99, the decrease in EDS was least in presence of AB74 though it was expected to be maximum as per the stoichiometry.

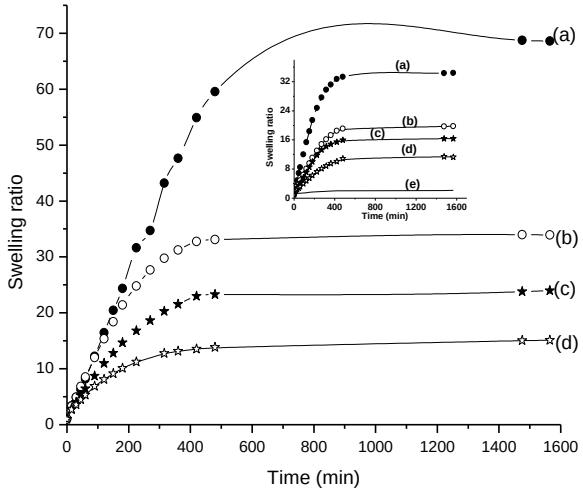

Figure 3.4: Swelling of HM31 gel in dye solutions at dye concentration of 250ppm (a) Water (b) AB74 (c) AY99 (d) AB25. Inset: Swelling of gels in dye (AB 74) solution of concentration 250 ppm (a) HM31 (b) HM32 (c) HM33 (d) HM34 (e) HM35

It may be due to the water binding sites available on the dye molecules itself; the expected decrease in EDS because of charge neutralization was probably compensated by water binding sites available on the dye molecule. The EDS in AB25 solution was lower than that in AY99 solution indicating more effective binding of AB25 in comparison with AY99, similar to HEMA-VBT system [105]. This indicates some role of the chemical structure of dye molecule in binding of the dye to the gel.

3.4.2 Swelling kinetic measurements

The dynamic swelling properties of a polymer include the solvent sorption rate, the rate of approach to equilibrium and the transport mechanism controlling the solvent sorption. Alfrey et al [57] have proposed that the transport mechanism, which indicates the relative importance of diffusion and relaxation, can be identified through the empirical equation 2.12 (refer to chapter 2). Equation 2.12 is applied to the initial stages

of swelling and the plots of $\ln(M_t/M_\infty)$ vs ln (t) yield straight line up to $M_t/M_\infty \leq 0.6$. The n and k values are obtained from the slope and intercept of the plot respectively.

The rate of approach to equilibrium can be characterized by a diffusion coefficient value "D" which can be calculated from the equation 2.13 (refer to chapter 2).This criterion was also used to confirm the transport mechanism of gels.

In order to investigate the swelling rate of different copolymer gels in water medium, the mean swelling time (MST) was determined as given by the equation 2.15 (refer to chapter 2). Rate of swelling at different temperatures was evaluated in terms of the penetration velocity (V) of solvent which is determined by weight-gain method by calculating from the slope of the initial portion of water uptake curve by equation 2.16 (refer to chapter 2).

(a) Dynamic swelling

Swelling kinetics i.e. time dependent swelling behavior of HEMA-co-MAETC gels containing different amounts of MAETC at 28^{o}C is shown in figure 3.5. It can be seen that the swelling ratio and rate of swelling of gel increased with the increase in the MAETC content in the gel matrix. In order to have more realistic insight into the effect of ionic monomers, the experimental swelling data was analyzed using power law equation 2.12 (refer to chapter 2).

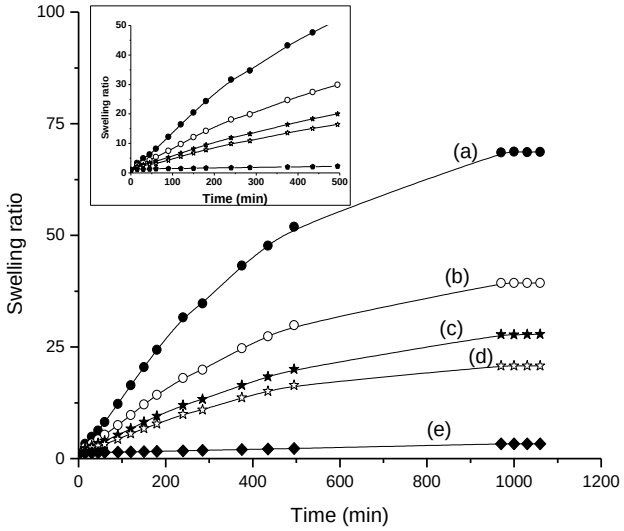

Figure 3.5: Swelling kinetics of HEMA-co-MAETC gels in double distilled water at 28^{o}C (a) HM31 (b) HM32 (c) HM33 (d) HM34 (e) HM35 Inset: Swelling kinetics at lower time

The dynamic swelling parameters of gels in aqueous medium are presented in Table 3.2. The n value for pure PHEMA gel was found to be 0.5, which is in good agreement with the results reported in earlier work for PHEMA gel prepared by different methods under different conditions [106, 107]. The swelling was found to be independent of sample thickness further indicating that the diffusion was Fickian. However, introduction of MAETC had an effect on the transport mechanism. For gel HM35, n=0.53 containing 0.03 mole fraction of MAETC indicating that introduction of MAETC in poly (HEMA) matrix even at low concentration causes shifting of swelling from Fickian to anomalous. The anomalous diffusion is characterized by rate of diffusion (k_d) ≈ rate of relaxation (k_r), whereas, for Fickian diffusion $k_d << k_r$. Thus the presence of MAETC either increases k_d to match with k_r or k_r decreases to become comparable to k_d. The first possibility is more likely as k_d may increase because of two reasons i) MAETC segments present in the matrix on ionization will repel each other to open up the matrix and cause faster diffusion of water into the matrix ii) the k_d will also be enhanced due to

the increase in concentration gradient of counter ions inside and outside of the gels as reported for several other ionic gels [108, 109]. These two factors contribute to increase in k_d, is supported by the experimentally observed fact that n values further increased with increase in MAETC content for other gels.

Table 3.2 Dynamic swelling parameters of different HEMA-co-MAETC gels in distilled water at different temperatures

S.No.	28°C		37°C		50°C		60°C	
	n	MST (min)	N	MST (min)	N	MST (min)	n	MST (min)
HM31	0.95	285.8	0.98	172.9	0.98	122.5	0.97	114.9
HM32	0.91	293.6	0.93	181.9	0.93	127.5	0.93	106.8
HM33	0.82	344.0	0.89	185.8	0.89	144.1	0.90	111.1
HM34	0.80	413.9	0.77	223.1	0.80	190.1	0.85	114.5
HM35	0.53	641.0	0.57	378.4	0.56	347.2	0.61	159.1

To further support this observation the mean swelling time (MST) and D values were estimated and are listed in Table 3.2 and Table 3.3 respectively. MST values decreased and D values increased monotonously with the amount of MAETC in the gel once again confirming that the presence of MAETC in the HEMA matrix facilitates the diffusion process. It has been reported that the transport mechanism is related to the extent of swelling of gels and it tends to shift from Fickian to non-Fickian after a certain threshold value of swelling ratio for a hydrogel [65,109].

(b) Effect of temperature

Hydrogels sometimes undergo a volume change in the response to a change in surrounding conditions such as temperature called thermo-sensitive hydrogels. Parameters like diffusion coefficient (D), mean swelling time (MST), swelling rate are and activation energy found to be function of temperatures which are important parameters to be characterized for particular applications like drug delivery, separation of biomolecules, dyes from effluents.

Table 3.3 Diffusion coefficients of water into different HEMA-co-MAETC gels at different temperatures and activation energy of diffusion

S. No.	D (cm^2s^{-1}) x 10^8				E_D (kJ/mole)
	28°C	37°C	50°C	60°C	
HM31	14.9	20.3	29.6	42.7	26.84
HM32	13.2	19.8	24.5	43.2	28.49
HM33	11.1	18.0	20.4	34.8	29.62
HM34	8.7	10.9	19.3	34.6	30.28
HM35	5.1	8.3	10.3	20.9	33.57

Therefore, the dynamic swelling parameters n, MST, diffusion coefficient and activation energy (E_a) for gels are calculated at different temperatures are given in Table 3.2 and Table 3.3. Figure 3.6 shows swelling of these gels at different temperatures. From the data in the Table 3.2, 3.3 and figure 3.6, it is clear that the extent of swelling did not change significantly with temperature, however the n values increased marginally but to the extent that the diffusion remained anomalous. Also from the slope of the profiles and from MST values it is can be inferred that swelling rate increases with temperature.

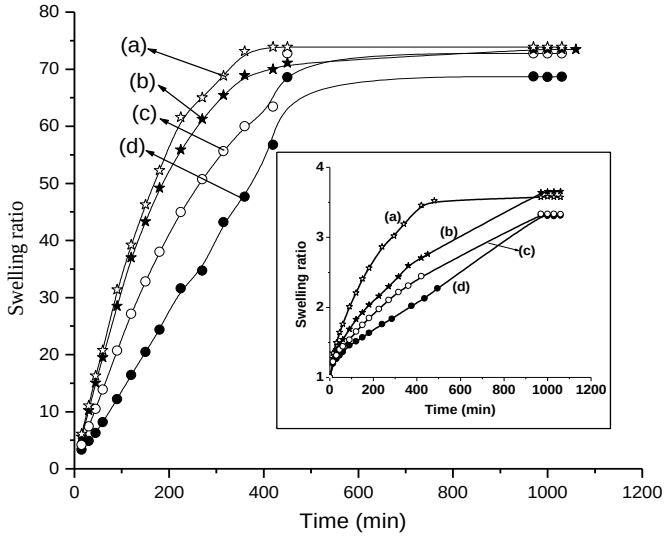

Figure 3.6: Swelling kinetics of gel HM31 in double distilled water at different temperatures (a) 60^{o}C (b) 50^{o}C (c) 37^{o}C (d) 28^{o}C. Inset: Swelling kinetics of gel HM35 at (a) 60^{o}C (b) 50^{o}C (c) 37^{o}C (d) 28^{o}C

The gel were more conducive to swelling with increase in amount of MEATC in the gel and with the temperature, was confirmed by increase in penetration velocity as shown in figure 3.7. The D values obtained using equation 2.13 (refer to chapter 2) at different temperatures is tabulated in Table 3.3. It was found that the diffusion coefficient increased with the increase in temperature of swelling medium.

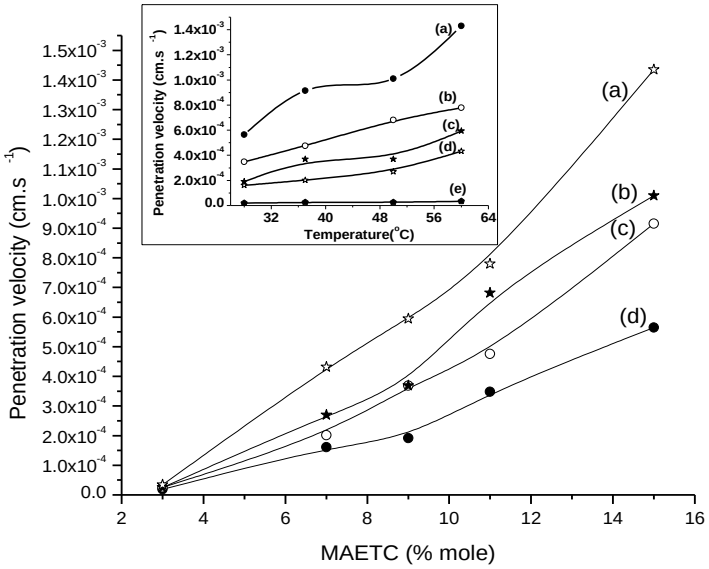

Figure 3.7: Penetration velocity as a function of gel composition (a) 60^{o}C (b) 50^{o}C (c) 37^{o}C (d) 28^{o}C. Inset: Penetration velocity as a function of temperature of swelling medium for different gels (a) HM31 (b) HM32 (c) HM33 (d) HM34 (e) HM35

Arrhenius equation 2.17 (refer to chapter 2) was used to estimate the activation energy of diffusion for gels by plotting ln (D) against 1/T plot for different HEMA-co-MAETC gels. Figure 3.8 represents the plot of and the E_D values estimated for different gels are given in Table 3.3. It is clear that E_D value decreased with the increase in the MAETC content in the HEMA gel matrix indicating incorporation of ionic monomer into a non-ionic gel matrix facilitates its rate of swelling in aqueous medium.

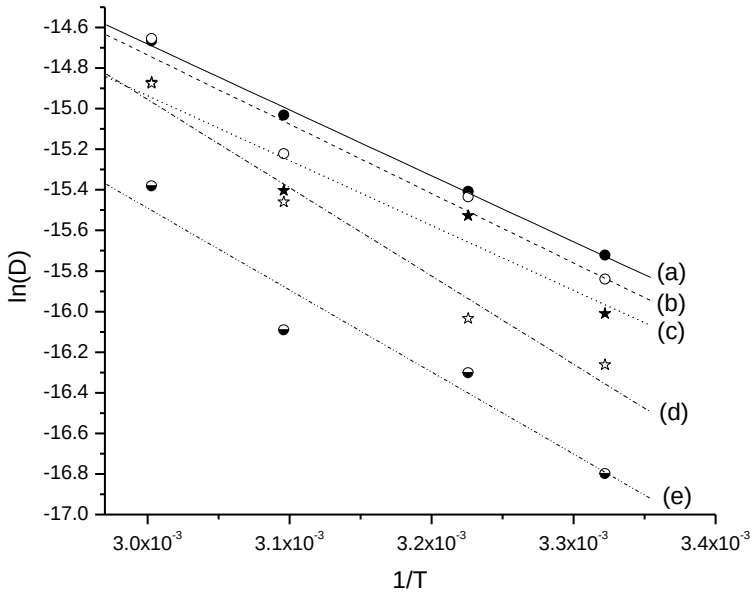

Figure 3.8: ln (D) against 1/T plots for activation energy of diffusion (E_D) determination for different HEMA-co-MAETC gels (a) HM31 (b) HM32(c) HM33 (d) HM34 (e) HM35

(c) Effect of electrolytes

The total osmotic swelling pressure of a polyelectrolyte gel given by equation (3.1) is zero at equilibrium swelling. The Donnan equilibrium theory evaluates one of the

osmotic pressure term π_{ion} of the hydrogel system by following equation (3.3) [110, 111]

$$\pi_{ion} = RT \sum_i (C_i^g - C_i^s) \quad (3.3)$$

Where, C_i is the mobile ion concentration of species i, g and s represent the gel and solution respectively.

Equation 3.3 indicates that the greater the difference between the ionic concentration inside the gel and in the external solution, larger the swelling. The mobile ion concentration inside the gel is typically much higher than the external solution, so π_{ions} is quite high. As a result, water flows into the gel to dilute the ion concentration, causing the gel to swell. As contribution due to π_{ions} is significant in extent of swelling of polyelectrolyte gels, the volume of such gels can change sharply with change in the pH or ionic strength of the swelling medium. Therefore, the swelling behavior of HEMA gels in presence of various electrolytes was investigated.

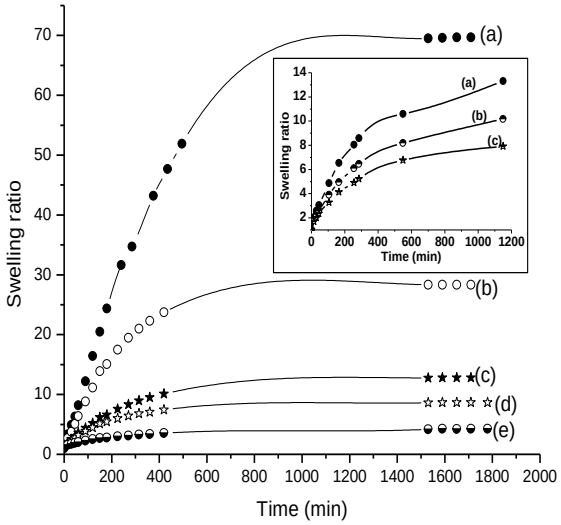

Figure 3.9: Swelling kinetics of HEMA-co-MAETC gel (HM31) in aqueous solution with different NaCl concentration (a) 0.0 N (b) 0.01 N (c) 0.05 N (d) 0.1 N (e) 0.5 N. Inset: Swelling in different salt solutions of concentration 0.05 M (a) NaCl (b) $CaCl_2$ (c) $AlCl_3$

Figure 3.9 shows swelling behavior of HM31 gel in NaCl solution of different concentrations at 28^{o}C. The swelling extent of gel decreased with the increase in the NaCl concentration. In absence of NaCl, π_{ion} is much higher due the large difference in the ion concentration inside the gel and external solution. When NaCl is added to the swelling medium, the ionic concentration in the medium C_i^s increases, which decreases the ionic concentration gradient ($C_i^g - C_i^s$) and eventually decreases the π_{ions} pressure term, resulting in lower swelling ratio. Also, the salt ions in the swelling medium cause the screening of the repulsive electrostatic interactions between ionized groups on the polymer chains and reduces the π_{elect} pressure term, resulting in coiling of the polymer chains reflected as a decrease in the equilibrium swelling of the gel (Table 3.1).

Table 3.4 lists the n, MST and D values calculated from experimental data on swelling in NaCl solution. The decrease in n value suggests that the transport mechanism tends to shift from anomalous to Fickian with increase in NaCl concentration. This may be attributed to the fact that presence of NaCl screens the repulsive forces between the ionic groups on MAETC, which causes comparatively less swelling of the gel and allows gel to behaves like non-ionic gel {like pure poly(HEMA), n=0.5}.

Table 3.4 Dynamic swelling parameters of HEMA-co-MAETC gels in NaCl solution at 28^{o}C

S.No.	0.01 N NaCl			0.05 N NaCl			0.1 N NaCl			0.5 N NaCl		
	n	MST$^{\#}$	D*	n	MST$^{\#}$	D*	n	MST$^{\#}$	D*	n	MST$^{\#}$	D*
HM31	0.87	178.6	13.7	0.72	215.7	12.7	0.70	153.3	13.7	0.49	195.8	12.2
HM32	0.82	186.4	17.2	0.75	178.9	15.2	0.66	198.1	15.6	0.54	198.9	14.5
HM33	0.80	187.2	12.1	0.68	234.9	11.7	0.63	206.3	14.9	0.47	169.5	14.5
HM34	0.62	304.5	10.7	0.61	296.6	11.5	0.53	250.2	11.0	0.49	245.4	15.0
HM35	0.53	478.5	3.7	0.51	322.4	13.3	0.49	225.5	12.3	0.44	249.2	10.0

MST$^{\#}$= Mean swelling time in minutes

D*= Diffusion values (cm^2s^{-1}) x 10^8

As expected the MST values decreased with MAETC content however D values did not show any defined pattern for gels with higher MAETC content (HM33-HM31) probably due to random neutralization of MAETC segments in copolymer matrices during swelling which causes tortuosity in the swelling channels. The swelling of gels was followed in mono, di and trivalent ions (inset figure 3.9). For same concentration of ions the swelling extent as well as swelling kinetics followed the pattern $Al^{3+} < Ca^{2+} < Na^{+}$ on the expected lines as each Al^{3+} furnishes three Cl^{-} ions in the medium which can neutralize more sites in the gel in comparison to less number of counter Cl^{-} ions furnished by Ca^{2+} or Na^{+} in the swelling medium. Also more Cl^{-} ions furnished by $AlCl_3$ would reduce the concentration gradient (equation 3.3) to a greater extent in comparison to $CaCl_2$ or NaCl.

(d) Swelling in presence of co-solutes

Hydrogels with equilibrium water content (EWC) of around 70% have special significance because of their potential use in biomedical applications such as extended wear contact lenses, wound dressings, sanitary napkins, and super absorbent baby napkins. Therefore, from application point of view, equilibrium swelling and swelling kinetics of hydrogels in presence of biologically important fluids, have to critically assessed. Effect of some of the biologically important additives (glucose, urea) and other additives like Triton-X and 7-Deoxycholic acid (DOCA) on the swelling kinetics and swelling mechanism of HEMA-co-MAETC gels was investigated. The swelling behavior of HM31 gel in presence of various solutes is shown in figure 3.10. The swelling behavior of hydrogels like PHEMA, HEMA-co-AA [103], HEMA-co-SSS [104], HEMA-co-NVP [65], polyampholytic SSS-co-VBT gels [112] and HEMA-co-VBT [103,

89] are known to be affected by presence of solutes of biological interest viz. NaCl, urea and glucose. Comparing the swelling kinetics profile it is clear that extent of swelling of these gels was not much influenced by presence of most of the solutes tried, the swelling extent followed the trend Water~Urea~Glucose~Triton-X>DOCA i.e. only the ionic surfactant DOCA decreased the extent of swelling of the gels.

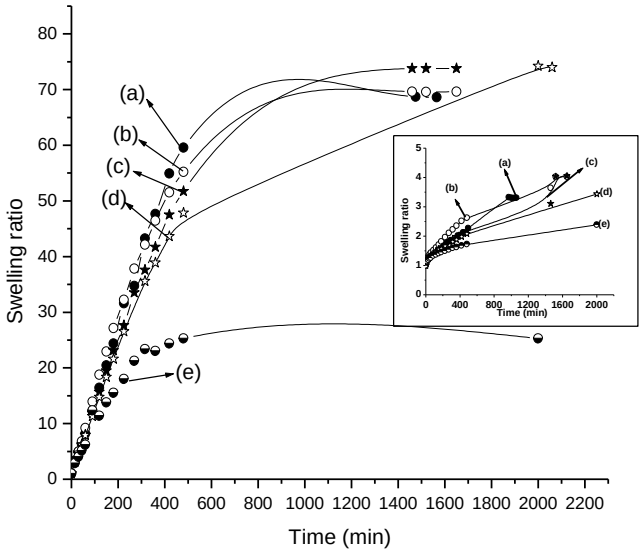

Figure 3.10: Swelling kinetics of HEMA-co-MAETC gel (HM31) in presence of solutes (a) Water (b) 0.1% Urea (c) 0.1% Glucose (d) 0.1 % Triton-X (e) 0.1% DOCA. Inset: Swelling of HM35 gel in (a) Water (b) 0.1 % Urea (c) 0.1% Glucose (d) 0.1% Triton-X (e) 0.1% DOCA

The lowest EDS in the presence of DOCA can be explained on the basis of interaction of carboxylic groups of DOCA and the quaternary ammonium group of MAETC, causing neutralization and hence, shrinking of the gel to significant extent. The urea is known to further swell matrices like PHEMA and other gels, explained on the molecular level by proposing the existence of a secondary non-covalent structure based upon hydrophobic interactions between the backbone chains [113, 114]. No such

appreciable increase in EDS for gels containing MAETC was observed indicating presence of MAETC segments in the matrix weakens the hydrophobic interactions among the chains so that no residual hydrophobic interactions are left in the matrix which could be later overcome in presence of urea to further swell the matrix. The hydrophobic interactions are too weak and are surpassed during swelling to equilibrium is confirmed by the fact that though the presence of urea did not affect the EDS but it decreased the MST (Table 3.2 & 3.5) for gels to significant extent.

Table 3.5 Dynamic swelling parameters of different HEMA-co-MAETC gels in solution of various solutes at 28^{o}C

S.No.	Glucose			Urea			Triton-X			DOCA		
	n	MST$^{\#}$	D*	N	MST$^{\#}$	D*	N	MST$^{\#}$	D*	n	MST$^{\#}$	D*
HM31	0.97	314.0	10.2	1.00	243.6	14.1	0.92	352.6	8.8	0.84	156.4	27.1
HM32	0.90	328.9	10.4	0.92	241.5	12.7	0.87	362.4	8.8	0.76	171.0	23.3
HM33	0.81	336.4	7.5	0.90	251.0	17.4	0.89	372.2	10.8	0.71	213.2	24.8
HM34	0.89	341.9	7.6	0.83	262.5	9.9	0.81	389.0	9.2	0.68	313.8	20.9
HM35	0.56	1020.9	3.0	0.58	581.3	5.6	0.55	815.9	6.5	0.48	609.3	8.3

3.5 Stimuli responsive property of gels

From the discussion in preceding part it could be established that the co-polymer gels swelled at different rates at different temperatures and swelled to different extent at different rates in presence of electrolytes. Thus swelling-shrinking of gels was allowed by initially swelling the gels at different temperatures and then shrinking them in 0.5M NaCl solution. Figure 3.11 shows swelling–shrinking kinetics of HM31 gel for which the swelling and shrinking were noticed to be fastest. The swelling of gel in water was slower as compared to shrinking in NaCl solution. The slow swelling may be due to closed pores of the gel in shrunken state through which water diffusion into the gel matrix is

comparatively difficult where as in the swelled state the pores are wide open through which water can flow out easily. Also, it has to be mentioned that the changes in the swelling ratio here were not rapid in terms of time; they were abrupt only in the sense that they could be provoked in the presence of NaCl in the medium.

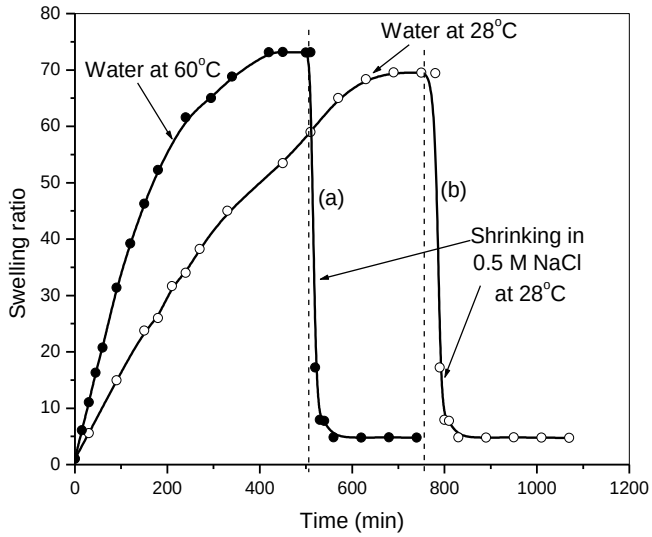

Figure 3.11: Effect of temperature on the time of swelling-shrinking cycle of hydrogel HM31 in NaCl solution

Thus the total time for one swelling-shrinking cycle was sufficiently high (~800 min) but for practical application time of swelling-shrinking cycle should be as short as possible. In order to decrease the time required for cycle the initial swelling was carried out at 60^{o}C as shown in figure 3.11. The cycle time was reduced to ~575 min under these conditions decreasing the cycle by substantial ~30 % of initial time without altering the swelling extent.

3.6 Conclusion

High energy gamma radiation can be effectively used to synthesize HEMA-co-MAETC hydrogels of good swelling extent. The increase in extent of swelling due to introduction of MAETC into HEMA matrix is many folds more than due to introduction of similar anion exchange type of monomer VBT into HEMA matrix. Dynamic swelling studies confirm that introduction of MAETC increases the rate of diffusion of water into the medium. The increase in k_d leads to its value comparable to k_r as a result the diffusion mechanism for pure poly(HEMA) matrix shifts from Fickian to anomalous for HEMA-co-MAETC gels. It was found that higher the extent of swelling of gels more was the possibility of swelling being anomalous.

The rise in temperature of the swelling medium only increases the rate of approach to EDS and not the EDS. The HEMA-co-MAETC hydrogel showed ionic strength responsive property and the swelling deswelling of the gels can be performed in water-NaCl solution for many cycles without affecting the shape and strength of the gel. A combination of higher temperature and suitable solute was demonstrated to reduce the time of swelling-deswelling cycle.

Chapter 4

Synthesis of antibacterial cotton fabric by radiation induced grafting of [2-(Methacryloyloxy)ethyl]trimethylammonium chloride (MAETC) onto cotton

Keywords: Radiation, Grafting, [2-(Methacryloyloxy)ethyl]trimethylammonium chloride, antibacterial

4.1 Introduction

Cotton is ubiquitous, extremely versatile, and most favorable clothing materials due its good folding endurance, breathability, moisture absorbency, comfort, durability, easy care, better conductor of heat, easy dye-ability, smooth feeling and bio-degradability [115]. However, the molecule structure of cotton is full of sugar components, and this makes it very vulnerable to microbes and fungi as well as bacteria under moist conditions. Growth of microbes can lead to disease, breaks down fabrics, create stains and produce odors.Cotton textile surfaces modification and functionalization provide a way to impart new and diverse properties to cotton while maintaining comfort and mechanical strength. Currently, functional finishes on textile fabrics are of critical importance to improve with multifunctional properties like antibacterial activity. Therefore, in recent years several groups have shown keen interest in developing antibacterial fibers and fabrics for various applications such as clothing for hospital workers, hospital beddings, sports clothing, underwear, ladies tights, shoe linings, armbands, sleeping bags and toys for children [116]. Silver,triclosan and trichlorocarban are the three compounds which are generally known for their efficacy as an antibacterial in clothing material.

The antibacterial property can be introduced into the fiber, either at the manufacturing step itself by incorporating antibacterial chemicals or by coating the finished product with antibacterial compounds [117]. However, such products have the limitation of leaching of physically bound antibacterial compounds leading to induced toxicity and decreased antibacterial efficacy of the substrate. Immobilization of antimicrobial agents through covalent bonding can be a solution of this problem. It is well established that grafting is an ideal and efficient technique for attaching polymer chains containing desired chemical groups via covalent bonding to existing polymeric backbones. Continuous efforts have been made to improve physico-chemical properties of polymers by grafting technique both by conventional chemical grafting technique [118] and by radiation grafting [119]. Radiation grafting has been shown to be advantageous over conventional chemical grafting method [3]. Radiation grafting is advantageous since it is generally applicable to many combination of polymers and monomers. Furthermore, the reactions process at low temperature and reaction products any chemical impurities such as fragments of inhibitor. Therefore, number of studies has been carried out using the techniques. Radiation grafting on cellulose has been investigated to impart and improve many desired properties like flame retardancy [120], high absorbency [121], water impermeability, abrasion resistance and anti-crease properties [122], rot resistance [123], thermo-responsive character [124], for bio-medical applications [125,126] and for many other applications. Polycationic antimicrobial agents, especially quaternary ammonium and phoshphonium salts containing polymers have been reported to be excellent antimicrobial agents [116, 117, 127-130].

In this chapter, radiation grafting of MAETC, which is polymerized with HEMA to have hydrogel with high water absorbency, chapter 3, has been investigated for

grafting on the surface of cotton fibrils in order to impart antibacterial property. Radiation grafting has been carried out in aqueous medium by mutual radiation grafting method and effect of various experimental variables on the grafting extent has been investigated. Further, grafted samples were characterized with various experimental techniques like FTIR, SEM, Elemental analysis, XRD etc. Finally, grafted cotton fibrils have been investigated for its anti-bacterial efficacy.

4.2 Synthesis of PMAETC and Grafting by gamma radiation

Linear poly[(2-(Methacryloyloxy)ethyl]trimethylammoniumchloride (PMAETC) was synthesized by irradiating aerated 20 % aqueous MAETC solution to total dose of 1.67 kGy at a dose rate of 5.0 $kGyh^{-1}$, using ^{60}Co γ-radiation from gamma chamber. The polymer formed was precipitated by pouring the irradiated solution in excess of acetone. The process of dissolving and precipitating was repeated until the polymer was free of monomer.

The cotton fabric procured from a local supplier in cloth form was washed and dried for 5 cycles finally followed by rinsing with double distilled water. The washed cotton samples were dried in vacuum at 50^oC and stored in desiccator for further use. Mutual radiation grafting method was used to graft MAETC onto cotton cellulose. Pre-weighed small pieces of dried cotton cloth (size 1 x 2 cm^2, weight = 0.1 – 0.15 g) were completely immersed in MAETC solution of suitable concentration in stoppered glass bottles for an hour. The samples in glass bottles were then irradiated in gamma chamber for required doses at desired dose rates. The grafted samples were washed with double distilled water in a soxhlet extraction assembly for 8 hours in order to remove PMAETC homopolymer adsorbed on the cotton substrates. The grafted sample was dried in vacuum

at 50 °C and grafting yield (%) was determined gravimetrically using following equation (4.1)

$$\text{Grafting yield } (\%) = \frac{W_f - W_i}{W_i} \text{ X } 100 \qquad (4.1)$$

Where, W_i and W_f are the weight of cotton samples before and after grafting.

The extent of radiation grafting depends upon many experimental variables such as dose, dose rate and ambient condition during the irradiation process. Therefore, effect of various experimental parameters onto grafting yield was investigated in order to optimize the experimental parameter to get desired grafting extent.

4.2.1 Effect of dose and dose rate

The number of grafted chains and their length in mutual radiation grafting process are dependent on total absorbed dose and the dose rate [131]. While the total absorbed dose governs the total number of free radicals generated on the trunk polymer, dose rate determines the rate of initiation of grafting polymerization process. The effect of radiation dose and dose rate was studied by carrying out the grafting reaction at different total dose and dose rate in 20% MAETC aqueous solution. The grafting yield increased with radiation dose and then leveled off at a dose of ~1.25 kGy as shown in figure 4.1. The increase in grafting with dose was expected as increase in dose would proportionally increase the number of radical grafting sites on the trunk polymer and no further increase in grafting extent at later doses may be either due to monomer exhaustion or due to increased viscosity of the bulk of grafting mixture which restricts the monomer diffusion to propagating grafted chains. Figure 4.1 and inset figure 4.1 clearly indicate that grafting

extent is an inverse function of dose rate. The lower grafting yield at higher dose rates can be attributed to major energy deposition in the bulk of the solution during grafting.

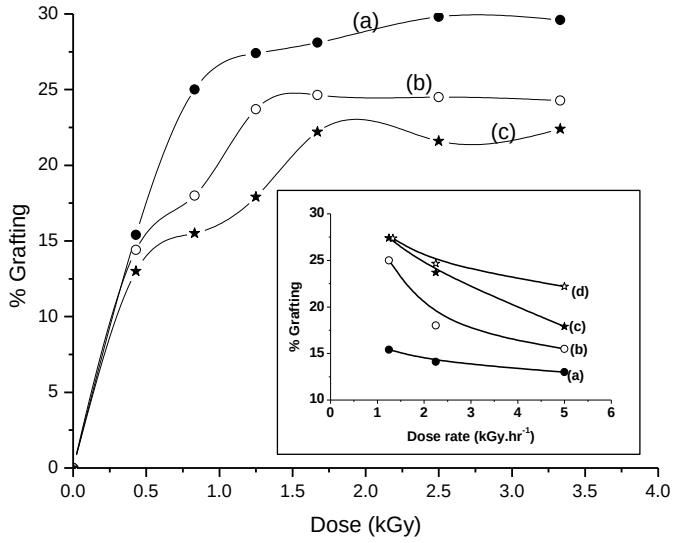

Figure 4.1: Effect of radiation dose on grafting: [MAETC] = 20% (w/w) in water, aerated solution. (a) 1.25 kGy.h^{-1} (b) 2.5 kGy.h^{-1}(c) 5.0kGy.h^{-1}Inset: Dose rate effect on grafting extent for total dose of (a) 0.43kGy (b) 0.83kGy (c) 1.25kGy (d) 1.67kGy

High dose rates produce higher radical density, which may favor recombination of radicals generated in close vicinity or faster generation of the homopolymer in bulk and its subsequent gelation. The homo-polymerization reduces the grafting extents in two ways (i) due to increased bulk viscosity the diffusion of monomer from bulk to the reactive site and growing chains at trunk polymer becomes difficult (ii) due to the consumption of monomer in homopolymer formation, less monomer would be available for grafting reaction.

4.2.2 Effect of ambient condition

The adverse effect of oxygen on polymerization behavior of vinyl monomer is well known and referred to as oxygen inhibition. Molecular oxygen has due to its ground state "biadical nature" a highly reactive towards radical species which yields peroxyradicals of low reactivity in respect of initiating capacity. An effective propagating radicals e.g. an initiator radical or growing polymer chain radical is scavenged by oxygen resulting in an ineffective propagating radical or chain termination [132]. Schematic mechanism of the inhibition is shown in scheme 4.1.

To study the effect of O_2 on the grafting reaction, the reaction has been studied under various ambient conditions. As shown in figure 4.2; the ambient conditions during grafting had a significant effect on grafting extent.

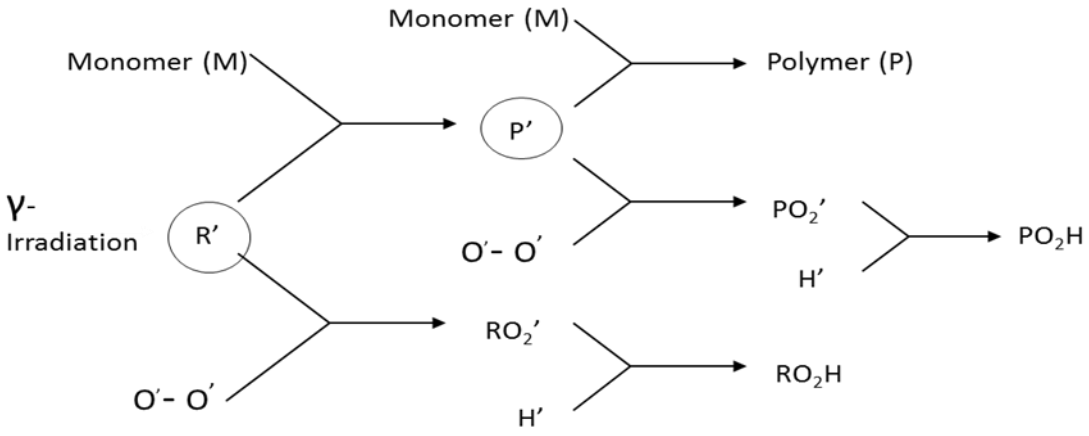

Scheme 4.1: Mechanism of the inhibition of radical polymerization by O_2

The extent of grafting was found to decrease under oxygenated and aerated condition in comparison to N_2 saturated conditions indicating that presence of O_2; a well-known efficient radical scavenger hindered the grafting reaction [133]. Comparing the dose at which the grafting started it is clear that dose requirement followed the trend O_2

purged>Aerated>N_2 purged indicating predominantly radical grafting mechanism for this system.

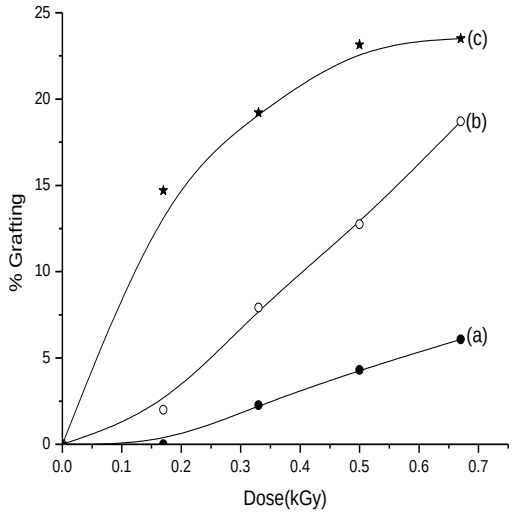

Figure 4.2: Effect of ambience on grafting: [MAETC] = 20% (w/w) in water, Dose rate: 5.0 $kGyh^{-1}$ (a) O_2 saturated (b) Air (c) N_2 purged

4.2.3 Effect of monomer concentration

The concentration of monomer during mutual grafting is an important parameter; therefore effect of monomer concentration on grafting extent was investigated keeping ratio of weight of substrate to volume of grafting solution constant. Figure 4.3 shows the result of this study. Grafting increased linearly with the concentration of monomer in the concentration range studied. However the homopolymer formation was equally favored with increasing monomer concentration. The retrieval of grafted product was increasingly difficult at higher with concentration of monomer and was not possible at concentration > 50%. Higher grafting yields were expected at higher monomer concentrations, as at any instant, radicals generated on the backbone are able to interact with more monomer molecules. However, at higher monomer concentrations, as more monomer radicals are generated in the bulk, homo-polymerization will be equally favored.

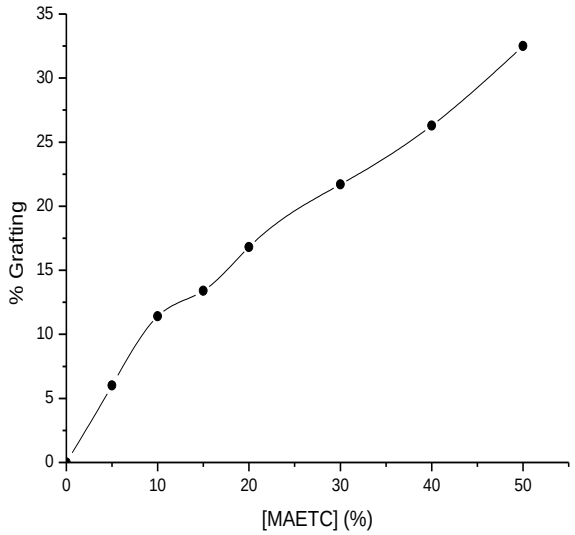

Figure 4.3: Effect of monomer concentration on grafting. Total dose=0.83kGy, Dose rate= 5.0 $kGyh^{-1}$ under aerated condition

4.2.4 Effect of homo-polymerization inhibitors (metal salts)

Mutual radiation grafting has the disadvantage of homo-polymer formation during grafting reaction, which leads to unproductive use of monomer and necessitates removal of physically adsorbed homo-polymers on the grafted copolymer. Addition of certain inorganic salts has been reported to suppress the production of undesirable homo-polymer during radiation induced grafting or redox grafting, thus leaving more monomer available for grafting and hence enhancing the grafting extent and facilitating easy retrieval of grafted product [134-136]. This has been attributed mainly to conversion of OH radical (generated due to radiolysis of water in the bulk of the mixture and due to decomposition of hydroperoxides formed on polymer backbone) to non-reactive OH anion (equation 4.2 & 4.3) thereby reducing the homo-polymerization formation in the bulk.

$$ROOH \text{—}\sim\sim\sim\rightarrow RO^{\bullet} + {}^{\bullet}OH \quad (4.2)$$

$$Fe^{2+} + {}^{\bullet}OH \rightarrow Fe^{3+} + OH^{-} \quad (4.3)$$

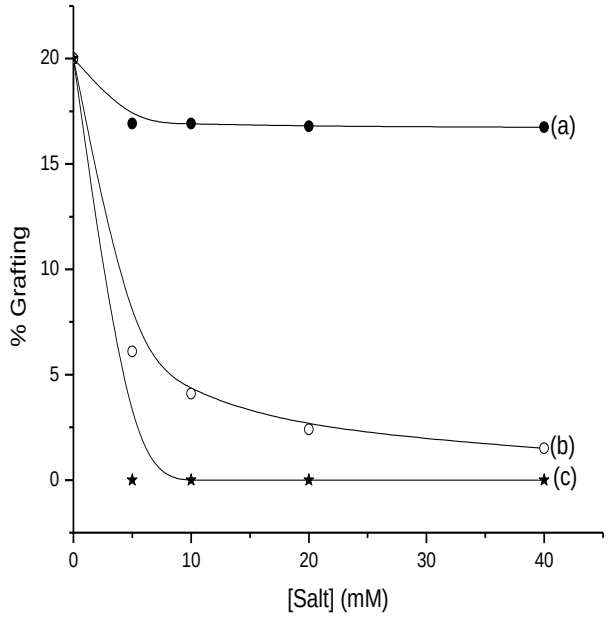

Figure 4.4: Effect of metal salts on grafting. Total absorbed dose= 0.83 kGy, Dose rate=5.0 $kGyh^{-1}$ (a) $FeSO_4(NH_4)_2SO_4.6H_2O$ (b) $Ce(SO_4)_2$ (c) $CuSO_4.5H_2O$

In the present study grafting was carried out in presence of salts such as $FeSO_4.(NH_4)_2SO_4.6H_2O$, $CuSO_4.5H_2O$ and $Ce(SO_4)_2$ in the concentration range of 0-40 mM. Figure 4.4 shows effect of these salts on grafting extent. It can be seen that grafting level decreases drastically in presence of these salts particularly in presence of cupric and ceric salts. Homopolymer formation was also found to decrease with the increase in metal ion concentration. This indicates that for MAETC-cotton aqueous system, the presence of salts effects both homo-polymerization and grafting reactions.

The decrease in grafting yield along with homopolymer in presence of metal ions has been reported for other grafting systems also. This has been explained on the basis of oxidizing (Cu^{2+}) and reducing properties (Fe^{2+}) of metal ions [137, 138]which cause

chain termination of the growing grafting chain ends as shown in scheme 4.2 below whereas Ce^{4+} is known to enhance grafting through formation of complex in aqueous medium [136].

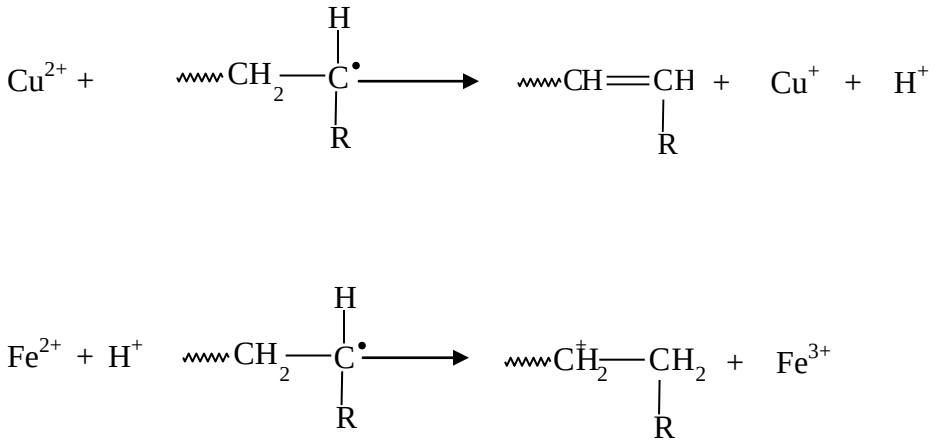

Scheme 4.2: Mechanism of the inhibition of homo-polymerization by metal salts

4.2.5 Effect of alcohols on grafting

Radiation induced grafting and free radical polymerization of vinyl monomers have been shown to depend on type and composition of solvent in the grafting medium [139, 140]. In order to study the effect of solvent, grafting reaction was carried out in presence of a series of alcohols. Results of these studies are shown in figure 4.5. It is clear from the figure that presence of alcohols affects the grafting extent adversely and at alcohol concentration > 80%, no grafting takes place. It was interesting to note that higher the hydrophobicity of the alcohol, lower the effect on grafting extent. In fact for alcohol series studied, decrease in grafting followed the trend Methanol>Ethanol>n-Propanol. It has been reported that solvents affect grafting yield in three ways namely (i) they can act as good wetting (swelling) agents for the polymer backbone [141] and thus enhance the monomers approach to the active sites, promoting the grafting. (ii) alcohols can act as an effective chain transfer agent, hence may quench the radical sites generated

on the substrate polymer and result in decrease of grafting yields or length of grafted polymer chain [142] and (iii) grafted polymer if, insoluble in the solvent, take compact globular shape hindering the availability of the reactive site on the growing chain to interact with the monomer, resulting in the lower grafting yields.

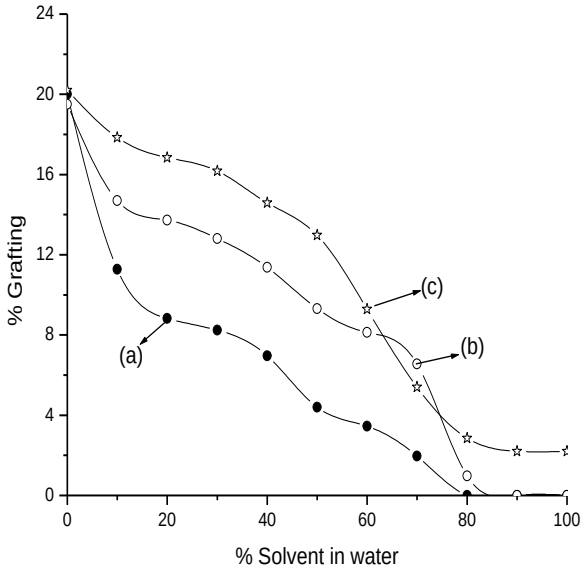

Figure 4.5: Effect of solvent composition on grafting (a) Methanol (b) Ethanol (c) n-Propanol , Total absorbed dose=0.83 kGy, Dose rate=5.0 $kGyh^{-1}$

These competing effects may take place simultaneously along with the presence of grafting reaction. The wetting ability of alcohol decreases with chain length, thus the wetting ability will follow the order methanol>ethanol>n-Propanol. The lower extent of grafting in presence of methanol can be due to ability of methanol to diffuse into the cotton substrate because of its smaller size as compared to other alcohols and may quench the reactive sites generated on the substrate decreasing the grafting extents. The decrease in grafting extent in presence of alcohols may also be due to efficient chain transfer properties of alcohols. It seems the wetting ability predominates over the chain transfer ability for this grafting system. Similar results, about the presence of alcohols affecting

grafting of even non-ionic monomers, have been reported earlier [3]. Moreover, it is interesting to note that there is almost no grafting in pure solvents (no water), which indicated that presence of water is an important factor in grafting of hydrophilic monomers. The absence of water probably reduces the number of grafting sites generated on cotton backbone due to abstraction reaction of $^{\bullet}H$ (generated as a result of radiolysis of water) with backbone.

4.3 Characterization of Grafted Cotton fibrils

4.3.1 Fourier Transform Infrared Analysis

Fourier transformed infrared spectroscopy (FTIR) measurements were performed using FTIR spectrophotometer. Samples were ground at liquid nitrogen temperature and mixed with KBr to prepare discs by compression molding press. FTIR spectra were recorded in the range from 400 to 4000 cm^{-1} with a resolution of 4 cm^{-1} and averaged over 100 scans. FTIR technique was also used to characterize the grafted cotton samples and to confirm the incorporation of MAETC onto cotton after radiation induced grafting. Figure 4.6 shows IR spectra of the radiation polymerized MAETC, grafted cotton and cotton sample. It can be seen from the spectra that for the MEATC-*g*-cotton cellulose sample, additional peaks are obtained at 1450 cm^{-1}, 1482 cm^{-1} and 1728 cm^{-1}. Peaks at 1428 cm^{-1} and 1488 cm^{-1} belong to the C-H bending of methyl groups and scissoring of methylene groups respectively, whereas, 1728 cm^{-1} corresponds to C=O of methacryloyl group. These peaks confirm the introduction of MAETC groups in the cotton cellulose structure.

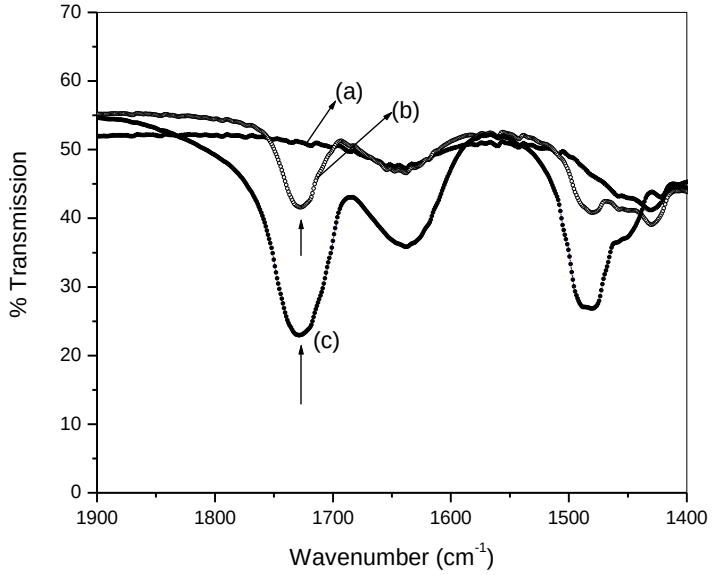

Figure 4.6: FTIR spectra of (a) Cotton (b) MAETC-g-cotton (20 % grafted) (c) poly (MAETC)

4.3.2 Elemental analysis

Elemental analysis of the grafted samples was carried out to determine nitrogen content of the grafted samples as MAETC monomer contains one nitrogen atom in quaternary ammonium group. nitrogen content of the MAETC-*g*-cotton cellulose matrix was determined using an Elemental analysis technique as explained in chapter 2. The % of nitrogen determined by elemental analysis for different grafted samples with varying grafting yields were correlated with the grafting yield estimated gravimetrically. Nitrogen content estimated theoretically and experimentally observed for grafted samples has been tabulated in Table 4.1. It is clear from the table that nitrogen content values determined theoretically and experimentally are in close agreement for samples grafted to different extents.

Table 4.1: Elemental analysis of grafted samples

S. No.	% Grafting(w/w) (Gravimetrically)	% N (theoretically)	% N (experimental)
1.	0.0	0.02	0.0
2.	3.8	0.14	0.19
3.	13.0	0.74	0.77
4.	14.6	0.82	0.85
5.	17.8	1.00	1.02

4.3.3 Water uptake study

Cotton is preferred choice for breathable garments, and its capacity to absorb water provides comfort to user as, it prevents build-up of sweat, when one perspires by easily absorbing into the garment from the body. Thus, the water absorbing capacity is among the important properties of cotton. MAETC grafted cotton samples grafted to different extents were immersed in water until equilibrium weight was reached. The water uptake (%) of the samples were estimated using the equation 4.4

$$\text{Water Uptake } (\%) = \frac{W_s - W_d}{W_d} \text{ X } 100 \qquad (4.4)$$

Where W_d and W_s are the weight of cotton samples before and after water uptake at equilibrium.

Water absorption characteristics of the MAETC-g cotton samples are depicted in figure 4.6. PMAETC prepared by radiation polymerization was highly hygroscopic therefore MAETC grafted cotton was expected to impart more hydrophilicity to the grafted product. Figure 4.7 shows the increase in water content of the grafted products. The equilibrium water content increased linearly with the extent of grafting and increased more than four times at a grafting extent of ~20%.

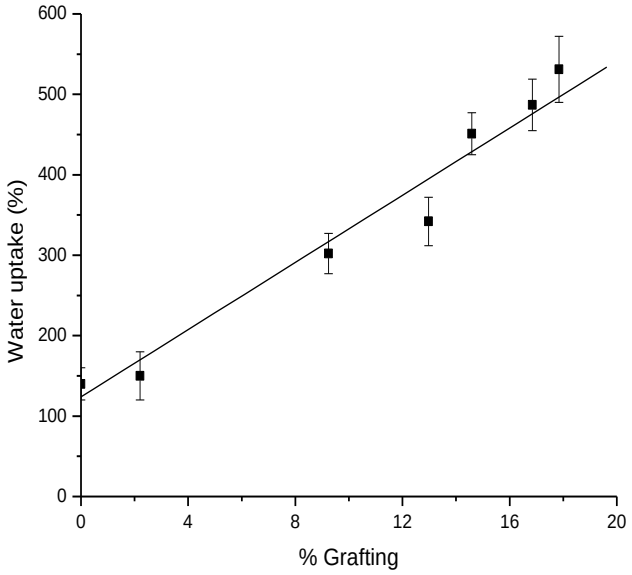

Figure 4.7: Water uptake of cotton grafted to different extents

4.3.4 Thermogravimetric analysis

Thermogravimetry analysis was carried out in order to study the thermal stability of the samples in air atmosphere at a heating rate of 10 $^{o}Cmin^{-1}$ and temperature range of room temperature to 600^{o}C.Thermo-gravimetric analysis of PMEATC, cotton and MEATC-g-cotton samples was carried out to study the change in the thermal stability of cotton after grafting. The results of this study are presented in figure 4.8. As evident from the figure thermal stability followed the trend cotton>MAETC-g-cotton>poly(MAETC).

As mentioned earlier poly(MAETC) being hygroscopic readily absorbs water from the surrounding. Thus, initial weight loss may be attributed to loss of water which follows the order poly(MAETC)>MAETC-g-cotton>cotton and the loss is much faster in case of poly(MAETC) (Inset figure 4.8). At higher temperatures cotton displayed better thermal stability than others as significant weight loss was observed at temperatures 295^{o}C, 250^{o}C and 240^{o}C for cotton, grafted cotton and poly(MAETC) respectively.

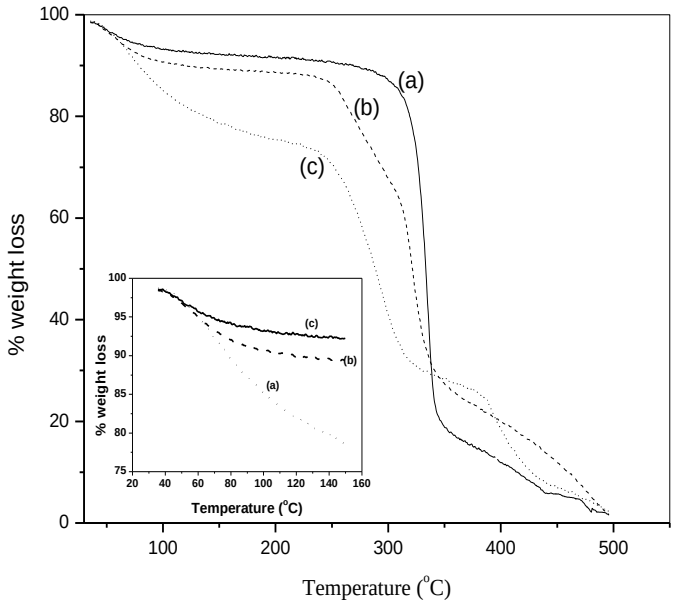

Figure 4.8: Thermograms of (a) Cotton (b) MAETC-g-cotton (20% grafted) (c) poly(MAETC)

At much higher temperatures poly(MAETC) and grafted samples showed multi-step weight loss probably due to decomposition of quaternary groups, removal of pendant groups of grafted chains or decomposition of backbone itself. The MAETC-g-cotton exhibited thermal stabilities of both the components cotton and poly(MAETC). The lower thermal stability of grafted cotton in comparison to parent cotton may be due to faster decomposition of loosely entangled grafted chains in comparison to strong compact pure cotton backbone. Similar results on decrease in thermal stability of cotton backbone on grafting of other monomers have also been reported recently [143].

4.3.5 Scanning Electron Microscope

The morphology of the control and MAETC-g-cotton fibrils was investigated by Scanning Electron Microscopy (SEM). SEM micrographs of cotton fibers were taken after coating with gold under vacuum and pasted on a conducting surface by carbon paste.

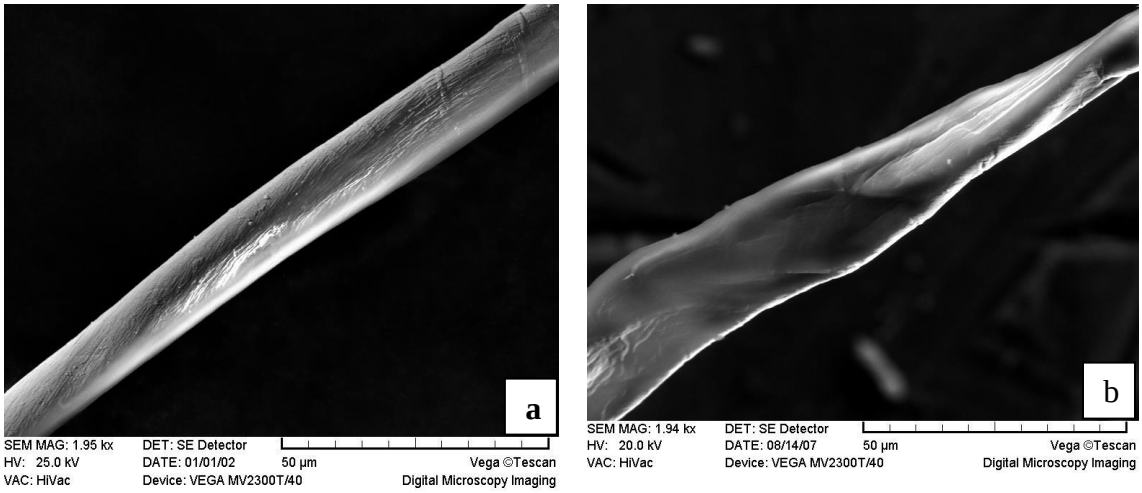

Figure 4.9: SEM of (a) Un-grafted cotton fibrils (b) MAETC-grafted cotton

Figure 4.9 (a) & (b) show SEM of the grafted and un-grafted cotton fiber. The results clearly show that the grafting changes the smooth morphology of the fiber to rough surface with increase in the diameter of the fiber.

4.3.6 XRD Analysis

XRD pattern of cotton and grafted cotton (grafting extent ~46%) shown in figure 4.10 clearly indicate that the intensity of the crystalline peak of cotton at around 23° decreased drastically on grafting. The crystallinity decreased by 60% as determined by area under the peak after appropriate correction for background from the peak area. Similar results regarding the decrease in crystallinity has been reported on post irradiation

grafting of N-Isopropylacylamide (NIPA) onto cotton [144]. The decrease in crystallinity has been explained by proposing a third phase i.e. inter-phase between crystalline and amorphous phase wherein the radical density is significantly higher than the crystalline phase after irradiation.

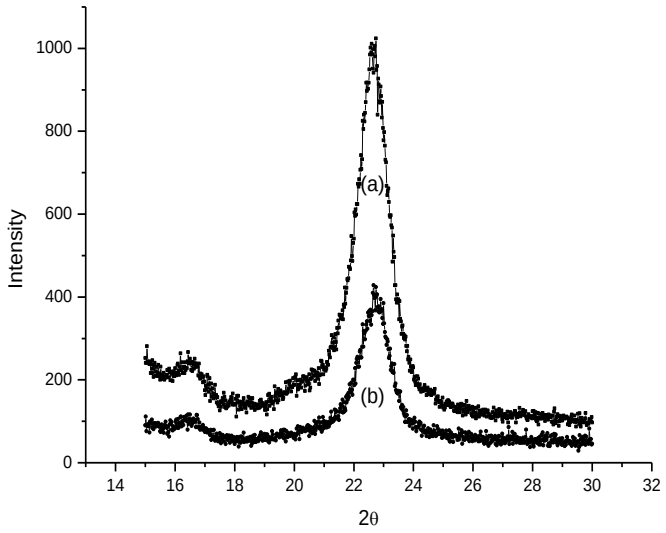

Figure 4.10: XRD Pattern of (a) Cotton (Net area of peak = 44491 counts) (b) MAETC-g-cotton (grafting extent ~46.33%) (Net area of peak = 17531)

These radicals act as center for additional grafting over and above the radicals generated in amorphous phase. These grafted chains, to some extent, are able to disturb the orderliness of the crystalline phases thereby decreasing the crystallinity. Similar analogy can be applied to the present study where the radicals generated in crystalline phase migrate to third phase by sequential abstraction reaction resulting in enhanced grafting.

4.4 Antibacterial assay of the grafted samples

To check whether PMAETC was bactericidal or bacteriostatic in nature, all four bacterial cultures were inoculated to the level of 10^3cells/ml in nutrient broth

individually. PMAETC was added (0.1% w/v) to this and incubated at 37˚ C for 24 h. Samples were withdrawn at regular intervals and growth was checked by measuring turbidity at 600 nm. The samples were also spread plated to count the colonies after incubation. Minimum bactericidal concentration (MBC) was defined as the lowest concentration at which complete elimination of cells was achieved at 37˚ C in 24 h.(MBC) was found out by addition of different concentrations of polymer to 0.1 M phosphate buffered saline (PBS) (pH 7.0). The cultures were grown in nutrient broth for 18h and centrifuged at 6000 rpm for 10 min to harvest the cells. The cells were washed twice with PBS and re-suspended in buffer containing PMAETC.

The qualitative test for antibacterial activity of radiation synthesized PMAETC in nutrient broth showed it to be bactericidal as there was no significant increase in turbidity and number of colonies formed on solid media reduced with time. These results indicated the polymer to be bactericidal in nature rather than inhibitory. The MBC of the polymer ranged from 0.025 to 0.075% depending on the organism used. The lowest MBC was found to be for *S. aureus*, followed by *E. coli*, *B. cereus* and *P. fluorescens*.

The antibacterial activity of samples grafted to different extents was assayed by colony count method. Cultures were grown; cells were harvested and suspended in similar way as described above for MBC. Aliquots of samples were withdrawn and spread plated on plate count agar to estimate the initial counts. The grafted sample as well as cotton fabric (control) was then added to this suspension and kept on rotary shaker at 37˚ C. Cell blank was also included in the experiment. Samples were withdrawn after different intervals of time and spread plated.

4.4.1 Antimicrobial tests

Figure 4.11(a-d) shows reduction in initial load of *E. coli*, *S. aureus*, *B. cereus* and *P. fluorescens* with time for samples grafted to different extents. Antibacterial assay showed variations in activity between pure PMAETC and grafted on cotton. The activity of grafted samples was less as compared to pure polymer, which may be due to its bound state on cotton but it was observed that grafted sample showed antibacterial activity against all these organisms at grafting levels as low as 2%. The antibacterial activity increased with extent of grafting up to 19% and thereafter there was no significant increase in activity. Maximum activity was found against *S. aureus,* as there was approximately 5-log cycle kill in 24 h (figure 4.11-b). This was expected as PMAETC had lowest MBC against this organism. In case of *B. cereus* (figure 4.11-c) and *E. coli* (figure 4.11-a), up to 4log cycle was observed with 19% grafting followed by *P. fluorescens* (figure4.11-d) where only 3 log cycle kill was observed. Decrease in E. *coli.* and *S. aure*us concentration was also monitored with time for sample grafted to an extent of ~33% and the results of these studies are shown in figure 4.12(a &b). It is clear from the figure that reduction in initial count reaches minimum value after 6 hours itself and thereafter no significant decrease in the number of organism is observed. When these results were compared with VBT grafted cotton as reported by us earlier [145], it was found that that decrease in bacterial count is lower than VBT grafted cotton.

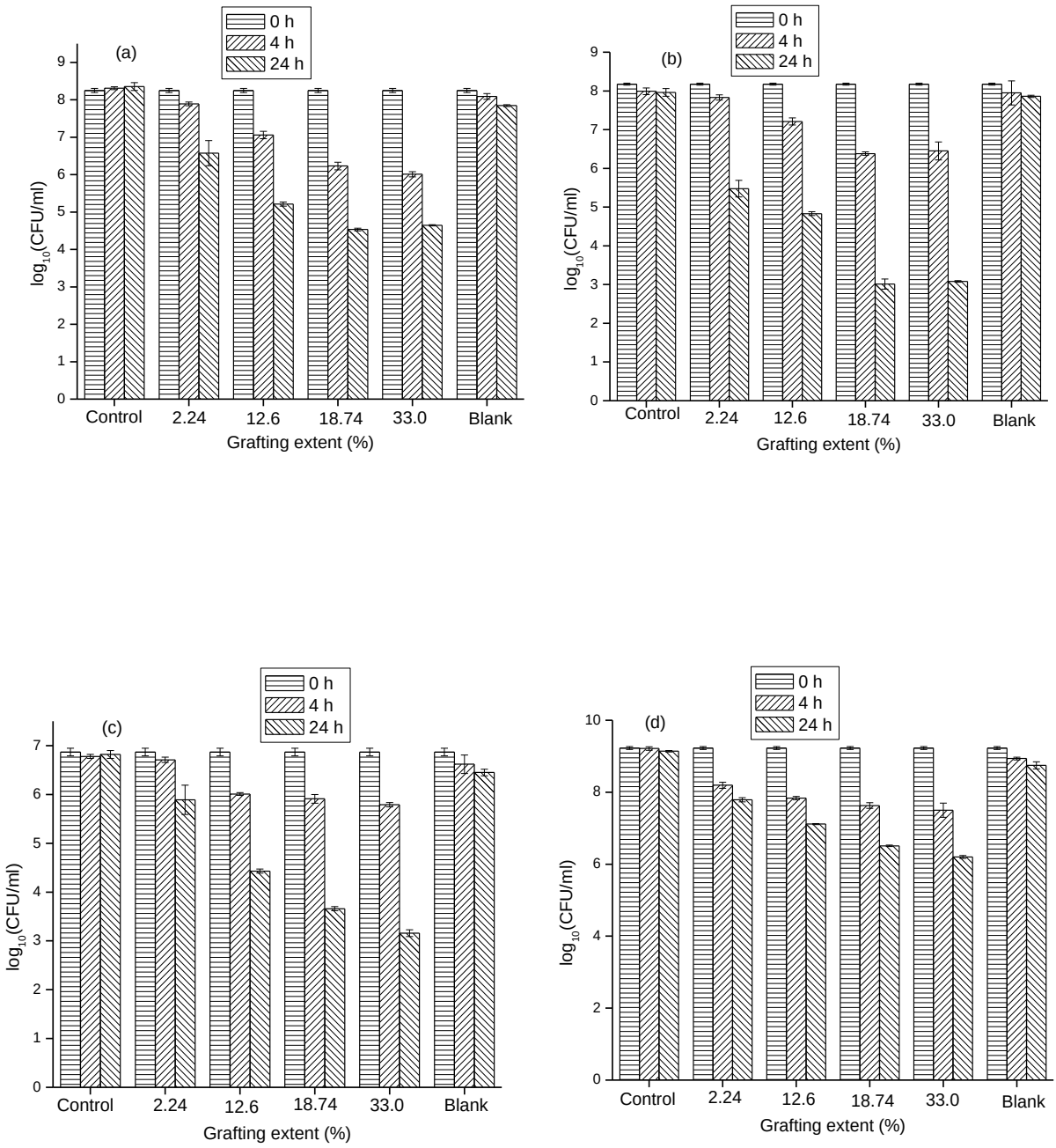

Figure 4.11: Anti-bacterial activity of MAETC-g-cotton against (a) *E.coli*(b) *S. aureus* (c) *B. cereus* (d) *P. fluorescens*

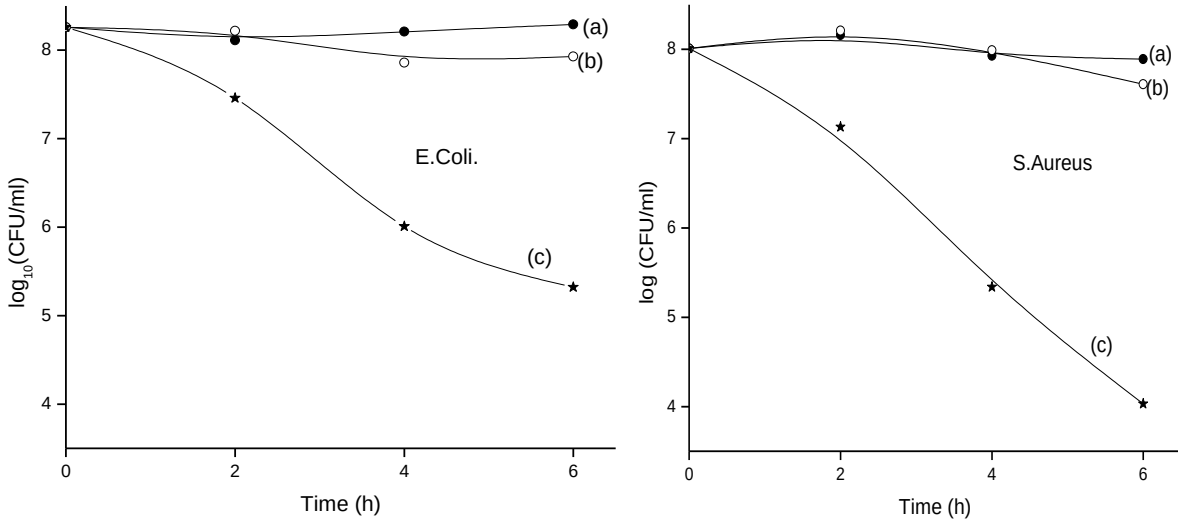

Figure 4.12: Anti-bacterial activity of MAETC-g-cotton (Grafting extent ~ 33%) with time against (A) *E.coli.* (a) Blank test medium (b) Ungrafted cotton (c) Grafted cotton (B) *S. aureus*(a) Blank test medium (b) Ungrafted cotton (c) Grafted cotton

4.5. Conclusion

Mutual radiation grafting technique can be effectively used to graft quaternary ammonium group containing MAETC onto cotton to desired extent under optimized experimental conditions. The presence of metal salts and solvents like methanol, ethanol, *n*-propanol and iso-propanol has an inhibiting effect on grafting. The MAETC grafted samples show significant increase in hydrophilicity. Radiation polymerized MAETC and MAETC grafted cotton show good antibacterial activity against gram-positive bacteria like *Staphylococcus aureus, Bacillus cereus* and gram-negative bacteria like *Escherichia coli, Pseudomonas fluorescens*. The efficiency and efficacy of grafted cotton to show antibacterial property is not solely dependent on presence of quaternary ammonium group in the grafted moiety as MAETC grafted cotton was found to be less efficient and effective than vinylbenzyltrimethylammonium chloride grafted cotton.

Chapter 5

Synthesis of antibacterial cotton fabric by radiation induced co-grafting of [2-(Acryloyloxyethyl)]trimethylammonium chloride and 2-Hydroxyethyl methacrylate onto cotton fibrils

Keywords: Radiation, Grafting, [2-(Acryloyloxyethyl)]trimethylammonium chloride (AETC), 2-Hydroxyethyl methacrylate (2-HEMA), Antibacterial

5.1. Introduction

Advanced medical textiles are a significantly developing area because of their major expansion in such fields like wound healing and controlled release, bandaging and pressure garments, implantable devices as well as medical devices, and development of new intelligent textile products [152]. Nowadays, it is common practice to combine traditional textile characteristics with multi-functionality to have smart textile products. Antimicrobial treatment for textile materials is necessary to fulfill the objectives like: i) to avoid cross infection by pathogenic micro ii) to control the infestation by microbes iii) to arrest metabolism in microbes in order to reduce the formation odor and iv) **t**o safeguard the textile products from staining, discoloration and quality deterioration [153]. A general term that is adopted to indicate the textile fibres with activity against micro-organisms growth is “bio-active fibres. The most used additives are based on organic compounds like halogenated salicylic acid, anilides, organotin compounds, quaternary ammonium compounds, organo-silicon, quaternary ammonium salts, and quaternary ammonium sulphonamide derivatives [152]. Researchers have also tried to incorporate silver nanoparticles for adding the antibacterial activities. But due to non-economical viability, require leaching for the antibacterial action, more importantly these silver ions are very mobile and can migrate into the body on contact with an open wound to cause “inflammatory, oxidative, genotoxic, and cytotoxic consequences. The silver particulates

primarily accumulate in the liver [154] but have also been shown to be toxic in other organs including the brain. [155]. But due to the excellent antimicrobial properties of quaternary ammonium and phosphonium salts, monomer containing the quaternary ammonium groups have been chosen to impart the antibacterial properties to the cotton fibrils.

From the investigation of antibacterial properties of polymer containing quaternary ammonium group, it has been observed that efficacy of the antibacterial polymer depends upon the extent of incorporation and structure of the alkyl groups attached to quaternary ammonium group. There are number of reports where investigators have reported the dependence of length of the free alky chains of the quaternary ammonium group on the efficacy of the antibacterial properties [105, 157**]**. In our studies it has been tried to investigate the effect of the structure of polymerizable alkyl chain on the antibacterial properties keeping all other three same methyl groups. In our previous studies, we have reported the incorporation of antibacterial property onto cotton by radiation grafting of [2-(Methacryloyloxy)ethyl]trimethylammonium chloride (MAETC) and Vinylbenzyltrimethylammonium chloride (VBT) for adding the antibacterial property [4,145].

Radiation induced grafting and co-grafting of 2-Acryloyloxyethyltrimethylammonium chloride (AETC), another quaternary ammonium based monomer with different polymerizable alkyl chain compared to MAETC and VBT, have been tried to add antibacterial properties. Also low minimum inhibitory concentrations (MIC) of poly (AETC) against the test microbes have suggested its incorporation to the cotton fibrils can add more efficacies of the antibacterial properties. Extent of grafting of pure AETC was found low compared to MAETC on to cotton

fibrils. Kohle, Tsenedo in their respective groups have earlier incorporated VBTAC, a highly ionisable group with a large hydration sphere that is incompatible with hydrophobic polymer, in presence of HEMA on base material such as nylon, polyethylene respectively [130, 152]. Therefore, Extent of AETC incorporation has been tried to increase on to cotton fibrils by copolymerization with 2-Hydroxyethyl methacrylate (HEMA). Radiation grafting has been carried out in aqueous and combination with other solvents medium by mutual grafting method and effect of various experimental variables on the grafting extent has been investigated. The grafted and co-grafted product has been investigated for its anti-bacterial efficacy against bacteria *E. coli, P. fluorescens, S. aureus* and *B. cereus*.

5.2 Radiation induced grafting studies

Grafting was carried out using mutual radiation grafting of AETC and HEMA onto cotton fabric by irradiating aerated AETC and HEMA in appropriate solution using γ-radiation from ^{60}Co radiation source. Washed cotton fibrils (weight=0.2 g) were completely immersed in known volume of AETC and HEMA solution in various solvents of fixed concentration in stoppered glass bottles and left for an hour for complete swelling of base polymer. The bottles were then irradiated in gamma chamber for required doses. The homo-polymer was removed from the grafted samples using water as an extractant by soxhlet extraction for 8 hours. The grafted sample was then dried and grafting yield was determined gravimetrically using equation 4.1 (refer to chapter 4).

The final property of the grafted product will depend upon the extent incorporation of AETC units along with HEMA (i.e. cumulative grafting yield) on to the backbone polymer. The extent of radiation grafting is a function of many experimental

variables such as dose, dose rate, monomer concentration, ambient condition etc. Therefore, effect of various experimental parameters onto grafting yield has been studied in detail in order to optimize the experimental parameter to get a desired extent of grafting.

A general description of the grafting mechanism in the by mutual radiation grafting can be illustrated using the following initiation, propagation and termination steps:

General Mechanism of Mutual Irradiation Radiation Grafting

	$C \xrightarrow{\gamma-ray} C^{\cdot}$	(primary Radicals)
Initiation	$C^{\cdot} + M \longrightarrow CM^{\cdot}$	(Grafted chains)
Propagation	$CM^{\cdot} + nM \longrightarrow CM^{\cdot}_{n+1}$	(Grafted growing chains)
Termination	$CM^{\cdot}_{n} + M^{\cdot}_{m} \longrightarrow CM_{m+n}$	(Grafted copolymer)

Where, C cotton fibrils, M is the monomer AETC or/and HEMA. $C^{\cdot}, CM^{\cdot}_{n+1}, CM_{m+n}$, are the cotton radicals, grafted growing chains and grafted copolymer respectively.

5.2.1 Effect of solvent and solvent mixture on grafting and co-grafting

Initially grafting of AETC was studied in aqueous medium in the concentration range 1-30% of AETC. The grafting solution above 10% AETC turned to soft transparent non-flowing mass even at a dose of 3.5kGy and it was difficult to retrieve cotton fiber for further characterization. It was further confirmed by the measuring the relative viscosity of aqueous solution 0 to 7.5 %(w/v) of AETC. Figure 5.1 shows the variation of relative viscosity before and after the irradiation as a function of monomer concentration. From the figure it is clear that there is increase in the relative viscosity as the concentration of

AETC increased and beyond 7.5% (w/v) concentration there was gel formation of non-flowing soft mass at the total absorbed dose of 1 kGy. Increase in relative viscosity with AETC concentration indicated the extent of homo-polymerization was increased due to more number of AETC radicals generation and hence gave highly viscous solution.

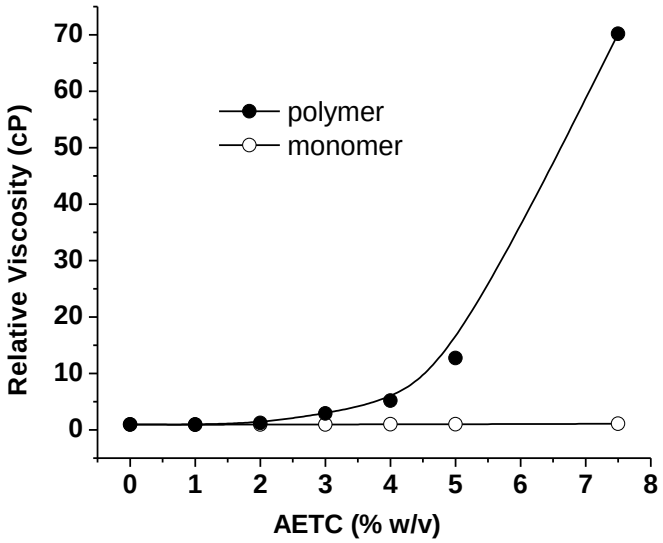

Figure 5.1 Relative viscosity of AETC solution at different w/v percent for total absorbed dose of 1 kGy

In grafting polymerization solvents plays very important role mainly in two ways: 1) Solvents can swell the base polymer such that diffusion can occur efficiently to the bulk of the base polymer and 2) solvents like water produce number of radiolytic products like OH. H. e^-_{aq} on radiolysis. These radiolytic radicals produce radicals on base polymer by abstracting H atom and hence produce the site for initiation of grafted chains. Therefore, grafting of AETC was tried to graft in number of solvents like methanol, its higher homologues and their aqueous solutions and mixture with dimethyl formamide (DMF). There are number of investigation in which grafting was tried in binary and ternary mixture of solvents reported earlier for similar grafting systems [130, 153].

Grafting was not observed in any of the alcohols or their aqueous solutions. However, low grafting yield was observed in DMF: H_2O mixture. Figure 5.2 shows grafting of AETC in different DMF: H_2O mixtures. From figure it is clear that maximum grafting extent obtained was <10 % in DMF: H_2O (80:20). Therefore, co-grafting of AETC with HEMA was studied, as it has been reported earlier that presence of combination of monomers in the medium increases the grafting extent significantly [154, 155]. It was found that methanol-water mixture was better mixture for co-grafting than any other alcohols or their mixture with water. The co-grafting of the monomers increased significantly in presence of methanol in the grafting solution (Inset figure 5.2). In view of the above observations, for further studies grafting of AETC was carried out in 10% (v/v) of stock monomer solution in DMF:H_2O (80:20) solution whereas co-grafting of AETC with HEMA was carried out in Methanol:H_2O (80:20) solution keeping AETC:HEMA:: 0.6M:1.1 M with total monomer concentration to be 10% unless, otherwise mentioned.

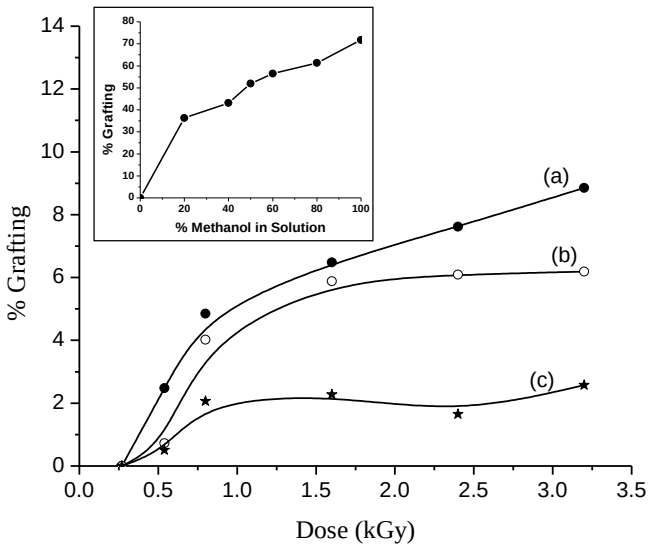

Figure 5.2 Grafting in DMF: H_2O mixture containing 10% AETC under aerated conditions, Dose rate=3.5 $kGyh^{-1}$ (a) DMF: H_2O (80:20) (b) DMF: H_2O (90:10) (c) DMF: H_2O (70:30). Inset: Variation in co-grafting of AETC-HEMA with methanol concentration. [AETC]: [HEMA]:: 0.6M:1.1 M, [Total monomer]=10%

5.2.2 Effect of total absorbed dose and dose rate

The effect of total absorbed dose and dose rate on grafting & co-grafting is shown in figure 5.3a and figure 5.3b for grafting of AETC and co-grafting of AETC and HEMA respectively. Both figures clearly show that grafting yield increased with radiation dose and then leveled off after certain dose. The observed effect can be attributed to the increase in the number of radicals formed in the grafting system, particularly in the cotton matrix as shown in the above mechanism of grafting in formation of primary cotton radicals. Consequently, more radicals take part in the grafting reaction and, as a result, the degree of grafting increases. Leveling off of the grafting yield at higher doses could be either due to the consumption of monomer or increase in the viscosity of the solution. This effect is already explained in more details in chapter 4 for MAETC and cotton fibrils system. Grafting yields decreased with the increase in the dose rate as shown in figure 5.3a and 5.3b for both grafting and co-grafting polymerization. Similar effect of dose rate on grafting of other quaternary ammonium salts like [2-(Methacryloyloxy)ethyl] trimethylammonium chloride (MAETC) and vinylbenzyltrimethylammmonium chloride (VBT) [4,145], has been observed in earlier studies. The high degree of grafting obtained at low dose rates can be illustrated due to the formation of efficient radicals, which have enough time to survive and react with the monomer molecules. This leads to efficient monomer diffusion due to low viscosity of the grafting solution and, as a result, long chain grafts are formed. As the dose rate increases, the formed radicals tend to decay by recombination leading to fast termination of the grafted growing chains [156].

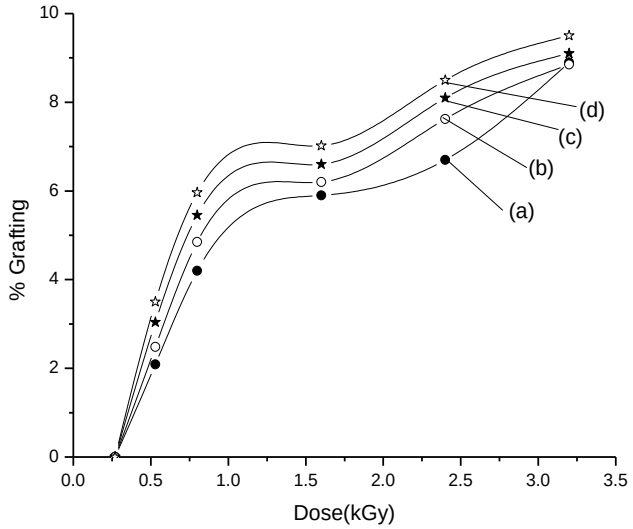

Figure 5.3a: Effect of total absorbed dose and dose rate on grafting AETC in aerated 10% solution of AETC in DMF:H_2O (80:20) solution (a) 7.8 $kGyh^{-1}$ (b) 3.5 $kGyh^{-1}$ (c) 1.75 $kGyh^{-1}$ (d) 0.87 $kGyh^{-1}$

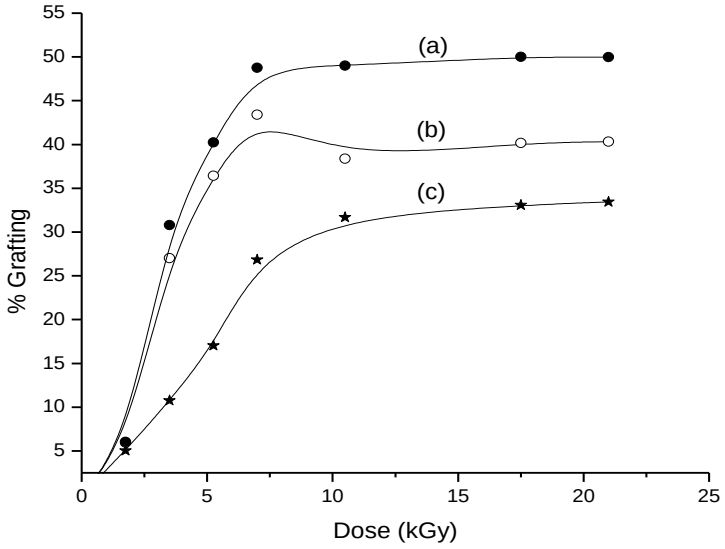

Figure 5.3b: Effect of total absorbed dose and dose rate on co-grafting of AETC-HEMA in aerated solution [AETC]:[HEMA]::0.6M:1.1M, [Total monomer]=10% in Methanol:H_2O (80:20) at a dose rate of (a) 1.75 $kGyh^{-1}$ (b) 3.5 $kGyh^{-1}$ (c) 7.8 $kGyh^{-1}$

More details about effect of dose rate have already been explained in chapter 4. Since co-grafting levels of 35-40% could be achieved at dose of ~6 kGy at dose rate of 3.5 $kGyh^{-1}$, dose rate of 3.5 $kGyh^{-1}$ was chosen for further studies.

5.2.3 Effect of monomer concentration

From above studies it was clear that extent of grafting increased with presence of HEMA in the grafting mixture. Therefore effect of monomer concentration on grafting was studied keeping the ratio of weight of the substrate to volume of grafting solution constant for a fixed radiation dose. It was found that for pure AETC in DMF:H_2O (80:20) solution the grafting increased from 5 to ~10% when the monomer concentration was increased from 5 to 30% and homo-polymer formation was more favored than grafting as the concentration of the monomer increased as observed and explained in earlier studies (refer to chapter 4). For co-grafting studies in Methnaol:H_2O (80:20) solution two experiments were carried out. In the first case the HEMA concentration was fixed (1.1 M) and AETC concentration was varied (0.2-0.9M) and in other case AETC concentration was held constant (0.6M) and HEMA concentration was varied. Figure 5.4 shows result of these studies. It is clear from the figure that co-grafting was almost independent of AETC concentration but increased linearly with concentration of HEMA in the grafting solution.

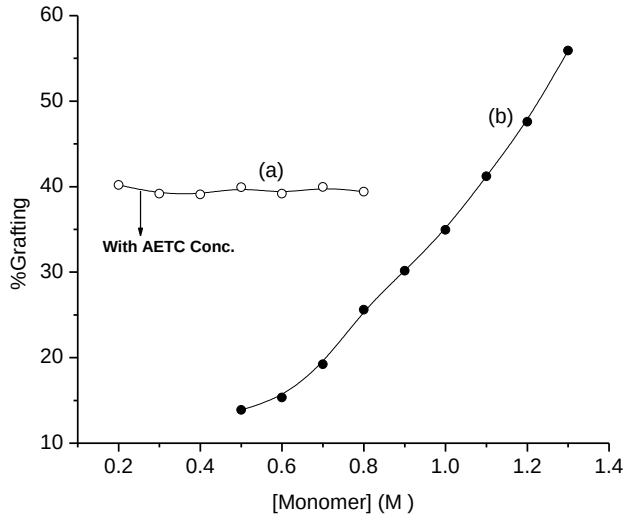

Figure 5.4: Effect of monomer concentration on co-grafting at dose rate of 3.5 $kGyh^{-1}$ for (a) Effect of AETC concentration when [HEMA] =1.1M for total dose of 2.7kGy (b) Effect of HEMA concentration when [AETC] =0.6M M for total dose of 3.2kGy

5.2.4 Effect of homo-polymerization inhibitors and additives

Mutual radiation grafting suffers from serious drawback of homo-polymerization during grafting which illustrated in our earlier studies (refer to chapter 4). In the present study grafting was carried out in presence of Mohr's salt $\{FeSO_4.(NH_4)_2SO_4.6H_2O\}$, an efficient homo-polymerization inhibitor. Grafting of pure AETC could not be studied in presence of Mohr's salt, because in the solvent mixture chosen Mohr's salt was not soluble in presence of AETC. Figure 5.5 (inset) shows effect of presence of the salt on co-grafting extents. It can be seen that grafting level decreased significantly in the presence of Mohr's salts even at concentrations as low as 5 x 10^{-3} $moldm^{-3}$ and homo-polymer formation was also found to decrease. This indicates that for cotton-HEMA-AETC co-grafting system the presence of salts effect the homo-polymerization and grafting to same extent. The grafted copolymers obtained in presence of Mohr's salt had yellowish tinge may be due Fe^{3+} formed due to oxidation of preferentially adsorbed Fe^{2+}

ions on cotton. The absorption of metal ions, which can act as efficient radical site quencher may be responsible for inhibiting the grafting reaction.

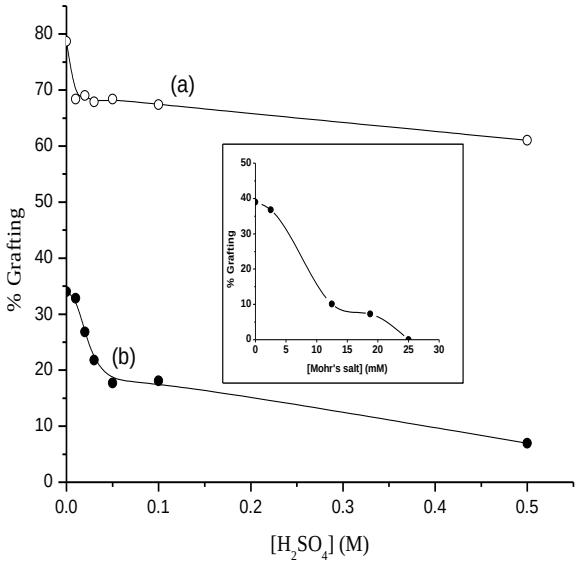

Figure 5.5: Effect of H_2SO_4 on co-grafting of AETC-HEMA in aerated solution [AETC]: [HEMA]: 0.6M: 1.1M, in Methanol: H_2O (80:20), Dose rate= 3.5 $kGyh^{-1}$, Total absorbed dose= 7 kGy, Inset: Effect of Mohr's salt on co-grafting.

Presences of additives like acid have been reported to enhance grafting in many systems [157, 158]. Therefore, effect of H_2SO_4 on grafting (shown in figure 5.5) was also studied. Presence of acid alone or in combination with Mohr's salt in fact inhibited grafting. This observation was contrary to observation made earlier for other grafting system where Mohr's salt alone enhanced grafting and its combination with H_2SO_4 further enhanced the grafting [159]. This also indicates that the explanations suggested by earlier workers [158, 160] do not hold good for all grafting systems and are more of grafting system specific.

5.2.5 Effect of ambient conditions on grafting

In order to study the effect of ambient conditions on grafting extent grafting of AETC and co-monomers was carried out in three ambient conditions namely, in N_2 saturated, aerated and O_2 saturated solutions. Results of this study, shown in figure 5.6 indicate that the grafting of AETC is suppressed due to presence of O_2, a well known efficient radical scavenger (scheme 4.1, chapter 4) which inhibits radical initiated reactions [161].

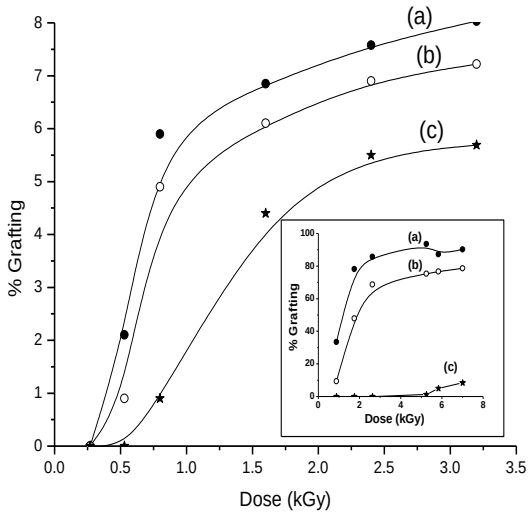

Figure 5.6: Effect of ambiance on grafting: [AETC] =10% in DMF: H_2O (80:20), Dose rate: 3.5 $kGyh^{-1}$ (a) N_2 purged (b) Air (c) O_2 saturated; Inset: [AETC]:[HEMA]::0.6M:1.1M in Methanol:H_2O (80:20), Dose rate=3.5 $kGyh^{-1}$ (a) N_2 purged (b) Air (c) O_2 saturated

In case of co-grafting also similar effect of ambiance was observed (figure 5.6 Inset). The grafting yields were significantly lower in oxygenated condition as compared to de-oxygenated and aerated conditions in the dose range studied, indicating that the presence of O_2 hinders the homo-polymerization and grafting reaction to nearly same extent. It appears that for hydrophilic backbones like cotton where the dissolved oxygen

is able to diffuse deep into the backbone, the radicals generated on backbone get quenched, hence decrease the grafting extents.

5.3 Characterization of grafted cotton

5.3.1 Elemental analysis

The nitrogen content of the grafted cotton fibrils was determined using an elemental analyzer and the % N in the grafted cotton samples was correlated with the grafting yield estimated gravimetrically.

The results of elemental analysis are given in Table 5.1. Assuming that for the samples grafted to the lowest extent (2.5%) the N content determined by elemental analysis matched with the grafting extent determined gravimetrically, the extent of grafted AETC incorporated in other grafted/co-grafted matrices was estimated. From the tabulated values it is clear that in case of pure AETC grafting the grafting extents determined by two methods were in close agreement whereas for co-grafted samples fraction of AETC incorporated decreased though the extent of grafting increased. This clearly indicated that reactivity of HEMA with cotton and with itself was much higher that with AETC which resulted in higher extent of grafting when HEMA was introduced in the grafting solution. The introduction of HEMA in grafting solution only increased the grafting extent due to incorporation of PHEMA chains in the co-grafted matrix was further confirmed by the antibacterial studies (described later in the text) whereas higher co-grafted matrix did not show the expected higher antibacterial activity.

Table 5.1: Comparison of grafting extent determined gravimetrically and by elemental analysis for grafted and co-grafted samples

Sample	% N	% C	% H	% $G_{(Gravi)}$	% $G_{(EA)}$ of AETC	% g-AETC in co-grafted matrix
Control	0.000	42.319	8.947	_	_	_
*Grafted1	0.191	42.534	8.386	2.5	2.5	_
Grafted2	0.434	42.479	8.941	7.6	5.6	_
#Co-grafted1	0.171	43.809	9.285	8.1	2.2	27.3
Co-grafted2	0.258	44.340	9.251	14.8	3.3	22.7
Co-grafted3	0.361	45.368	9.699	32.0	4.7	14.6
Co-grafted4	0.630	46.225	9.597	64.0	8.2	12.8

*Grafting condition: 10% AETC in DMF:Water (80:20)
#Grafting condition: HEMA:AETC::1.1M:0.6M in Methanol:Water (80:20)
% $G_{(Gravi)}$= % Grafting determined gravimetrically
% $G_{(EA)}$= % Grafting determined from elemental analysis

5.3.2 Water uptake study

Cotton samples grafted with AETC and HEMA was supposed to add more hydrophilic character, as poly(AETC) is highly hygroscopic in nature because of high charge density of quaternary ammonium group. Hydrophilicity of the grafted samples with different grafting yields was tried to characterize by water uptake study and percentage of water uptake was determined by using equation 4.4 (refer to chapter 4). Figure 5.7 shows equilibrium water uptake of the grafted and co-grafted samples.

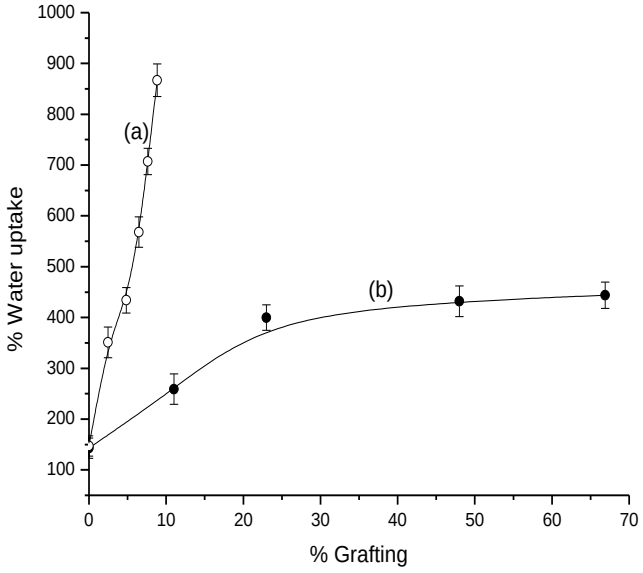

Figure 5.7: Water uptake of cotton (a) AETC grafted (b) HEMA-co-AETC grafted

The water uptake of AETC-grafted cotton was comparable to VBT or MAETC grafted cotton whereas that of co-grafted was much lower. This further establishes the role of HEMA incorporated in the co-grafted matrix. Water uptake by radiation polymerized poly(HEMA) has been reported to be much lower than that of radiation polymerized ionic polymers. Incorporation of ionic monomers in fact has been reported to enhance water uptake of poly(HEMA) by several folds [99]. No significant increase in water uptake with grafting extent on co-grafting is clear indicator that presence of HEMA in grafting solution leads to significant increase in HEMA content in co-grafted chains without much enhancing the incorporation of AETC as described earlier section.

5.3.3 Thermogravimetric analysis

Thermogravimetry analysis was carried out using under dynamic nitrogen atmosphere at a heating rate of 10^{o}C/min in the temperature range of room temperature to 550^{0}C. Thermo-gravimetric analysis of pristine cotton, grafted matrices and radiation

polymerized HEMA & AETC was carried out to study the change in the thermal stability of cotton after grafting and co-grafting. The results of this study are presented in figure 5.8 and figure 5.8 Inset. From inset, thermograms it is pretty evident that the poly(AETC) shows weight loss as soon as it is heated and at temperature >225^{o}C drastic multi-step weight loss follows. Poly(HEMA) on the other hand shows significant weight loss only at temperature >325^{o}C. The thermal stability of cotton was in between these two polymers. Poly(AETC) being hygroscopic readily absorbs water from the surrounding therefore the initial weight loss may be attributed to loss of water whereas weight loss beyond 225^{o}C may be due to decomposition of quaternary groups, removal of pendant groups. Also better thermal stability of poly(HEMA) in comparison to poly(AETC) may be attributed to the nature of polymers formed on irradiation. It was found that AETC sets to non-flowing polymer mass at a dose as low as ~0.5 kGy. The polymer formed was soluble in excess of water indicating that on radiation the AETC forms linear poly(AETC). HEMA on irradiation on other hand formed a non flowing mass at dose of ~5 kGy which was not soluble in any of the solvents indicating it forms crosslinked polymer matrix on irradiation. Crosslinked polymer matrices have better thermal stability than the linear polymers. Probably this may be one of the reason which provides better thermal stability to poly(HEMA) than to poly(AETC). In view of the thermal stability of poly(AETC), poly(HEMA) and cotton it was expected that the thermal stability of the grafted matrices will follow the order AETC-g-Cotton<Cotton<HEMA-g-Cotton. In fact, as shown in figure 5.8 the trend was on expected lines. However it was interesting to see that the co-grafted cotton showed initial weight loss at temperature even lower than the AETC-g-cotton.

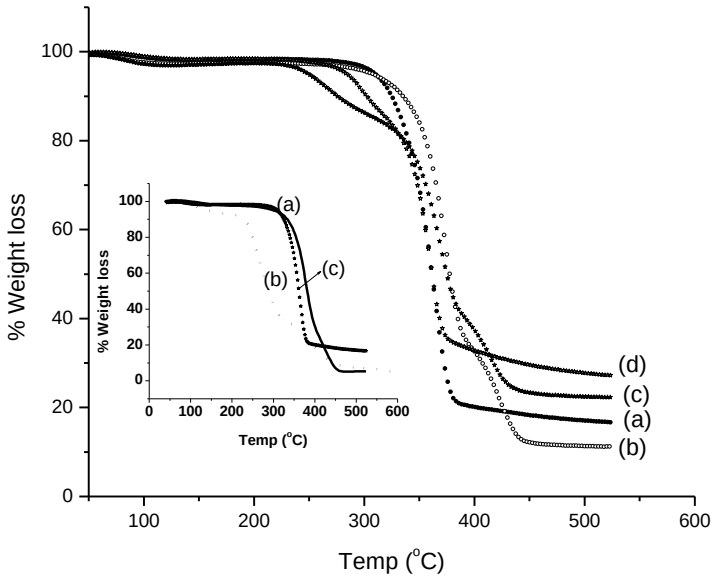

Figure 5.8: Thermograms of (a) Cotton (b) HEMA-g-cotton (c) Co-grafted cotton (d) AETC-g-cotton; Inset: (a) Radiation polymerized poly(HEMA) (b) Radiation polymerized poly(AETC) (c) Cotton

From co-grafting studies discussed above it is clear that when grafting extent of AETC grafting was tried to increase, in presence of HEMA the net result was that grafting extent increased, but due to incorporation of HEMA segments in the grafted chains with no significant increase in AETC segments. This may due to higher reactivity of HEMA than AETC. Thus it can be fairly assumed that in co-grafted chains there were huge blocks of HEMA segments separated intermittently by AETC segments. On heating these AETC segments probably act as weak links at which polymer chain breakage takes place and which causes higher weight loss percentage in comparison to that of pure AETC grafted chains. Other interesting observation was that in the temperature range studied the grafting/co-grafting onto cotton resulted in lower weight loss in comparison to pure polymers.

5.3.4 Scanning Electron Microscopy

Scanning Electron Microscopy (SEM) were recorded to investigate the surface morphology of the control and grafted cotton fibrils. SEM pictures of cotton fibers were taken after coating with gold under vacuum and pasted on a conducing surface by carbon paste.

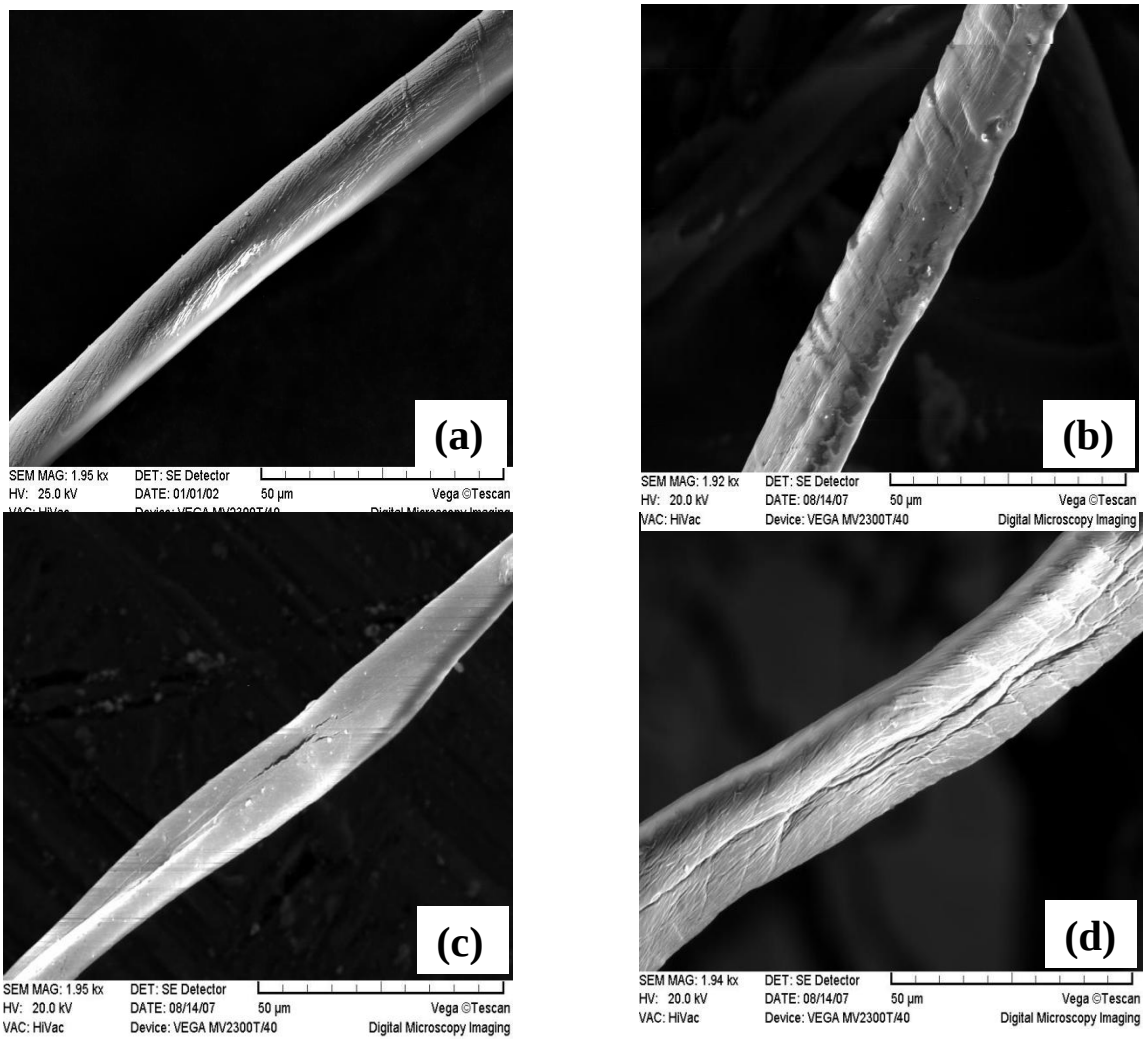

Figure 5.9: SEM micrographs of cotton fibrils (a) Pristine (b) HEMA-grafted (c) AETC grafted (d) HEMA-co-AETC grafted

Figure 5.9 shows SEM micrographs of pristine, grafted and co-grafted cotton fibrils. Micrographs clearly show that surface morphology of the cotton fibrils visibly changes from smooth to rough with increase in the diameter of the fiber on grafting.

5.4 Anti-bacterial tests

To confirm whether AETC and its co-polymer were bactericidal or bacteriostatic in nature, all four bacterial cultures were inoculated to the level of 10^3cells/ml in nutrient broth individually. AETC was added (0.1% w/v) to this and incubated at 37˚C for 24 h. Samples were withdrawn at regular intervals and growth was checked by measuring turbidity at 600 nm as reported earlier by other workers [162]. The samples were also spread plated to count the colonies after incubation. The minimum bactericidal concentration (MBC) was found out by addition of different concentrations of polymer to 0.1M phosphate buffered saline (PBS) (pH 7.0). The cultures were grown in nutrient broth for 18 h and centrifuged at 6000 rpm for 10 min to harvest the cells. The cells were washed twice with PBS and re-suspended in buffer containing AETC or co-polymer. MBC was defined as the lowest concentration at which complete elimination of cells was achieved at 37˚C in 24h. The antibacterial activity of samples grafted to different extents was assayed by colony count method. All the bacterial counts were done on plate count agar, (Himedia, Mumbai, India) incubated at 37°C for 24h during the course of this work. The overnight grown cells of all four bacteria were harvested by centrifuging at 6000rpm and washed twice in 0.1M phosphate buffer (pH 7.0) and re-suspended in buffer to give final concentration of about 10^7 to 10^8cells/ml. The grafted as well as control cotton fabrics were then introduced into this bacterial suspension and stirred in rotary shaker at room temperature. The aliquot was drawn at regular interval and spread plated on nutrient

agar in triplicate after appropriate dilution. The bacterial colonies were counted after 24 hours incubation at 35^{o}C.

The qualitative test for antibacterial activity of radiation synthesized PAETC in nutrient broth showed it to be bactericidal as there was no significant increase in turbidity and number of colonies formed on solid media reduced with time. These results indicated the polymer to be bactericidal in nature rather than inhibitory. The MBC of the polymer (PAETC) ranged from 0.0025 to 0.05% depending on the organism studied. These values were much lower than for poly[2-(Methacryloyloxy)ethyltrimethylammonium chloride] reported by us recently [4]. The lowest MBC was found to be for *S. aureus* & *B. cereus*, followed by *E. coli*, but for *P. fluorescens* it was effective at higher concentration of 0.2%. The MBC of the co-polymer poly(AETC-co-HEMA) was found to be 0.05% for *S. aureus & B. cereus* but no bactericidal activity of the co-polymer was observed against *E. coli & P. fluorescens* even at 0.2%.

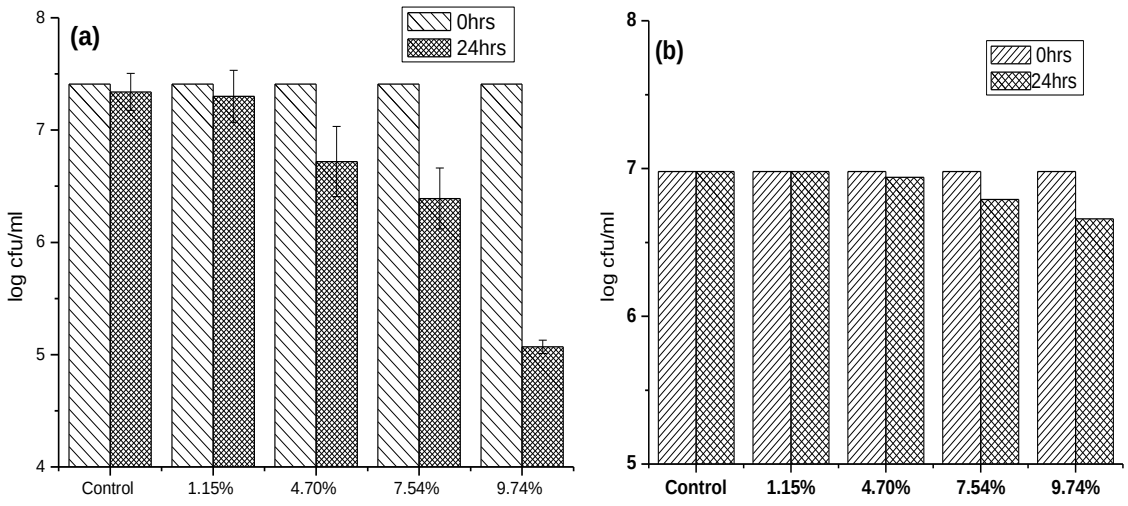

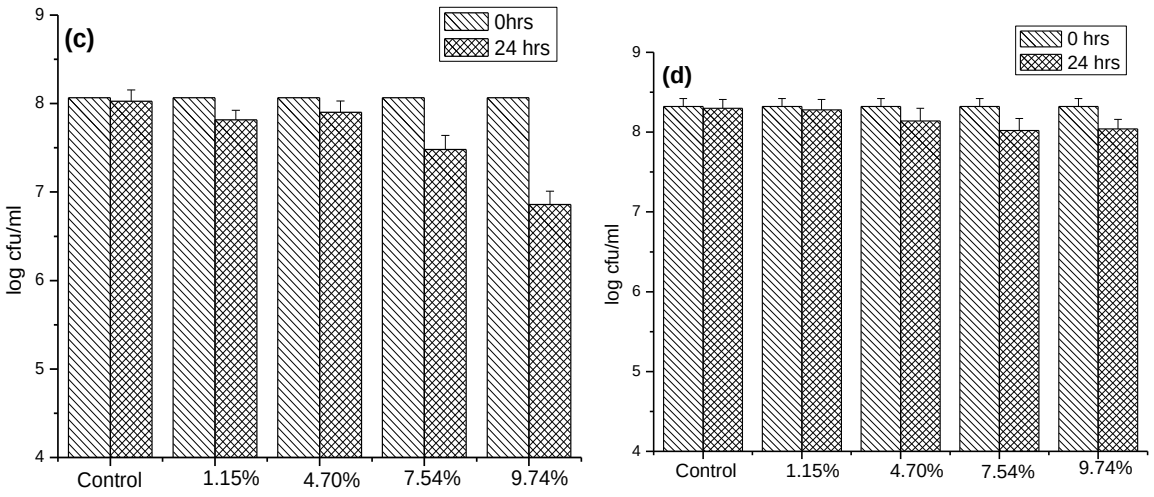

Figure 5.10: Anti-bacterial activity of PAETC-g-cotton against (a) *S. aureus* (b) *B. cereus* (c) *E. coli* (d) *P. fluorescens*

Figure 5.10(a-d) shows effect on initial load of *S. aureus, B. cereus, E. coli* and *P. fluorescens* for samples grafted to different whereas figure 5.11 (a-d) shows effect on initial load for co-grafted samples. Antibacterial assay showed variations in anti-bacterial activity between pure polymer and grafted samples. The anti-bacterial activity followed the order pure polymers>grafted cotton>co-grafted cotton>co-polymer. The lower activity of the grafted matrices may be due to bound state of these polymer/co-polymer chains wherein the flexibility of the grafted chains in restricted which in turn restricts the diffusion of hydrophobic chain into the bacteria once the bacteria held onto by charged interactions [163]. The AETC-grafted cotton showed antibacterial activity against all these organisms at grafting levels as low as 4.7% and increased with grafting extent. The co-grafted matrices showed noticeable antibacterial activity at much higher grafting extent of ~11% which didn't improve on increase in co-grafting extent.

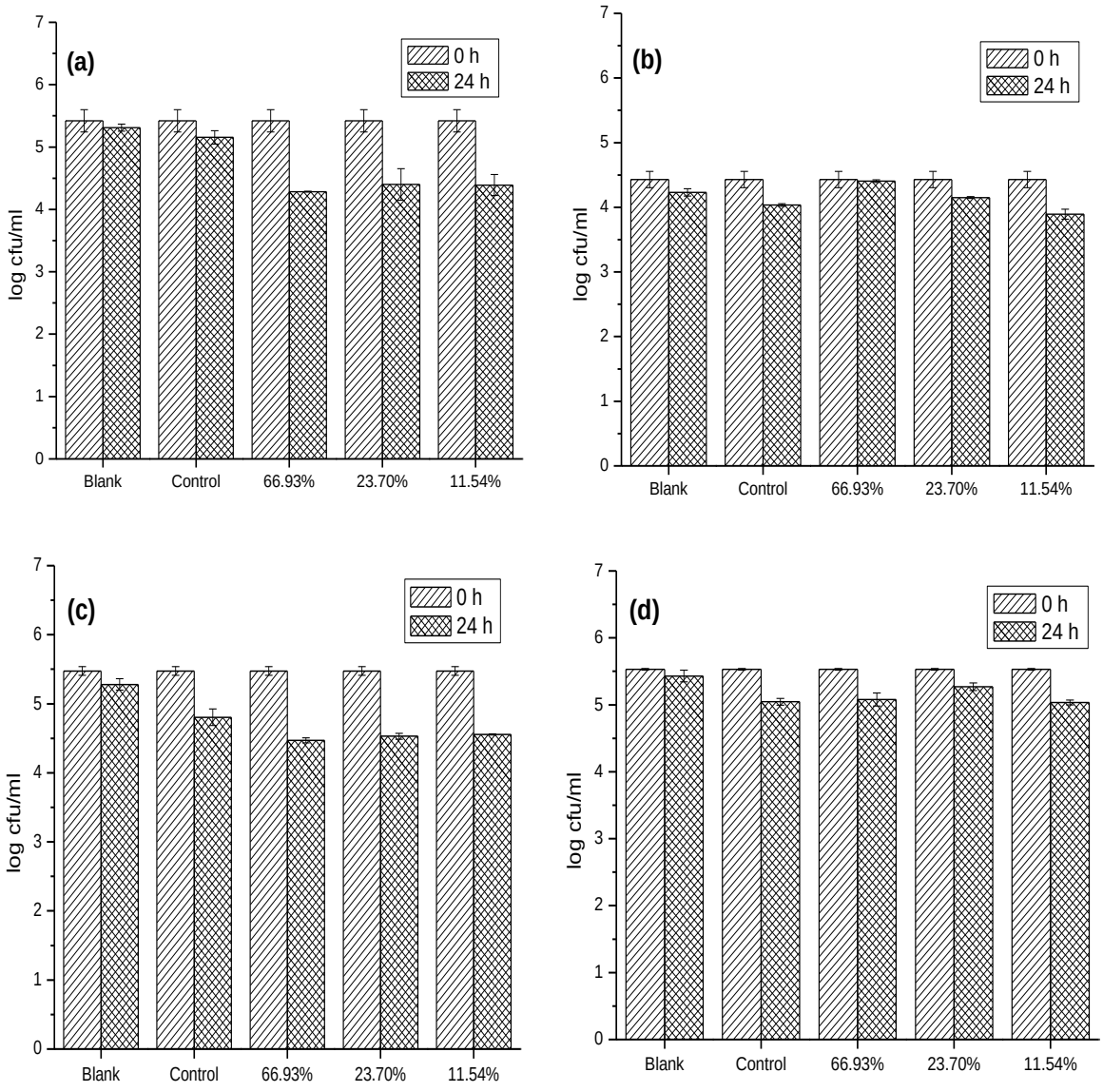

Figure 5.11: Anti-bacterial activity of co-grafted cotton against (a) *S. aureus* (b) *B. cereus,* (c) *E. coli* (d) *P. fluorescens*

Maximum activity was found against gram positive *S. aureus & B. cereus* and not so significant against gram negative *E. coli & P. flourescens.* This was on expected lines as poly(AETC) had highest MBC against *E. coli & P. flourescens.* This observation was important in the sense that AETC grafted matrices were effective against gram positive bacteria whereas our earlier studies show that MAETC and VBT were more effective

against gram negative organisms which are known to have lipopolysacchride layer present over their cell walls [164].

5.5 Conclusion

The mutual radiation grafting of quaternary ammonium group containing AETC onto cotton is difficult in aqueous solution. The grafting extent of AETC can be enhanced only to limited extent in optimized binary solvent mixture of DMF and water. The co-grafting of AETC with HEMA is favored in methanol-water mixture. The presence of metal salts and acid had detrimental effect on grafting extent. The change in ambiance of grafting mixture also did not improve the grafting extent. AETC grafted samples show significant increase in hydrophilicity. Radiation polymerized AETC and AETC grafted cotton show good antibacterial activity against gram-positive bacteria like *S. aureus* and *B. cereus*. The samples co-polymerized or co-grafted with HEMA showed lower antibacterial activity. The efficiency and effectivity of grafted cotton to show antibacterial property is not solely dependent on presence of quaternary ammonium group in the grafted moiety as AETC grafted cotton was found to be more effective than VBT and MAETC against gram positive bacteria but less effective than VBT and MAETC against gram negative bacteria. AETC grafted product has potential for dress material of high-risk group like hospital staff and also in developing the hygienic inner wears.

Chapter: 6

Functionalization of textile adsorbent from textile cotton cellulose waste via radiation grafting process for acid dye removal: Equilibrium and kinetic adsorption studies

Keywords: Functionalization, Textile, Grafting, Equilibrium, Langmuir, Freundlich, Elution

6.1. Introduction

Many investigators have changed the surface properties of the cotton fabrics for the target applications in the field of biotechnology, bioengineering, and most recently in nanotechnology by many physical (corona discharge, plasma, laser, electron beam and neutron irradiations, Ion beam), and chemical (ozone-gas treatment, surface grafting, enzymatic modification, sol-gel technique, micro-encapsulation method and treatment with different reagents) methods. Most recently investigators have targeted applications like self cleaning textiles, antibacterial cotton, flame retardant, dyeability, stimuli responsive fabrics are called smart textiles. The development of permanent self-cleaning cotton textiles with a life cycle of 25–50 washings or more is an objective sought by the textile industry in the framework of new products classified as intelligent textiles [165, 166]. The cost saving on cleaning using these fabrics, presenting total or partial self-cleaning properties, is one benefit. The other is to prolong the lifetime of the textile due to the continuous self-cleaning taking place at the fabric surface under daylight irradiation. Such an innovation comprises TiO_2 nano-clusters thin films deposited on the cotton textile. Scientist also have attempted to impart stimuli responsive to the surface of textiles cottons, particularly NIPPAM for the thermo-sensitivity which has the well defined LCST around 32-37^oC which is close human body temperature [167]. Paosawatyanyong et. al. have tried to develop a methodology to impart a fire resistant

properties of cotton by grafting of vinyl phosphate ester as nanometer residue structure onto cotton surface using plasma-induced graft copolymerization methods [168].

This chapter describes the brief studies related to the conversion of low cost textile cotton waste to the highly efficient functionalized adsorbent for the treatment of the textile effluents. Brush like cationic grafted polymer chains offer three dimensional spaces for adsorption of dye molecules resulting in the high adsorption capacity and fast adsorption kinetics [4, 169,170]. The cotton cellulose based cationic adsorbent, was synthesized by radiation induced grafting of Polyvinylbenzyltrimethylammonium chloride (PVBT), characterized for extent of cationization and finally tested for adsorption and elution of acid dyes AB25, AY99 and AB74. Adsorption isotherm models, namely, Langmuir [171], Freundlich [172], Redlich-Peterson [172, 174] Langmuir-Freundlich [175] isotherms were employed to analyze the equilibrium adsorption of acid dyes, whereas, adsorption kinetics of the dyes was analyzed using pseudo-first-order, pseudo-second-order and intra-particle diffusion models [176, 177]. The chemical structures of monomer and acid dyes used in this study are shown in figure 6.1.

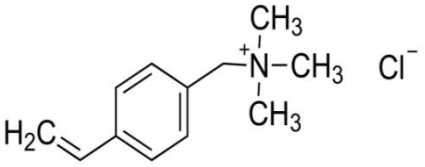

Vinylbenzyltrimethyl ammonium chloride

(VBT)

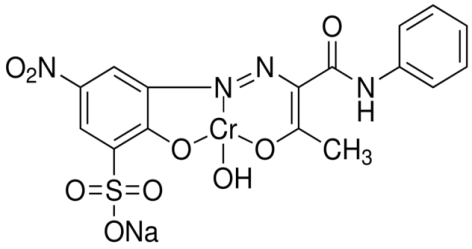

Acid Yellow 99 ((λ_{max}= 450 nm)

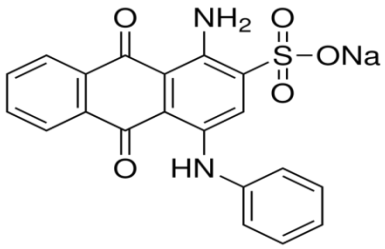

Acid Blue 25 (λ_{max}= 602 nm)

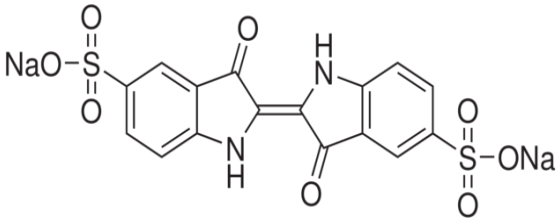

Acid Blue 74 (λ_{max}= 610 nm)

Figure 6.1: Chemical structure of acid dyes & monomer

6.2. Cationization of cotton by radiation induced Grafting

Cationization of cotton cellulose backbone was carried out by mutual- irradiation grafting of PVBT containing strong ammonium group. Cotton cellulose samples of known weight were immersed in a known concentration and volume of aqueous solution of VBT in stoppered glass tubes and left for an hour to get complete swelling of the backbone. The glass tubes were then put for irradiation in gamma chamber for various known absorbed radiation doses at known dose rates. After irradiation, the grafted samples were washed to remove the homopolymer which is physically adsorbed or trapped in the grafted samples during the grafting process in Soxhlet extraction assembly, using water as an extractant. The washed grafted samples were dried under vacuum at 50^{o}C and stored in desiccator for further use. The probable mechanism of the grafting is shown as schematic diagram in scheme 6.1.

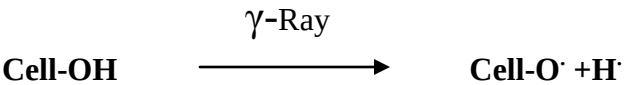

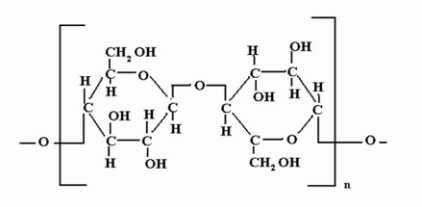

Cellulose

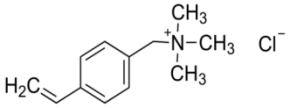

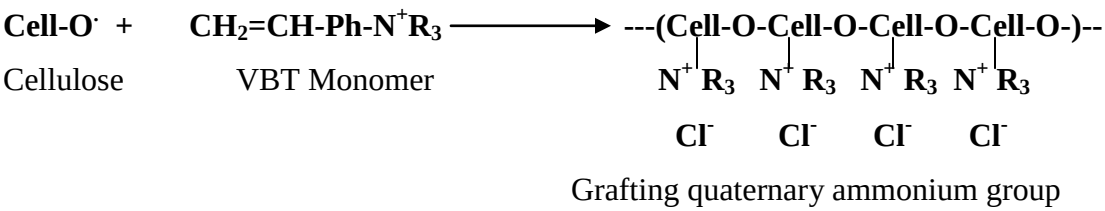

Scheme 1: Schematic diagram of the grafting of VBT having quaternary ammonium group

6.3. Characterization of PVBT-g-Cellulose samples

6.3.1 Grafting yield determination

Radiation grafting extent of PVBT on cotton cellulose substrate was ascertained by grafting yield (G.Y.) measurement determined gravimetrically using equation 4.1 (refer chapter 4). Variation in grafting yield with total radiation dose and dose rate is shown in figure 6.2 which is already published by the Kumar et. al. [145]. From the figure 6.2, it is clear that change in grafting extent with dose and dose rate is followed the same pattern as in case of MAETC [4]. Grafting extent increased with total absorbed dose and decreased with increase in the dose rate. As explained in chapter 4, total absorbed dose give more number of sites for grafting chains while higher dose rate leads to increase in homo-polymerization hence lesser grafting extent. In case of VBT, grafting

extent was not fully saturated even at 4 kGy with 20% VBT solution compared to MAETC where it got saturated at ~2 kGy with lower extent of grafting. Therefore, there is scope to have more anion exchangeable groups by increasing the extent of grafting of VBT and hence efficiency of adsorption can be increased compared to cationized cotton with MAETC.

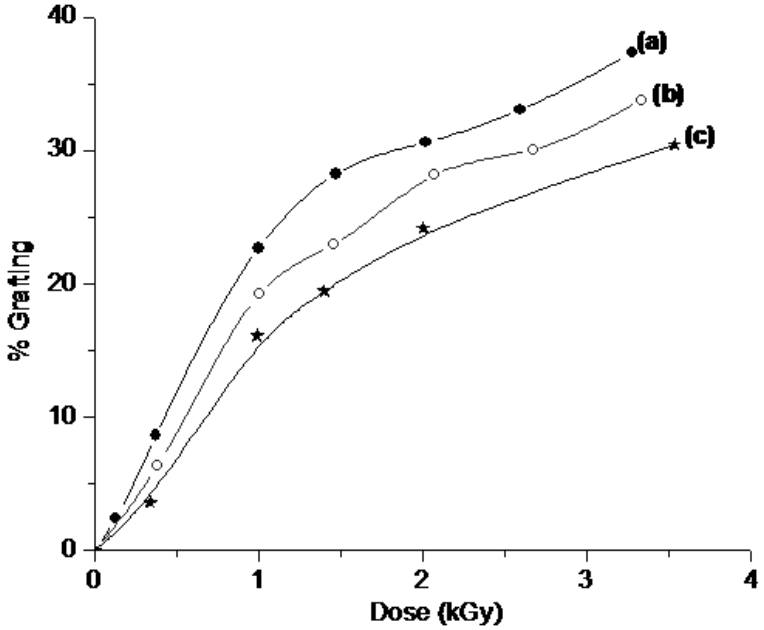

Figure 6.2: Effect of dose rate on grafting: [VBT] = 20% (w/w) in water, aerated solution. (a) 2 $kGyh^{-1}$ (b) 4 $kGyh^{-1}$ (c) 8 $kGyh^{-1}$

6.3.2. FTIR analysis

The grafting of PVBT on to cotton cellulose matrix was further confirmed by Fourier transformed infrared (FTIR) spectroscopy using FTIR spectrophotometer in attenuated total reflectance (ATR) mode. The FTIR spectra were recorded in the range 400 to 4000 cm^{-1} with a resolution of 4 cm^{-1} and averaged over 100 scans. The FTIR spectra of pristine and grafted samples are shown in Figure 6.3. The PVBT-*g*-Cellulose sample exhibited additional peaks at 1428 cm^{-1} (C-H bending of methyl groups), 1488 cm^{-1} (scissoring of methylene groups) and 890 cm^{-1} (out of plane bending of aromatic ring C-

H bonds). These additional peaks in grafted sample confirmed grafting of PVBT on the cotton cellulose substrate.

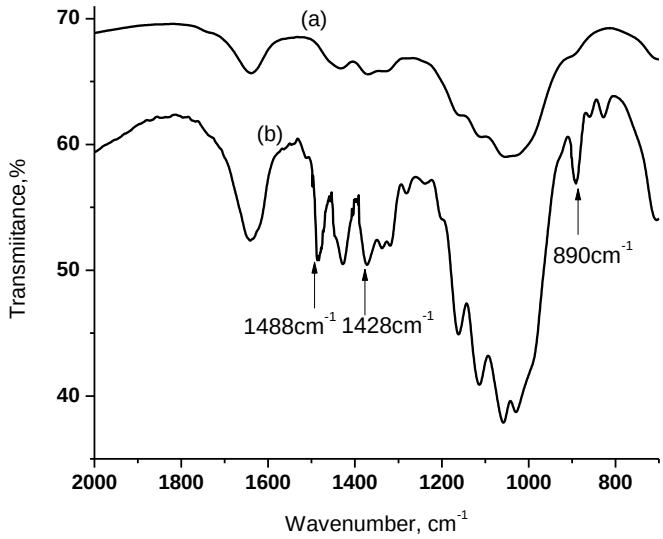

Figure 6.3: FTIR spectra of (a) Pristine cotton cellulose (b) PVBT-g-Cellulose

6.3.3. Elemental analysis

As the quaternary ammonium group of VBT contains nitrogen atom, extent of PVBT incorporation onto backbone can also be determined by nitrogen content estimation. The results of elemental analysis of the samples grafted to different extent are presented in Table 6.1. As expected, nitrogen content of the grafted matrix increased with increase in the G.Y. Moreover, the nitrogen contents of grafted samples, determined by elemental analysis, were found to be in good agreement with the theoretical values of nitrogen content calculated from gravimetrically estimated grafting yield data. The results of elemental analysis of the samples grafted to different extent are presented in Table 6.1. As expected, nitrogen content of the grafted matrix increased with increase in the G.Y. Moreover, the nitrogen contents of grafted samples, determined by elemental analysis, were found to be in good agreement with the theoretical values of nitrogen content calculated from gravimetrically estimated grafting yield data.

Table 6.1: Nitrogen content values

Dose (kGy)	G.Y. (%)	N content (%) ([1]EA)	N content (%) ([2]G.Y.)
0.25	5.2	0.30	0.33
0.50	9.5	0.61	0.72
0.70	14.8	1.05	0.98
1.04	20.4	1.39	1.46
1.25	25.4	1.59	1.65

[1]EA= Estimation by elemental analysis
[2]G.Y= Estimation by grafting yields

6.3.4. Scanning electron microscopy (SEM)

The surface morphology of the pristine cotton and PVBT grafted cotton fibrils was investigated by Scanning Electron Microscopy (SEM) analysis at acceleration voltages of 20-25kV. SEM micrographs of cotton fibers were taken at 1.95 kx magnification after gold the gold coated sample were pasted onto a conducing surface by carbon paste.

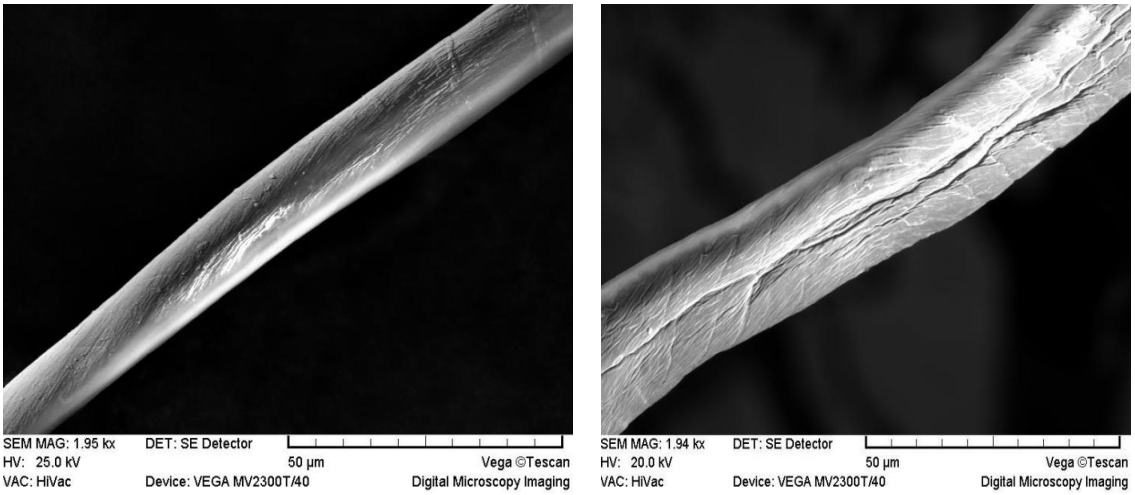

Figure 6.4: SEM micro-images presenting surface morphology of (a) pristine cotton fibrils (b) Cotton fibrils grafted with PVBT (G.Y~25%).

Figure 6.4 shows the SEM images of pristine cotton fibrils and cotton fibrils grafted with PVBT, which clearly revealed a marked difference in the surface morphology of cotton fabrils before and after grafting with PVBT. In fact, the PVBT-g-cotton fibrils became rougher and thicker in comparison with the control cotton fibrils because of the incorporation of grafted PVBT chains into the cotton cellulose backbone.

6.4. Adsorption behavior on the grafted cationized cotton samples of dyes

6.4.1 Effect of grafting yield on adsorption of dyes

PVBT-g-Cellulose samples of varying grafting yields were obtained by irradiating to different absorbed doses under conditions optimized, discussed elsewhere [145]. Figure 6.5 shows the equiibrium adsorption of three acid dyes as a function of grafting yield. The adsorption capacity increased with increase in grafting yield. This was very much expected as increase in grafting would increase the number of cationic group on the grafted matrix which act as binding sites for acid dye molecules.

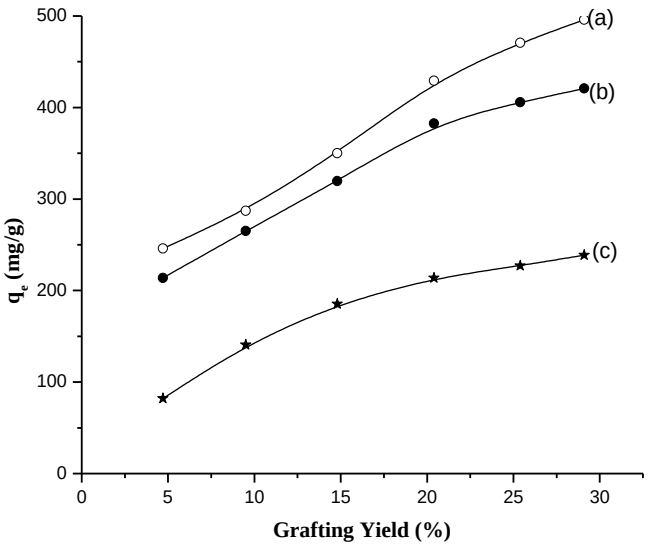

Figure 6.5: The equilibrium dye uptake capacity of the PVBT-g-Cellulose adsorbent as a function of grafting yield ([Dye] =2000 ppm) (a) AB25 (b) AY99 (C) AB74

Interestingly, for all three dyes the adsorption capacity did not increase linearliy with the grafting yield. Lower dye uptake capacity than expected values for samples grafted to higher grafting extent may be due to two factors (i) Assuming higher grafting yield corresponds to longer grafted chains, the binding sites on the longer tangled grafted chains would be less accessible to dye molecules; and if higher grafting yield is assumed to be due to higher density of grafted chains, which would hinder diffusion of bulkier dye molecule from surface to core of the grafted matrix. (ii) At higher radiation doses, in addition to increase in grafting yield the grafted chains may also crosslink, which may hinder swelling and hence uptake of dye molcules. At lower grafting extent, the grafted chain length or chain density will be lower which will facilitate the approach of bulkier dye molecule to adsorption sites on the grafted chains.

6.4.2. Equilibrium adsorption

For equilibrium dye adsorption experiments, a fixed mass (0.2 g) of PVBT-g-Cellulose adsorbent (grafting yield =25%) was weighed into 50 mL stoppered conical flasks containing 25 mL of aqueous dye solution of known concentration. The residual dye concentration in solutions were determined using UV/Vis spectrophotometer using calibration curves established for each dye, at wavelength corresponding to the maximum absorbance i.e., λ_{max}= 602 nm, 450 nm and 610 nm for AB25, AY99 and AB74, respectively. The amount of dye adsorbed at equilibrium q_e (mg/g) was estimated using equation (6.1)

$$q_e = \frac{(C_0 - C_e)}{m X\, 1000} X\, V \qquad (6.1)$$

Where C_o and C_e are initial and equilibrium liquid phase concentrations (mg/L) of dye, V is the volume (mL) of dye solution and m is the mass (g) of the adsorbent.

Linear and non-linear regression analysis using Origin 7.5 was used to determine the best fit isotherm models using coefficient of determination (r^2) as error function. The average percentage error values were used as the supporting criteria for selection of the most suitable isotherm model. The average percentage error between the experimental and the predicted values were calculated using equation (6.2) [175].

$$\varepsilon\,(\%) = \frac{1}{N}\left[\sum_{i}^{N}\frac{q_{e,exp} - q_{e,cal}}{q_{e,exp}}\right] X\ 100 \qquad (6.2)$$

Where $q_{e,exp}$ is the experimental equilibrium solid phase dye concentration and $q_{e,cal}$ is the equilibrium solid phase dye concentration estimated from the isotherm models.

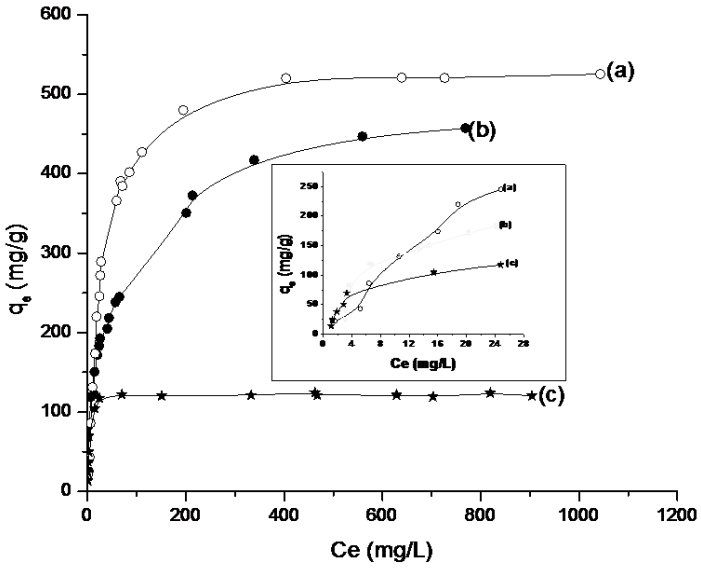

Figure 6.6: Adsorption isotherms (a) AB25 (b) AY99 (c) AB74. Inset: Adsorption isotherms at lower times (a) AB25 (b) AY99 (c) AB74

Dye adsorption is governed by the mass transfer and the adsorption equilibrium is established when the amount of solute being adsorbed is equal to the amount being desorbed. The adsorption isotherms are shown in figure 6.6, which indicates that the equilibrium adsorption capacity of PVBT-g-Cellulose adsorbent for acid dyes follows the order AB25>AY99>AB74. Linear regression method (using least-square method) has been widely applied to the linear form of isotherm equations to investigate degree of agreement between predicted and experimental equilibrium data.

(a) Langmuir adsorption isotherm

Langmuir's isotherm model postulates that theoretically, the adsorbent has a finite adsorption capacity and represented by equation (6.34) [171]

$$q_e = \frac{K_L C_e}{1 + a_L C_e} \tag{6.3}$$

Where q_e is the solid-phase equilibrium dye concentration (mg/g), C_e is the liquid phase equilibrium dye concentration (mg/L); K_L (L/g) and a_L (L/mg) are Langmuir isotherm constants.

The Langmuir isotherm equation can be rearranged into four different linear equations (6.4-6.7). These linear expressions of the Langmuir isotherm equation were used for linear regression analysis of the experimental equilibrium adsorption data.

Langmuir-1: $$\frac{C_e}{q_e} = \left(\frac{1}{K_L}\right) + \left(\frac{a_L}{K_L}\right) C_e \tag{6.4}$$

Langmuir-2: $$\frac{1}{q_e} = \left(\frac{a_L}{K_L}\right) + \left(\frac{1}{K_L}\right)\left(\frac{1}{C_e}\right) \tag{6.5}$$

Langmuir-3: $$q_e = \left(\frac{K_L}{a_L}\right) - \left(\frac{1}{a_L}\right)\left(\frac{q_e}{C_e}\right) \tag{6.6}$$

Langmuir-4: $$\frac{q_e}{C_e} = K_L - a_L q_e \quad (6.7)$$

The theoretical monolayer saturation capacity q_{max} (mg/g) can be evaluated from the Langmuir equilibrium constants K_L (L/g) and a_L (L/mg) using equation (6.8)

$$q_{max} = \frac{K_L}{a_L} \quad (6.8)$$

An another important parameter obtained from Langmuir isotherm is dimensionless separation factor R_L defined as equation (6.9) [177, 178]

$$R_L = \frac{1}{(1+a_L C_0)} \quad (6.9)$$

Where, C_o is the initial dye concentration (mg/L) and a_L is the Langmuir constant (L/mg). The value of R_L can be used to predict the adsorption behavior of dyes. $0<R_L<1$ indicates favorable adsorption, $R_L>1$ indicates unfavorable adsorption, $R_L=1$ indicates linear adsorption and $R_L=0$ indicates irreversible adsorption [177, 178].

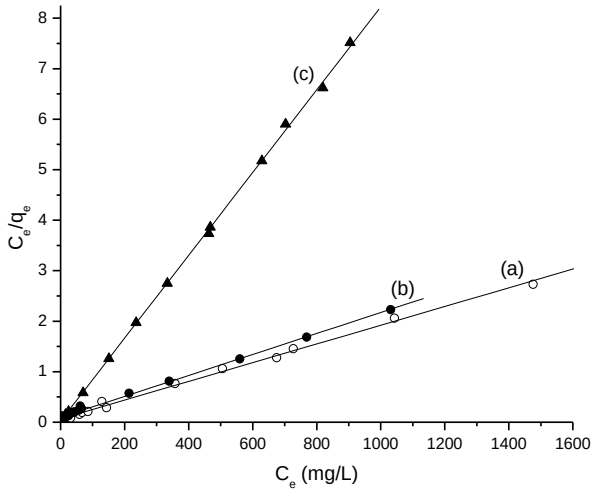

Figure 6.7: Langmuir-1 adsorption isotherm plots at 25^{o}C. (a) AB25 (b) AY99 (c) AB74

Langmuir isotherm parameters,i.e., a_L, K_L, q_{max} were estimated using Langmuir-1 equation (6.4) from the slope and intercept of the linear plot between C_e/q_e and C_e (figure 6.7). Other parameters were estimated by plotting suitable parameters of linear equation (6.4-6.7), and the obtained values for different parameters are shown in Table 6.2. For all three dyes, a spread in values of isotherm parameters and coefficient of determination (r^2) was obtained, indicating linear regression analysis is not a perfect method for analyzing equilibrium adsorption data. However, among four linearized forms of Langmuir equations, Langmuir-1 gave highest r^2 values (>0.99) for all three dyes.

Table 6.2 Langmuir adsorption parameters obtained using different linearized Langmuir equations

Dyes	q_{exp} (mg/g)	Isotherm	K_L(L/g)	a_L (L/mg)	q_{max} (mg/g)	r^2
AB25	525.0	Langmuir 1	14.8	0.027	540.0	0.9962
		Langmuir 2	13.5	0.022	613.5	0.9694
		Langmuir 3	16.2	0.029	552.6	0.8350
		Langmuir 4	14.8	0.024	601.4	0.8350
AY99	457.0	Langmuir 1	10.4	0.022	473.6	0.9966
		Langmuir 2	13.1	0.027	487.8	0.7986
		Langmuir 3	21.7	0.058	347.2	0.6063
		Langmuir 4	15.0	0.035	427.0	0.6063
AB74	123.8	Langmuir 1	40.6	0.333	121.9	0.9994
		Langmuir 2	17.9	0.114	156.7	0.8703
		Langmuir 3	28.4	0.232	122.5	0.7784
		Langmuir 4	23.6	0.180	130.6	0.7784

Also, theoretical monolayer saturation capacity values (q_{max}) obtained from Langmuir-1 equation, were close to that of the experimental adsorption capacity (q_{exp}) of adsorbent. Thus it can be said for the studied adsorbent-adsorbate adsorption is best explained by Langmuir-1, linear form of Langmuir equation. Langmuir parameter a_L,

also known as binding constant, is related to energy of adsorption and indicates the affinity or the binding strength of adsorbent for the dye; higher the value of a_L stronger is the adsorption of dye on the adsorbent.

Moreover, from the Langmuir equation, the value of a_L is the reciprocal of the dye concentration at which half of the sites of adsorbent are saturated (i.e., at $q_e = q_{max}/2$), so the higher value of a_L indicates a steep beginning of the isotherm (i.e., q_e vs C_e), which reflects the high affinity of the adsorbent for the dyes. The a_L value for three dyes followed the order AB74>AB25≈AY99. The higher value of a_L for AB74 implies stronger bonding of AB74 with the cationized adsorbent, which may be attributed to divalent nature of AB74. Figure 6.8 shows separation factor (R_L) values, as a function of initial dye concentration.

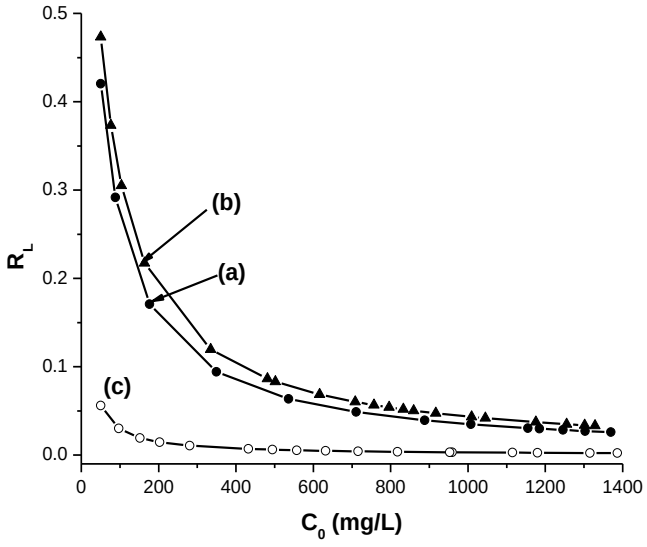

Figure 6.8: R_L as a function of dye concentration (a) AB25 (b) AY99 (c) AB74

The R_L values for all three dyes decreased drastically with the increase in C_o. It can be seen that for monovalent dyes, i.e., AB25 and AY99, the R_L values were in the range $0.42<R_L<0.02$ and $0.47<R_L<0.03$, respectively; whereas, for divalent dye, i.e.,

AB74, the R_L values are very low in the range $0.05<R_L<0.002$. R_L values for adsorption of all dyes were between 0 and 1 indicated a favorable adsorption of dyes onto adsorbent. Lower R_L values for AB74 (a divalent dye) indicated strong and probably irreversible types of adsorption.

(b) Freundlich isotherm

Freundlich isotherm is an empirical equation employed to describe heterogeneous systems [9], expressed as equation (6.10)

$$q_e = K_F C_e^{1/n} \tag{6.10}$$

The linear form of Freundlich isotherm is expressed by equation (6.11)

$$\ln(q_e) = \ln(K_F) + \frac{1}{n}\ln(C_e) \tag{6.11}$$

Where K_F is the Freundlich constant (L/mg), and 1/n is the heterogeneity factor. Unlike Langmuir model, Freundlich isotherm advocates reversible adsorption and is not restricted to the formation of the monolayer. An exponent (n) value between 1 and 10 represents favorable adsorption [179]; higher the n value, stronger the adsorption intensity, while higher value of K_F indicates a higher capacity of adsorption [175].

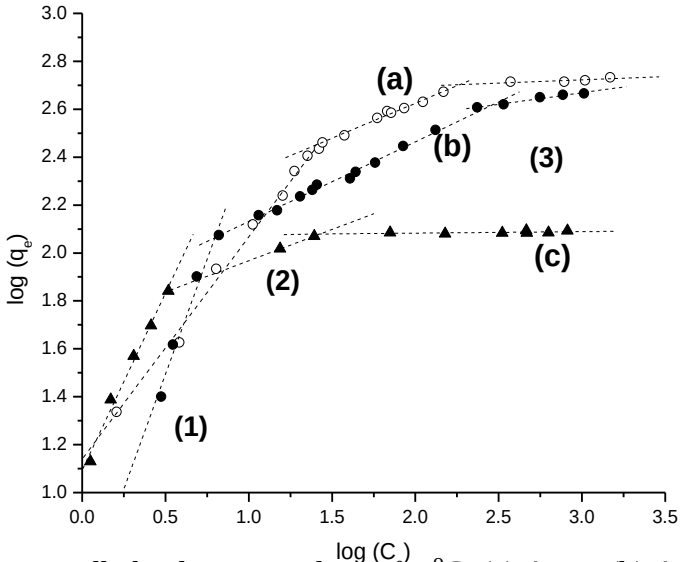

Figure 6.9: Linear Freundlich adsorption plots at 25°C. (a) AB25 (b) AY99 (c) AB74

Figure 6.9 shows profiles obtained using linear form of Freundlich equation (6.11). The plots clearly exhibit deviation from linearity.

However, when the concentration range was divided into three regions, region 1, region 2 & region 3, a good linear fit (r^2>0.98) for all three regions was observed for AY99; whereas, for AB25 and AB74 good fit was observed only in lower concentration range. Values of Freundlich parameters are tabulated in Table 6.3. Multi-linearity observed is normally attributed to irregular energy distributions due to different surface groups with different levels of activation energies for the range of sorption reactions [180].

Table 6.3 Freundlich adsorption isotherm parameters in different concentration ranges (region 1, 2 & 3 shown in figure 6.9)

Dyes	**Region**	**K_F (L/g)**	**n**	**r^2**
AB25	1 2 3	13.8 108.1 446.3	1.1 3.7 36.6	0.9936 0.9609 0.6523
AY99	1 2 3	34.3 62.8 244.8	0.5 3.0 10.4	0.9747 0.9834 0.9735
AB74	1 2 3	12.4 50.9 114.1	0.6 3.8 89.9	0.9874 0.9998 0.4039

From the linear regression analysis, it is clear that for whole concentration range, the equilibrium adsorption data was better explained by Langmuir isotherm. In addition, the shape of the isotherms q_e vs. C_e (figure 6.6), indicate that there is a limiting or saturation value of the solid-phase dye concentration (q_e), which satisfies the assumption

of Langmuir isotherm. However, studies also indicated that linear regression method using linearized Freundlich and Langmuir equations is not a perfect method to analyze the experimental data [181], therefore, the non-linear fitting method using non-linear isotherm equations of four isotherm models were also used here to analyze the adsorption data.

(c) Non-linear analysis

The R-P model, given by equation (6.12), combines elements of both, the Langmuir and Freundlich equation and is widely used as a compromise between Langmuir and Freundlich systems [180].

$$q_e = \frac{K_F\, C_e}{1+a_R c_e^{\beta}} \tag{6.12}$$

Where, K_R, a_R and β are the R-P parameters. The exponent β lies between 0 and 1. For $\beta=1$, R-P isotherm i.e. equation (6.12) takes Langmuir form i.e., equation (6.3).

Langmuir-Freundlich (L-F) model given by equation (6.13) suggests that equilibrium data follows Freundlich isotherm at low sorbate concentration and follows Langmuir pattern at higher sorbate concentration.

$$q_e = \frac{K_{LF}\, c_e^{m}}{1+a_{LF} c_e^{\beta}} \tag{6.13}$$

Where, K_{LF}, a_{LF} and m are the Langmuir-Freundlich isotherm parameters. Values for *m* (heterogeneity factor)>>1 indicates heterogeneous adsorbent, while value of m closer to 1 indicates an adsorbent with relatively homogeneous binding sites, at m=1, the L-F equation reduces to the Langmuir equation. A non-linear regression analysis of the equilibrium adsorption data was carried out using Langmuir, Freundlich, Redlich–

Peterson and Langmuir-Freundlich isotherm models. The simulated isotherms using four models and experimental profiles for adsorption of AB25, AY99 and AB74 are shown in figure 6.10a-6.10c. The values of different parameters for different isotherm models estimated by nonlinear regression analysis are presented in Table 6.4. From results shown in Table 6.4, it is clear that Langmuir model is better than Freundlich model to represent the equilibrium adsorption data of all three dyes.

Based on r^2 and ε(%) values, the quality of non-linear fitting using Langmuir model follows the order AB25>AB74>AY99. The validity of Langmuir model was also supported by good agreement between the experimental equilibrium uptake capacity ($q_{e,exp}$) and calculated theoretical monolayer saturation capacity (q_{max}) values for the three dyes. Among all four models, Langmuir-Freundlich model represented the experimental adsorption data the best, which is manifested in highest values of r^2 and lowest values of ε (%). Furthermore, for AB25 and AB74, the non-linear analysis on Redlich-Peterson and Langmuir-Freundlich yielded β and m values near to 1.0, i.e., converging to Langmuir model suggesting homogeneous adsorption with monolayer dye adsorption. From figure 6.10a-6.10c and Table 6.4, it can be concluded that the quality of non-linear fitting of adsorption isotherm models to adsorption data of all three dyes followed the order Langmuir-Freundlich>Redlich-Peterson>Langmuir> Freundlich.

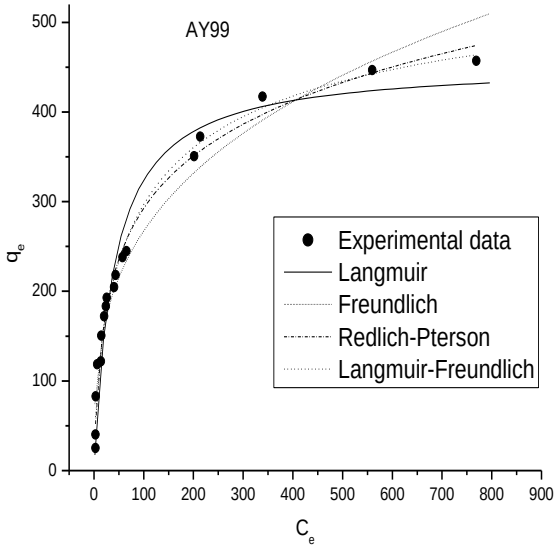

Figure 6.10a: Experimental & simulated isotherms for different isotherm models for AY99

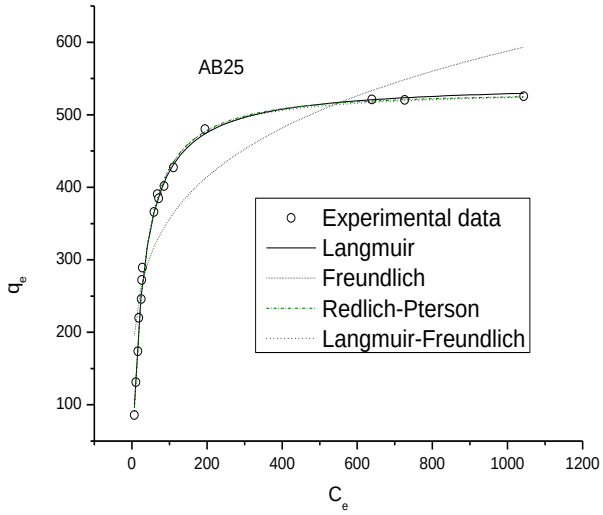

Figure 6.10b: Experimental & simulated isotherms for different isotherm models for AB25

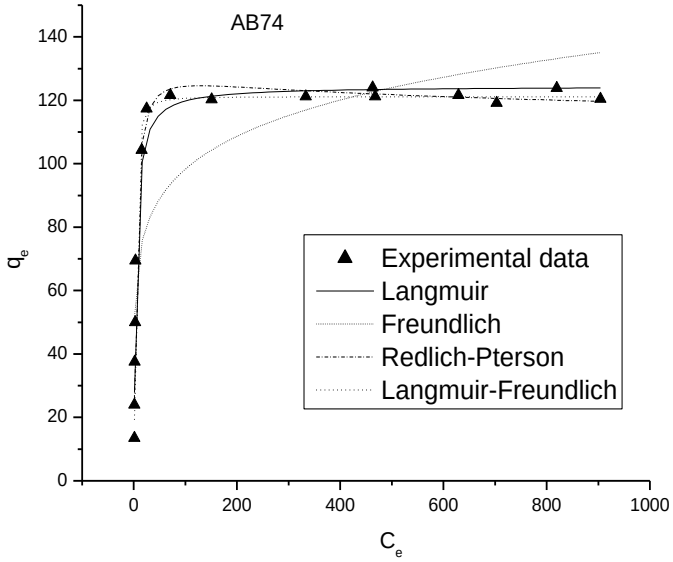

Figure 6.10c: Experimental & simulated isotherms for different isotherm models for AB74

Table 6.4 Langmuir, Freundlich, R-P and Langmuir-Frendlich adsorption isotherm parameters for dyes from non-linear regression method

Dye	Langmuir					
	$q_{e,exp}$ (mg/g)	K_L (L/g)	a_L (L/mg)	q_{max} (mg/g)	r^2	ε(%)
AB25	525	18.7	0.034	543.7	0.9943	3.8
AY99	457	11.3	0.024	455.6	0.9606	14.6
AB74	123.8	32.0	0.257	124.6	0.9754	12.2

Dye	Freundlich			
	K_F $(mg/g)/(mg/L)^{1/n}$	n	r^2	ε(%)
AB25	131.0	4.6	0.8278	23.0
AY99	63.9	3.2	0.9578	27.3
AB74	50.6	6.9	0.7359	38.5

Dye	Redlich-Peterson				
	B	K_R (L/g)	a_R $(L/mg)^{\beta}$	r^2	ε(%)
AB25	1.01	17.9	0.03	0.9947	3.5
AY99	0.81	25.1	0.18	0.9867	14.3
AB74	1.03	27.7	0.17	0.9834	9.6

Dye	Langmuir-Freundlich				
	K_{LF} $(mg^{1-m}.L^m.g^{-1})$	a_{LF} $(L/mg)^m$	m	r^2	ε(%)
AB25	14.8	0.02	1.0	0.9953	3.1
AY99	33.7	0.05	0.6	0.9865	13.5
AB74	19.1	0.15	1.3	0.9920	5.4

6.4.3. Adsorption kinetics

A vital evaluation element for an adsorption operation unit is the adsorption kinetics i.e., rate of adsorption reaction, which depends on the adsorbate-adsorbent interaction and system conditions. The uptake rate determines the time required for completion of adsorption process and can be enumerated from kinetics analysis using different kinetic models. For adsorption kinetic studies 0.1 g of adsorbent (Grafting yield =25%) was immersed in 100 mL of 500 ppm aqueous dye solutions and dye concentration in solution was measured spectrophotometrically at different time periods at 25^{o}C. Pseudo-first-order [182], pseudo-second-order kinetic models [183] and intra-particle diffusion model [187] were used to characterize the rate of adsorption of dyes. Figure 6.11 shows a relative change in the dye concentration of the liquid phase as a function of the adsorption time. Rapid uptake of dyes during initial stage (first 10 min) of adsorption indicates high affinity of adsorbent for anionic dye molecules

.

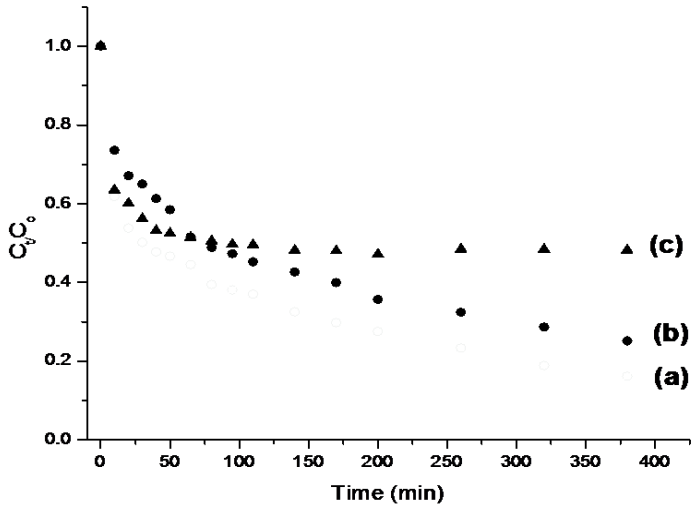

Figure 6.11: Adsorption kinetics of dyes (a) AB25 (b) AY99 (c) AB74

Rapid uptake is followed by slower adsorption and finally saturation at different times, depending on the dye. The adsorption of bivalent AB74 was much faster and the

equilibrium reached within 60 minutes; whereas, AB25 and AY99 took much longer time (> 300 min) to reach the equilibrium adsorption.

(a) Pseudo-first order kinetic model

The differential form of pseudo-first order equation is given as:

$$\frac{dq_t}{dt} = k_1 (q_e - q_t) \quad (6.14)$$

Equation (6.14) on integrating under boundary conditions q_t=0 at t=0 to q_t=q_t at t=t, transforms into the pseudo first order linear expression, also known as Lagergren equation [182-184], expressed as equation (6.15)

$$\ln (q_e - q_t) = \ln(q_e) - k_1 . t \quad (6.15)$$

where q_e (mg/g) and q_t (mg/g) are the solid phase dye concentration at equilibrium and at time 't', respectively, and k_1 (min^{-1}) is the pseudo-first order rate constant. The slope and intercept of the linear plot of ln(q_e-q_t) Vs t were used to estimate the pseudo-first order rate constant k_1(min^{-1}) and equilibrium solid phase dye concentration $q_{e,cal}$ (mg/g), respectively.

(b) Pseudo-second order kinetic model

The differential expression of the pseudo-second order model is given by equation 6.16 [185]

$$\frac{dq_t}{dt} = k_2(q_e - q_t)^2 \quad (6.16)$$

Integrating equation (6.16) and rearranging gives linear expression of the pseudo-second order model given as equation (6.17), which is mostly used for solid-liquid adsorption systems [185].

$$\frac{t}{q_t} = \frac{1}{k_2 q_e^2} + \frac{t}{q_e} \quad (6.17)$$

Where, k_2 is the pseudo-second-order adsorption rate constant (g/mg.min); and other parameters are same as in pseudo-first order model. If adsorption follows pseudo-second order kinetics, plot of t/q_t Vs t of equation (6.17) should give a linear relationship and adsorption amount $q_{e,cal}$ and k_2 can be calculated from slope and intercept of this plot.

The initial adsorption rate (h) and half-adsorption time ($t_{1/2}$) can be estimated from equation (6.18) and (6.19) respectively [186].

$$h = k_2 q_e^2 \quad (6.18)$$

$$t_{1/2} = \frac{1}{k_2 \ q_e} \quad (6.19)$$

It has been reported that the pseudo-first order equation is applicable to the initial stage of the adsorption process [187], whereas, pseudo-second order model is considered to explain adsorption behavior over the entire adsorption process [168]. Figure 6.12 and figure 6.13 show pseudo-first order and pseudo-second order kinetics plots, respectively. The kinetic parameters estimated from these plots (Table 6.5) show that the r^2 values are higher (>0.98) for pseudo-second order kinetic model. Therefore, it can be said that the adsorption kinetics of dyes follow pseudo-second order kinetics. It was found that r^2 values for AB25 is lower than that for AY99 and AB74. Moreover, for AB25, there is a large difference in the experimental capacity ($q_{e,\ exp}$) value and predicted value ($q_{e,cal}$).

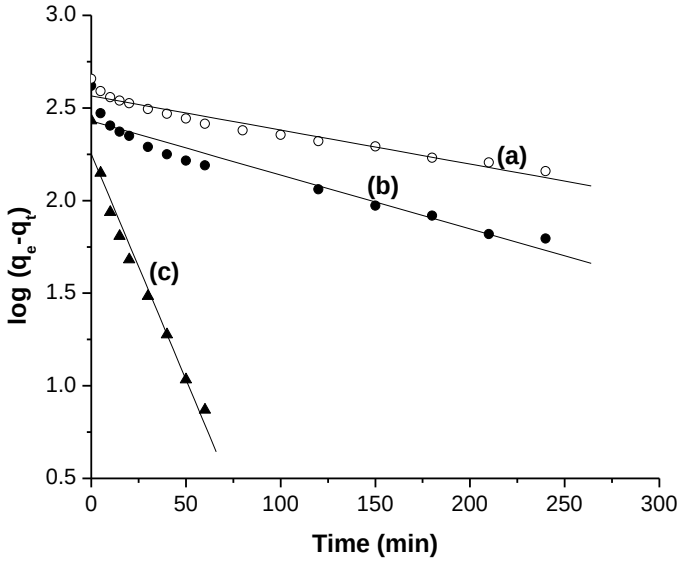

Figure 6.12: Pseudo-first order kinetic plots (a) AB25 (b) AY99 (c) AB74

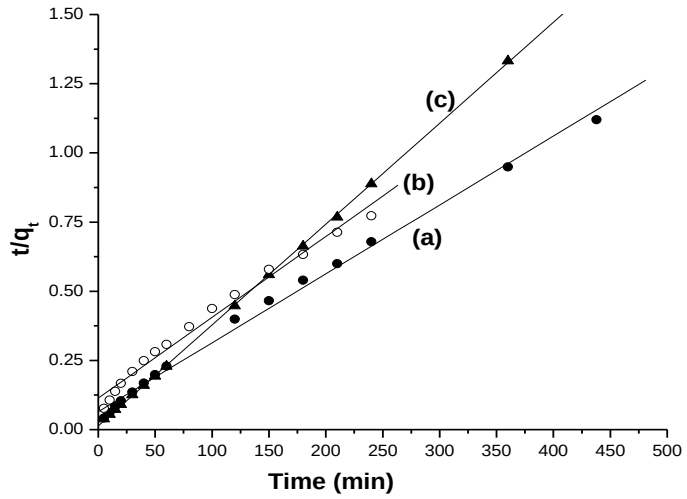

Figure 6.13: Pseudo-second order kinetic plots (a) AB25 (b) AY99 (c) AB74

Based on these observations, it can be inferred that pseudo-second order kinetic model shows better fitting for AY99 and AB74 in comparison to AB25. The values of adsorption rates, i.e., k_1, k_2 and h follows order AB25<AY99<AB74, whereas, the value of $t_{1/2}$ follows opposite trend, i.e., AB25>AY99>AB74 (Table 6.5).

Table 6.5: Pseudo-first order and pseudo-second order kinetic parameters

Dye	$q_{e,exp}$ (mg/g)	First order kinetic model		
		$q_{e,cal}$ (mg/g)	k_1 (min^{-1})	r^2
AB25	455	367.2	$4.2x10^{-3}$	0.9439
AY99	416	268.7	$6.7x10^{-3}$	0.9254
AB74	270	178.9	$5.6x10^{-2}$	0.9723

Dye	$q_{e,exp}$ (mg/g)	Second order kinetic model				
		$q_{e,cal}$ (mg/g)	k_2 (g/mg.min)	h (mg/g.min)	$t_{1/2}$ (min)	r^2
AB25	455	342.5	$7.5x10^{-5}$	8.8	38.9	0.9852
AY99	416	401.6	$9.5x10^{-5}$	15.4	26.0	0.9953
AB74	270	273.9	$9.7x10^{-4}$	27.3	3.7	0.9998

(c) Intra-particle diffusion model

As pseudo-first order and pseudo-second order model are used to determine type and extent of adsorption but cannot identify the diffusion mechanism, the intra-particle diffusion model (equation 6. 20) was used to study diffusion mechanism and to determine intra-particle diffusion rate constant (k_i) ($mg.g^{-1}\ min^{-0.5}$) (from slope of linear plot of q_t *vs* $t^{1/2}$) [168, 177, 188].

$$q_t = k_i\ t^{1/2} \qquad (6.20)$$

The intra-particle diffusion model (equation 6.20) was employed to find the probable adsorption mechanism of dyes onto adsorbent. It has been reported that if the linear plot of q_t vs $t^{1/2}$ passes through the origin then intra-particle diffusion is the only

rate determining step [175], otherwise other mechanisms along with the intra-particle diffusion are also involved, which is also manifested as the multi-linearity of the q_t vs $t^{1/2}$ plot [189].

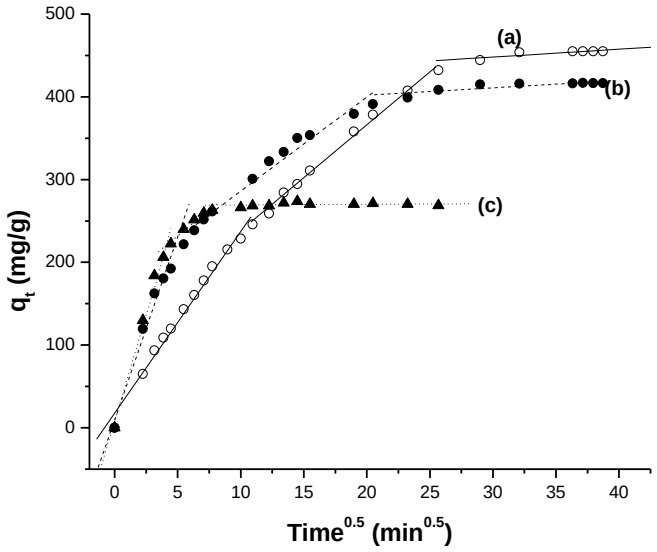

Figure 6.14: The intra-particle diffusion plots (a) AB25 (b) AY99 (c) AB74

Figure 6.14 shows intra-particle diffusion plot. The multi-linearities in three different stages, i.e., an instantaneously extremely fast uptake, a transition stage and an almost flat plateau portion was observed. The slope of the lines in each stages is termed as the rate parameter $k_{i,n}$ (n=stage number) and indicates the rate of the adsorption process. Rate parameters of the different stages for the adsorption of dyes are listed in Table 6.6. The adsorption rate for different stages was found to follow the order the first stage ($k_{i,1}$) > the second stage ($k_{i,2}$) > the third stage ($k_{i,3}$). The first-fast stage represents the mass transfer of dyes through boundary layers of liquid and an instantaneous utilization of the most readily available sites on the external surface of the adsorbent.

Table 6.6: The intra-particle diffusion rate parameters in three different regions of plots shown in figure 6.14

Dyes	Region (1)		Region (2)		Region (3)	
	$K_{i,1}$ (mg/g.min$^{0.5}$)	r^2	$K_{i,2}$ (mg/g.min$^{0.5}$)	r^2	$K_{i,3}$ (mg/g.min$^{0.5}$)	r^2
AB25	21.9	0.9934	12.7	0.9966	0.9	0.8593
AY99	44.1	0.9876	11.3	0.9872	0.9	0.8529
AB74	51.0	0.9919	12.5	0.9834	0.1	0.2017

In second stage the dye molecule enters the porous structures of the adsorbent and eventually gets adsorbed on the active sites at internal surface of the adsorbent. The transportation of dye molecule from external surface to bulk of the adsorbent sees increasing diffusion resistance, which is reflected as slower second stage adsorption. Finally third, the slowest stage represents the equilibrium region where the concentrations of the dye in the solution as well as the concentration of the adsorption sites on the adsorbent are limited [190, 191].

6.5 Thermodynamics aspects of the dye adsorption

Free energy (ΔG^o), an indication of spontaneity of the adsorption process, was estimated using relations (6.21) and (6.22) [186]

$$\Delta G^0 = -RT \ln K_d \tag{6.21}$$

$$K_d = \frac{C_A}{C_e} \tag{6.22}$$

Where, K_d is the distribution coefficient for the adsorption, C_A the amount of dye (mg) adsorbed on the adsorbent per liter of the solution at equilibrium and C_e is the equilibrium concentration (mg/L) of the dye in the solution. T is the solution temperature (K) and R is the gas constant (8.314 J/mol.K). The ΔG^o values for adsorption of AB25, AY99 and AB74 at 300 K, were estimated to be -9.7 kJ/mol, -8.8 kJ/mol and -7.4 kJ/mol,

respectively. The negative value of ΔG^o confirms the feasibility of the adsorption process and also indicates spontaneous adsorption of dyes onto adsorbent.

6.6 Desorption studies

The regeneration of the adsorbent by desorption of adsorbed dyes in a suitable eluent is prerequisite for the success of the adsorption process. Desorption experiments were carried out by immersing the adsorbent loaded with acid dyes, in 40 mL of de-sorption solution containing 1N KSCN in varying Water: Methanol mixture, for 3 hours at room temperature. The desorbed dye concentration was estimated spectrophotometerically after suitable dilution. The quantity of desorbed dye was quantified in terms of elution percentage (EP) given by relation (6.23).

$$EP\ (\%) = \frac{W_d}{W_a} X\ 100 \qquad (6.23)$$

Where, W_d,W_a are the weights of desorbed dye and weight of adsorbed dye

It was observed that dyes adsorbed onto PVBT-g-Cellulose did not desorb even in 1N NaCl aqueous solution. This indicated that adsorption of anionic dyes on to adsorbent was not solely due to ionic interaction but might be due to cumulative effect of many attractive forces viz. ionic interactions, hydrophobic interactions, van der waals forces, hydrogen bonding, etc. [186]. Similar results have been reported earlier for desorption of anionic reactive dyes from commercial anion-exchange membranes, where 1N KSCN solution in 60 % methanol solution in water was reported to be the optimum desorbent for breaking these non-specific interactions [1, 192]. The reported eluent mix was used for elution of dyes from adsorbent. The elution percentage for AB25, AY99 and AB74 was found to be ~95%, ~70% and ~20%, respectively.

6.7 Conclusion

Mutual radiation induced grafting methods have been used to cationize the cotton wastes in a single step-environment benign-aqueous solvent. Extent of cationization is found the function of radiation absorbed dose and monomer concentration. 25% extent of grafting yield has been achieved at 25% (w/v) of VBT at the total absorbed dose of 2.7kGy at the dose rate of $4kGyh^{-1}$. Cationized cotton wastes further have been utilized for treatment of textile dye effluents for removal of acid dyes. Various important parameters like equilibrium adsorption, kinetic study, thermodynamics aspects have been studied. Radiation grafted PVBT-g-Cellulose showed separation factor (R_L) values in the range $0<R_L<1$, indicating favorable adsorption of dyes on the adsorbent while negative ΔG^o value showed spontaneity of the adsorption. The fitting of non-linear adsorption isotherm models to adsorption data followed the order Freundlich<Langmuir<Redlich-Peterson<Langmuir-Freundlich. The kinetic adsorption data was in close agreement with pseudo-second order kinetic model. The elution percentage of ~95%, ~70% and ~20% for AB25, AY99 and AB74, respectively, could be achieved using optimized eluent composition.

Refrences

[1] N. K. Goel, V. Kumar, Y. K. Bhardwaj, S. Pahan, S. Sabharwal, J. Hazard. Mater. 193, 17 (2011)

[2] G. Z. Kyzas, M. Kostoglou, N. K. Lazaridis, D. N. Bikiaris, J. Hazard. Mater. 29, 244, (2013)

[3] A. Bhattacharya, B. N. Misra, Prog. Polym. Sci. 29, 767 (2004)

[4] N. K. Goel, S. Rao, V. Kumar, Y. K. Bhardwaj, C. V. Chaudhari, K. A. Dubey, S. Sabharwal, Radiat. Phys. Chem. 78, 399 (2009)

[5] M. M. Nasefa, O. Güvenc, Prog. Polym. Sci. 37, 1597 (2012)

[6] N. Seko, A. Ktakai, S. Hasegawa, M. Tamada, N. Kasai, H. Takeda, T. Sugo, K. Saito, Nucl. Technol. 144 (2), 274 (2003)

[7] P. A. Kavakli, N. Seko, M. Tamada, O. Gu¨ven, J. Appl. Polym. Sci., 105, 1551 (2007)

[8] M. Yamato, M. Utsumi, A. Kushida, C. Konno, A. Kikuchi, T. Okano, Tissue engineering. 7, 473 (2001)

[9] C. Bi , H. Zhang, S. Xiao, Y. Zhang, , Z. Mai, X. Li, J. Membr. Sci. 376, 170 (2011)

[10] M. M. Nasef, H. Saidi, H. M. Nor, J. Appl. Polym. Sci. 77, 1877 (2000)

[11] I. Y. Farber, J. Golenser, N. Beyth, E. I. Weiss, A. J. Domb, J. Nanomater. 2010 (2010)

[12] H. Kourai, T. Yabuhara, A. Shirai, T. Maeda, H. Nagamune, Eur. J. Med. Chem. 41, 437 (2006)

[13] K. Saito T. Sugo, in (Eds. Jonah C. D., B. S. M. Rao), Elsevier Science, Amsterdam-London-New York-Oxford-Paris-Shanon-Tokyo, 671 (2001)

[14] J. H. Hubbell, Radiat. Phys.Chem. 75 (6), 614 (2006)

[15] H. Fricke, S Morse. Philos. Mag. 7129 (1929)

[16] E. M. Fielden, N. W. Holm Manual on Radiatio Dosimetry, (Eds. Holm N. W., Berry R. J.) Dekker, New York, 261 (1970)

[17] S. L. Caër, Water. 3, 235 (2011)

[18] E. J. Hart, M. Anbar, The Hydrated Electron,Wiley Interscience, New York 42 (1970)

[19] J. M. Wisenfield, E. P. Ippen, Chem. Phys. Lett. 73, 47 (1980)

[20] T. J. Sworsk, J. Am. Chem. Soc. 764, 786 (1954)

[21] L. Zhao, J. M. Wssikiewicz, H. Mitomo, N. Nagasawa, F. Yoshii, J. Nucl. Sci. Technol. 18, 42 (2007)

[22] X. Z. li, W. Gen-hua, W. Han-ing, C. Gyn, N. Min-hua, Radiat. Phys. Chem. 22, 939 (1983)

[23] G. V. Sriryaeva, V. V. Bydanova, V.A. Khoromskaya, T.A. Bolshakova, Radiat. Phys. Chem. 46, 995 (1995)

[24] R. L. Clough, S. W. Shalaby, Radiation Effects on Polymers," ACS Symposium Series 475, eds., ACS Washington, D.C. (1991)

[25] R. P. Lagendijk, A. H. Hogt, A. Buijtenhuijs, A. D. Gotsis. Polymer. 42, 10035 (2001)

[26] O. Gueven, Advances in radiation chemistry of polymers**,** Proceedings of a technical meeting held in Notre Dame, Indiana, USA 33 (2003)

[27] S. Korenev, Radiat. Phys.Chem. 71, 521 (2004)

[28] S. Fukui, S. Shimaski, T. Tohzuka, US patent 4724092, assigned to daikin industries ltd. feb9, 1988 or Fluoropolymer additives by Sina ebnesajjad, Richard morgan, ISBN: 978-1-4377-3461-4

[29] K. Arai, Block and Graft Copolymers John Wiley, New York, 193 (1973)

[30] H. A. J. Battaerd, W Tregear, "Graft Copolymers", Wiley Interscience, New York, 56 (1967)

[31] S. K. Shukla, D. Shrivatava, J. Plym. Mater. 20, 207 (2003)

[32] M. M. Nasef, E. A. Hegazy, Prog. Polym. Sci. 29, 499 (2004)

[33] J. M. Rosiak, I. Janik, S. Kadlubowski, M. Kozicki, P. Kujawa, P. Stasica, P. Ulanski, Radiation Formation of Hydrogels for Biomedical Applications IAEA report 1-50 (2002)

[34] L. Varshney, Nucl. Instrum. Methods Phys. Res. Sect. B-Beam Interact. Mater. Atoms. 255(2), 343 (2007)

[35] R. L. Clough. Nucl. Instrum. Methods Phys. Res., Sect. B 185, 8 (2001)

[36] D. De Rossi, K. Kajiware, Y. Osada, A. Yamauchi; Polymer Gels. Fundamentals and Biomedical Applications. Plenum Press, New York (1991)

[37] H. Hasa, M. Ilavsky, K. Dusek, J. Polym. Sci. Polym. Phys. Ed., 13, 253 (1975)

[38] M. Ilavsky, Polymer. 22, 1687 (1981)

[39] J. Ricka, T. Tanaka, Macromolecules 17, 2916 (1984)

[40] D. Schmaljohann, Adv. Drug. Deliv. Rev. 58, 1655 (2006)

[41] V. Kudela "Encyclopedia of Polymer Science and Engineering", Vol 7, 2nd ed. (Eds. H. F. Mark, N. M. Bikales, C. G. Overberger, G. Menges, J. I. Kroschwitz eds.), John Wiley, New York, 783 (1987)

[42] IUPAC, Compendium of Chemical Terminology, 2nd ed. (the "Gold Book") (1997)

[43] D. K. Brannon, Cosmetic microbiology: a practical handbook. CRC Press, Inc., Boca Raton, Fla. (1997)

[44] G. J. Hucker, S. Watkins, D Metcalf, J. Stone N. Y. Agri. Expt. Sia., Tech. Bull. 281, 37 (1948)

[45] E. W. Kivela, W. L., Mallmann E. S. Churchill, J. Bact. 55, 565 (1948)

[46] D. E. Hughes, Biochem. J. 46, 231 (1950)

[47] E.-R. Kenawy, F. I. Abdel-Hay, A. E.-R. R. El-Shanshoury, M. H. El-Newehy, J. Controlled Release, 50, 145 (1998)

[48] R. K¨ugler, O. Bouloussa, F. Rondelez, Microbiology, 151(5), 1341 (2005)

[49] H. Fricke, E. J. Hart, J. Chem. Phys. 3, 60 (1935)

[50] ICRU Report "Radiation Dosimetry: X-rays and Gamma rays with maximum Photon Energies Between 0.6 and 50MeV. 14 (1969)

[51] H. Fricke, E. J. Hart. Radiation Dosimetry, Second Edition" (Eds. Attix F.H., Roesch W.C. and Tochilin E.) Acad., New York, Vol 1 Chap. 12 (1969)

[52] K. Sehested. Manual on Radiation Dosimetry" (Eds. Holm N. W., Berry R.J.) Dekker, New York, 313 (1970)

[53] American Society for testing and Materials Standards E, 1026 (1995)

[54] J. W. T. Spinks, R. J. Woods. An Introduction to Radiation Chemistry. Wiley Interscience New York, 289 (1990)

[55] ICRU Report. Radiation Dosimetry: Electrons with energies between 1 and 50MeV. 35 (1984)

[56] B. G. Kabra, M. A. Akhtar, S. H. Gehrke. Polymer 3, 3990 (1992)

[57] A. Alfrey, E. F. Gurnee, W. G. Lloyd, J. Poly. Sci. C12, 249 (1966)

[58] P. L. Ritger, N. A. Peppas, J. Control. Release. 537 (1987)

[59] N. A. Peppas, L. Brannon-Peppas, J. Food. Eng. 22, 189 (1994)

[60] H. B. Hopfenberg, H.L. Frisch, Polym. Letters 7, 405 (1969)

[61] H. Fujita. Fortsch. Hochpolym. Forsch. 3, 1 (1961)

[62] B. G. Kabra, S. H., Gherke S. T. Hwang, W.A. Ritschel, J. Appl. Polym. Sci. 42, 2 409 (1991)

[63] J. CrankIn, The Mathematics of Diffusion. 2nd Ed. Oxford University Press (1975)

[64] J. E. Mockel, B. C. Lippold, Pharm. Res. 90, 1066 (1993)

[65] W. F. Lee, P. L. Yeh, J. Appl. Polym. Sci. 68(10), 1597 (1998)

[66] S. J. Kim, K. J. Lee, I. Y. Kim, S. I. Kim, J. Macromol. Sci. A-Pure Appl. Chem. A40 (5), 501 (2003)

[67] M. E. Brown, Introduction to Thermal Analysis, Kluwer Academic Publisher, London (2001)

[68] K. R. Aneja, Experiments in Microbiology, Plant Pathology and Biotechnology. New Age Publishers, ISBN 81-224-1494-X 69 (2005)

[69] M. Tokita, M. J. Tanaka, J. Chem. Phys. 95, 4613 (1991)

[70] N. A. Peppas, A. G. Mikos, in: Hydrogels in medicine and pharmacy: Fundamentals, N. A. Peppas (Ed.), Vol. I, pp. 1-25. CRC Press, Boca Raton Fla (1986)

[71] K. Park, W. S. W. Shalaby, H. Park, in: Biodegradable hydrogels for drug delivery, K. Park, W. S. W. Shalaby and H. Park (Ed.), Technomic, Lancaster PA 1-12, (1993)

[72] D. W. Hutmacher, J. Biomater. Sci. Polymer Ed. 12, 107 (2001)

[73] M. Shahinpoor, J. Intell. Mater. Syst. Struct. 6, 307 (1995)

[74] E. V. Farahani, D. G. Cooper, J. H. Vera and M. E. Weber, Chem. Eng. Sci. 47(1), 31 (1992)

[75] A. A. Vaidya, B. S. Lele, M. G. Kulkarni, R. A. Mashelkar, Biotechnol. Bioeng. 64(4), 418, (1999)

[76] V. Kumar, Y. K. Bhardwaj, S. Sabharwal, Eur. Polym. J. 40, 1495 (2004)

[77] L. F. Gudeman, N. A. Peppas, J. Membrane Sci., 107, 239 (1995)

[78] C. L. Bell, N. A. Peppas, Biomaterials, 17, 1203 (1996)

[79] G. Chen, A. S. Hoffman, Nature, 374, 240 (1995)

[80] J. Kalal, J. Makromol. Chem. Suppl. 7, 31 (1984)

[81] A. B. Majali, Y. K. Bhardwaj, S. Sabharwal, H. L. Bhalla, P. Raj, in: Proceedings of the ACS symposium series 520, Washington D. C. pp. 288-296 (1993)

[82] P. Y. Ghi, D. J. T. Hill, D. Maillet, A. K. Whittaker, Polymer 38(15), 3985 (1997)

[83] J. P. Montheard, M. Chatzopoulos, D. Chappard, JMS Rev. Macromol. Chem. Phys. C32 (1), 1 (1992)

[84] B. D. Ratner, Biomaterials Science, An Introduction to Materials in Medicine. Elsevier Academic Press. ISBN 0-12-582463-7, (2004)

[85] J. Sague, J. Vogt, B. Andreatta, R. Egli, R. Luginbuehl, J. Bone Joint Surg. Br. 94-B :(SUPP XL) 210 (2012)

[86] R. A. Gemeinhart, J. Chen, H. Park, K.Park, J. Biomater. Sci. Polymer Edn. 11(12), 1371 (2000)

[87] H. Omidian, K. Park, U. Kandalam, J. G. Rocca, J. of Bioact. and Compat. Polym. 25,483 (2010)

[88] B. Isik, Turk. J. Chem. 24, 147 (2000)

[89] N.K. Goel,V. Kumar, Y. K. Bhardwaj, J. Biswal, S. Sabharwal, J. Macromol. Sci., Pure Appl. Chem., 43 (8), 1151 (2006)

[90] S. Dragan, D.Dragan, M. Cristea, A. Airinei, L. Ghimci, J. Polym. Sci. Polym. Chem. Ed. 37, 409 (1993)

[91] J. Byun, Y. M. Lee, C. S. Cho, J. Appl. Polym. Sci. 61, 697 (1996)

[92] W. Xue, S. Champ, M. B. Huglin, Polymer 42, 3665 (2001)

[93] K. A. Smeds, M. W. Grinstaff, J. Biomater. Sci. Polymer Edn. 54 (1), 115 (2001)

[94] A. S. Hoffman, Radiat. Phys. Chem. 18, 323 (1981)

[95] D. Saraydin, E. Karadag, O. Guven, J. Appl. Polym Sci. 79, 1809 (2001)

[96] I. Kaetsu, M. Kamakura, T. Fujimura, M. Yoshida, M. Asano, M. Kasai, M. Tamada, Radiat. Phys. Chem. 27, 245 (1986)

[97] W. Gombotz, A. Hoffman, G. Schmer, S. Venoyama, Radiat. Phys. Chem. 25, 549 (1985)

[98] O. Z. Higa, N. L. Delmastro, A. C. Castagnet, Radiat. Phys. Chem. 27, 311 (1986)

[99] Y. K. Bhardwaj, S. Sabharwal, A. B. Majali, J. Polym. Mater. 17(3), 239 (2000)

[100] Y. K. Bhardwaj, S. Sabharwal, A. B. Majali, J. Polym. Mater. 18(1), 37 (2001)

[101] P. J. Flory, in: Principles of Polymer Chemistry,P. J. Flory (Ed.), Cornell University Press, Ithaca New York , 541-594 (1953)

[102] S. H. Gherke, P. I. Lee, in: Specialized drug delivery systems: Manufacturing and production technology, Marcel Dekker Inc. New York and Basel, 333-392, (1990)

[103] S. N. Vinogradov, R. H. Linnell, in: Hydrogen bonding, Van Nostrand Reinhold Co. New York, 198-222 (1971)

[104] V. Kumar, C. V. Chaudhari, Y. K. Bhardwaj, N. K. Goel, S. Sabharwal, Eur Polym. J. 42, 235 (2006)

[105] N. K. Goel, V. Kumar, Y. K. Bhardwaj, S. Sabharwal, J Macromol. Sci. Pure and Appl. Chem. 43, 327 (2006)

[106] Y. K. Bhardwaj, S. Sabharwal, A. B. Majali, J. Polym. Mater. 11, 29 (1994)

[107] D. Biren, B. G. Kabra, S. H. Gherke, Polymer 33, 554 (1992)

[108] J. L. Valada, Y. Liu, M. Huglin, Macromol. Chem. Phys. 199, 1127 (1998)

[109] M. Yi, J. Li, J. B. Zhang, G. L. Jiang, J. H. Qiao, H. F. Ha, Radiat. Phys. Chem. 52, 261 (1998)

[110] J. Israelachvilli, in: Intermolecular and surface forces, 2nd Edition,. San Diego, Academic Press, 191-237 (199)

[111] A. K. Bajpai, J. Bajpai, S. Shukla, R. A. Kulkarni, J. Macromol. Sci. A: Pure Appl. Chem. A41 (2), 211 (2004)

[112] Y. K. Bhardwaj, V. Kumar, S. Sabharwal, J. Appl. Polym. Sci. 88, 730 (2003)

[113] J. W. Wood, D. Attwood, J. H. Corllett, Int. J. Pharmaceutics. 7, 189 (1981)

[114] K. Dusek, M. Bohdencky, V. Vosicky, Coll. Czech. Chem. Commun., 42, 1599 (1977)

[115] V. R. Gowariker, N. V. Viswanathan., J. Sreedhar, Individual polymers. In: Gowariker, V. R., Viswanathan, N. V., Sreedhar, J., (Eds.), Polymer Science. Wiley Eastern Limited, New Delhi, 215 (1993)

[116] G. Reyerouck., W. B. Hugo, A. D. Russel, Evaluation of antibacterial and antifungal efficiency. In: Russel, A. D., Hugo, W. B., Ayliffe, G. A. J., (Eds.), Blackwell Scientific Publications, Oxford, 124 (1992)

[117] B. Gottenbos, H. C.Vander Mei, F. Klatter, P. Nieqwenhuis, H. J. Busscher, Biomaterials 23, 1417 (2002)

[118] S. Wu, C. Jou, M. C. Yang. Biomaterials 24, 2695 (2003)

[119] E. Princi, S. Vicini, N. Proietti, D. Capitani, Eur. Polym. J. 41(6), 1196 (2005)

[120] A. H. Zahran, V. T. Stannet, R. Liepins, N. Morosoff, Radiat. Phys. Chem. 16(4), 265 (1980)

[121] V. Bilgin, J. T. Guthrie, Radiat. Phys. Chem. 36, 581 (1990)

[122] H. Lönnberg, L. Fogelström, M. A. S. S. Samir, L. Berglund, E. Malmström, AHult, Eur. Polym. J. 44(9), 2991 (2008)

[123] M. L. Sagu, K. K. Bhattacharyya, J. Macromol. Sci. Chem. A. 23(9), 1099 (1986)

[124] H. I. Meléndez-Ortiza, E. Bucio, G. Burilloa, Radiat. Phys. Chem. 78(1), 1 (2009)

[125] J. Chen, Y. C. Nho, A. S. Hoffman, J. Biomater. Sci. Polym. Ed. 35, 841 (2004)

[126] B. Gupta, R. Jain, N. Anjum, H. Singh, Radiat. Phys. Chem. 75(1), 161 (2006)

[127] N. Yoshinari, Y. Oda, M. Kato, K. Okuda, Biomaterials. 22, 2043 (2002)

[128] A. Kanazawa, T. Ikeda, T. Endo, J. Polym. Sci. Polym. Chem. Ed. 32, 1997 (1994)

[129] P. R. Murray, A. C. Niles, R. L. Heeren, J. Clin. Microbiol. 26(9), 1884 (1998)

[130] S. M. Kolhe, A. Kumara, Radiat. Phys. Chem. 76(5), 901 (2007)

[131] A. Chapiro, In: Chapiro, A. (Ed.), Radiation chemistry of polymeric systems. John Wiley & Sons, New York, 596 (1962)

[132] V. A. Bhanut, K. Kishore, Chemical Reviews. 91(2), 99 (1991)

[133] J. W. T. Spinks, R. J. Woods, In: Spinks, J. W. T., Woods, R. J. (Eds.), Wiley, New York, 127 (1990)

[134] K. Gargan, E. Kronfli, K. V. Lovell, Radiat. Phys. Chem. 36(6), 757 (1990)

[135] L. N. Grushevskaya, R. E. Aliev, V. Y. Kabanov, Rad. Phy. Chem. 36(3), 475 (1990)

[136] B. N. Misra, I. K. Mehta, M. P. S. Rathore, S. Lakhanpal, J. Appl. Polym. Sci. 49(11), 1979 (1979)

[137]Y. C. Nho, J. L. Garnett, P. A. Dworjanyn, J. Polym. Sci. Part A: Polym. Chem. 30(6), 1219 (1995)

[138] S. Steenken, P. Neta, J. Am. Chem. Soc. 104, 1244 (1982)

[139] I. K. Mehta, D. S. Sood, B. N. Misra, J. Polym. Sci. Part A: Polym. Chem. 27(1), 53 (1986)

[140] L. Albertin, M. H. Stenzel, C. L. Barner-Kowollik, J. R. Foster, T. P. Davis, Polymer 46, 2831 (2005)

[141] S. Dilli, J. L. Garnett, E. C. Martin, D. H. Phuoc, J. Polym. Sci. C. 37, 118 (1972)

[142] K. D. N. Lawrence, D. Verdin, J. Appl. Polym. Sci. 17(9), 2653 (1973)

[143] S. M. Badawy, H. H. Sokker, S. H. Othman, A. Hashem, Radiat. Phys. Chem. 73(2) 125 (2005)

[144] O. H. Wen, S. Kuroda, H. Kubota, Eur. Polym. J. 37(4), 897 (2001)

[145] V. Kumar, Y. K. Bhardwaj, K. P. Rawat, S. Sabharwal, Radiat. Phys. Chem. 73(3), 175 (2005)

[146] S. Petrulyte, 55(1), 72 (2008)

[147] T. Ramachandran, K. R. Kumar, R Rajendran, IE (I) Journal—TX, 84, 42 (2004)

[148] H. J. Johnston, G. Hutchison, F. M. Christensen, S. Peters, S. Hankin, V. Stone, Crit. Rev. Toxicol. 40 (4), 328 (2010)

[149] M. Ahamed, M. S. Alsalhi, M. K. Siddiqui, Clin. Chim. Acta. 411, 1841 (2010)

[150] Y. H. Xiao, J. H. Chen, M. Fing, X-D. Xing, H. wang, Y-J. Wang, F. Li, J. oral sci. 50(3), 323 (2008)

[151] V. Alptüzün , S. Parlar, H. Taşlı, E. Erciyas, Molecules. 14, 5203 (2009)

[152] S. Tsunedo, K. Saito, H. Mitsuhara, T. Sugo, J. Electrochem. Soc. 142 (11), 3659 (1995)

[153] C. K. Na, H. J. Park, J. Appl. Polym. Sci. 116, 2723 (2010)

[154] E. Bucio, G. Burillo, Radiat. Phys. Chem. 76, 1724 (2007)

[155] P. R. S. Reddy, G. Agathian, Radiat. Phys. Chem. 73, 169 (2005)

[156] M. M. Nasef, Polym. Int. 50, 338 (2001)

[157] H. Hongfei, L. Xiaohong, W. Jilan, Radiat. Phys. Chem. 39, 513 (1992)

[158] J. L. Garnett, L. T. Ng, Radiat. Phys. Chem. 48, 217 (1996)

[159] N. K. Goel, Y. K. Bhardwaj, R. Manoharan, V. Kumar, K. A. Dubey, C. V. Chaudhari, S. Sabharwal, Express Polym. Lett. 3, 268 (2009)

[160] P. A. Dworjanyn, J. L. Garnett, Radiat. Phys. Chem. 33, 429 (1989)

[161] J. W. T. Spinks, R. J. Woods. In: Spinks J. W. T., Woods R. J. (Eds) Wiley, New York, 163 (1990)

[162] A. Metris, S. M. George, M. W. Peck, J. Baranyi, J. Microbiol. Methods. 55, 821 (2003)

[163] G. Suvet, S. Dupond, K. Kazmierski, J Chojnowski, J. Appl. Polym. Sci. 75(8), 1005 (2000)

[164] J. Bozja, J. Sherrill, S. Michielsen, I. Stojiljkovic J. Polym. Sci., Part A: Polym. Chem. 41, 2297 (2003)

[165] A. Fujishima, K. Hashimoto, T. Watanabe, Photocatalysis, Fundamental and Applications Bkc Inc., Tokyo, Japan, 1999

[166] A. Mills, S. Lee, J. Photochem. Photobiol. A, 152, 233 (2002)

[167] J. Hu, Adaptive and functional polymers, textiles and their applications, Imperial College press. 2010

[168] B. Paosawatyanyong P. Jermsutjarit, W. Bhanthumnavin, J. Nanosci. Nanotechnol. 12, 748 (2012)

[169] V. Kumar, Y. K. Bhardwaj, K. Tirumalesh, K. A. Dubey, C. V. Chaudhari, N. K. Goel, J. Biswal, S. Sabharwal, Sep. Sci. Technol. 41, 3123 (2006)

[170] C.V. Chaudhari, J. Paul, L. Panicker, K.A. Dubey, V. Kumar, N.K. Goel, Y.K. Bhardwaj, S. Sabharwal, Environ. Prog. Sustain. Ener. 31(1), 77 (2012)

[171] I. Langmuir, J. Am. Chem. Soc. 38, 2221 (1916)

[172] H. M. F. Freundlich, Chemie Z. Phys. Chem. 57A, 385 (1906)

[173] O. Redlich, D.L. Peterson, J. Phys. Chem. 63, 1024 (1959)

[174] Y. S. Ho, Carbon. 42, 2115 (2004)

[175] O. Tunc, H. Tanaci, Z. Aksu, J. Hazard. Mater. 163, 187 (2009)

[176] Y. S. Ho, J. C. Y. Ng, G. McKay, Review, Separ. Purif. Method. 29, 189 (2000)

[177] K. G. Bhattacharyya, A. Sharma, Dyes Pigments. 65, 51 (2005)

[178] Y. S. Ho, G. McKay, Chem. Eng. J. 70, 115 (1998)

[179] R. E. Treyball, Mass transfer operations, third ed., McGraw Hill, New York, 1980

[180] G. Mckay, Y. S. Ho, Water Res. 33, 578, (1999)

[181] K. V. Kumar, S. Sivanesan, Dyes Pigments. 72, 130 (2007)

[182] M. S. Chiou, H. Y. Li, Chemosphere. 50, 1095 (2003)

[183] L. Semerjian, J. Hazard. Mater. 173, 236 (2010)

[184] S. Kapsabelis, C.A. Prestidge, J. Colloid Interf. Sci. 228, 297 (2000)

[185] Y. S. Ho, G. McKay, Process Biochem. 34, 451 (1999)

[186] W. Zhijian, J. Hyeonwoo, L. Kangtaek, Chem. Engg. J. 112, 227 (2005)

[187] Y. C. Wong, Y. S. Szeto, W. H. Cheung, G. McKay, Process Biochem. 39, 693 (2004)

[188] F. C. Wu, R. L. Tseng, R. S. Juang, Water Res. 35, 613 (2001)

[189] Q. Qin, J. Ma, K. Liu, J. Hazard. Mater. 162, 133 (2009)

[190] V. L. Snoeyink, R. S. Summers, Water Quality and Treatment: A Handbook of Community Water Supplies, 5th ed., McGraw-Hill Inc., New York, 1999

[191] W. H. Cheung, Y. S. Szeto, G. McKay, Bioresource Technol. 98, 2897 (2007)

[192] C. H. Liu, J. S. Wu, H. C. Chiu, S. Y. Suen, K. H. Chu, Water Res. 41, 1491 (2007)